THE GENERATION OF DOMAIN-SPECIFIC MONOCLONAL ANTI-CD4 ANTIBODIES AS NOVEL CANDIDATE HIV THERAPIES

Vinesh Mervyn JUGNARAIN

A dissertation submitted to the Faculty of Health Science, University of the Witwatersrand, in fulfilment of the requirements for the degree of Master of Science in Medicine

JOHANNESBURG, 2015

DECLARATION

I, Vinesh Mervyn Jugnarain, declare that this dissertation is my own work. It is being submitted for the degree of Master of Science in Medicine, at the University of the Witwatersrand, Johannesburg. It has not been submitted before for any degree or examination at this or any other University.

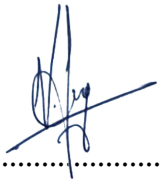

.....

Vinesh Mervyn Jugnarain

.....22/06/2015….....

Date

ABSTRACT

Directing antibodies against CD4, the primary receptor for HIV entry on its host T-cells, has been explored as an alternative way of inhibiting viral infection. Here, a panel of 40 CD4 targeting monoclonal antibodies (MAbs) were generated from mice immunized with bacterially expressed recombinant 2-domain CD4 (2dCD4). Firstly, the first two individual domains of CD4, termed D1 and D2, were generated. Whilst the mutant D1 generated was based on a previous work, the expression and characterisation of individual wild-type domain D2 has not yet been reported in detail. D1 and D2 cassettes were cloned and expression in *E.coli* was optimised. After the establishment of an optimised purification protocol, the purified protein were assessed by means of basic biophysical analyses (analytical SDS-PAGE, CD Spectroscopy), which allowed us to gain insights into the structural and functional integrity of the purified products. Recombinant D1 and D2 were then used to define the domain specificities of the MAbs by ELISA. We also demonstrated the ability of the MAbs to inhibit CD4-gp120 binding *in vitro* by ELISA, and inhibit viral infection by a pseudovirion inhibition assay. These preliminary results reinforce the potential of CD4-directed MAbs as candidate anti-HIV agents, and provide a solid platform for further pre-clinical development of this class of antiviral compounds.

***Key words*: CD4, HIV, gp120, Monoclonal Antibodies, Pseudovirion Assay**

ACKNOWLEDGMENTS

I would like to thank my principal supervisor, Dr Alexio Capovilla, for his guidance and help throughout the entire project; and for his understanding and encouragement when things were not working! I would also like to thank my co-supervisors Prof. Maria Papathanasopoulos and Prof. Caroline Tiemessen for their support. Thanks to all of my laboratory colleagues, especially Mark, Michelle, Nichole and Nazneen for their help and advice in the laboratory on a daily basis. Also, thanks to Michelle Bronze for her help with statistics. Not to forget all of the laboratory mates (which are quickly growing in number; soon no more space!): Irene, Roberto, Rafeeka, Dean and Karolina; thanks for your friendliness. I would also like to thank the entire Molecular Medicine and Haematology Department, 7th Floor, Wits Medical School, for the years of continuous friendliness and support.

FUNDING

This project was funded from Medical Research Council (MRC), National Research Foundation (NRF) and Poliomyelitis Research Foundation (PRF). Tuition fees were covered by the Wits Post-Graduate Merit Award Scholarship. The author received grant-linked bursaries from the MRC (PI, Dr Alexio Capovilla) and the NRF (PI, Prof. Caroline Tiemessen).

TABLE OF CONTENTS

DECLARATION 2

ABSTRACT 3

ACKNOWLEDGMENTS 4

FUNDING 4

TABLE OF CONTENTS 5

LIST OF FIGURES 11

RECURRING ABBREVIATIONS 13

CHAPTER 1: INTRODUCTION 14

1.1. INTRODUCTION 15

1.1.1. Epidemiology 15

1.1.2. Basics of HIV 16

1.1.2.1. Pathophysiology of HIV and AIDS 16

1.1.2.2. Viral Classification and Diversity 17

1.1.2.3. Viral Genome and Structure 18

1.1.2.4. Life-Cycle and Replication 19

1.1.2.5. Viral Entry 20

1.1.3. Current Antiretroviral Treatment and Prevention Strategies 21

1.1.3.1. Approved Anti-HIV Drugs 21

1.1.3.2. Antibody Development against HIV 22

1.1.3.3. The Problems with Antibody-Based HIV Treatments 24

1.1.3.3.1. HIV Diversity and Rapid Mutation Rates 24

1.1.3.3.2. Inaccessible Neutralizing Epitopes on the Envelope Glycoprotein 25

1.1.3.3.3. The Envelope Glycoprotein as an Immune Decoy 26

1.1.3.3.4. Extensive Somatic Hyper-mutation 26
1.1.4. Project objectives 27
CHAPTER 2: THE CD4 RECEPTOR 29
2.1. INTRODUCTION 30
2.1.1. General Overview 30
2.1.2. Function of CD4 31
2.1.3. Structure of Extracellular CD4 32
2.1.4. The CD4-Gp120 Interaction 35
2.1.5. Conformational Changes in CD4 37
2.1.6. Redox Changes in CD4 38
2.1.6.1. The Role of Disulphide Bonds 38
2.1.6.2. The Role of Disulphide Bonds in CD4 39
2.1.6.3. Redox Changes in CD4 and HIV infection 39
2.1.7. Project Objectives for this Chapter 40
2.2. MATERIALS AND METHODS 41
2.2.1. Design of CD4 Variants Cassettes 41
2.2.2. Preparation of Competent *E. coli* DH5α and BL21 42
2.2.3. Bacterial Cloning 43
2.2.4. Plasmid Extraction 43
2.2.5. Molecular Cloning of DNA Cassettes into Host Expression Vectors 44
2.2.6. Restriction Enzyme Analysis, Molecular Screening and Isolation of Pet-15b-D1 (M1.1), Pet-15b-D2, Pet-4dcd4 (Wt) and Pet-4dcd4 (D2A) 45
2.2.7. Bacterial Expression of CD4 variants 46
2.2.7.1. CD4 Expression 46
2.2.7.2. Protein Solubility Analysis 47

2.2.7.3. Protein Isolation and Purification 47
2.2.7.4. Protein Re-folding 48
2.2.7.5. Protein Analysis 49
2.2.7.6. Assessing Functionality of Bacterial Expressed CD4 variants 49
2.3. RESULTS 52
2.3.1. *In silico* analysis of CD4 variants 52
2.3.1.1. D1 52
2.3.1.2. D2 54
2.3.2. Protein Expression Studies 55
2.3.2.1. IPTG Induction and Temperature Optimisation for Protein Expression 55
2.3.2.2. Protein Solubility analysis 56
2.3.2.3. Protein Isolation and Purification 57
2.3.3. Protein Analysis: Structural 59
2.3.4. Protein Analysis: Low resolution Structure/Function analysis 61
2.4. DISCUSSION 66
CHAPTER 3: ANTI-CD4 ANTIBODIES AS ALTERNATIVE HIV THERAPIES 72
3.1. INTRODUCTION 73
3.1.1. Anti-CD4 Antibodies against HIV 73
3.1.1.1. Early Development 73
3.1.1.2. Immune Suppressive Effects 74
3.1.2. Description of MHCII-TCR-CD4 interaction 75
3.1.2.1. MHCII 75
3.1.2.2. MHCII-CD4 interaction 76
3.1.2.3. MHCII-CD4-TCR Interaction 77

3.1.3. Ibalizumab: Model Anti-CD4 Antibody against HIV 79
3.1.3.1. Drug Discovery and Development 79
3.1.3.2. Epitope Mapping of Ibalizumab 81
3.1.3.3. Mechanism of Action of Ibalizumab 83
3.1.3.4. Resistance to Ibalizumab 85
3.1.4. Project Objectives 85
3.2. MATERIALS AND METHODS 87
3.2.1. Generation of Monoclonal Anti-CD4 Antibodies Producing Hybridomas 87
3.2.2. Detection of Anti-CD4 Antibodies in Hybridoma Supernatants 87
3.2.2.1. Screening against Recombinant Expressed 2dcd4 (WT) 87
3.2.2.2. Low-Resolution Epitope Mapping: Elucidation of CD4 Antibody Domain Specificities 88
3.2.2.3. CD4-Gp120 Binding Assay 88
3.2.3. HIV-1 Pseudovirion Inhibition Assay 89
3.2.3.1. Determination of Working Viral Dilution 89
3.2.3.2. Viral Assay 91
3.3. RESULTS 92
3.3.1. Screening Supernatants 92
3.3.1.1. Preliminary Binding to 2dCD4-WT 92
3.3.1.2. Interaction of CD4-MAbs with Recombinant CD4 variants 93
3.3.1.3. Binding towards Hexahistidine Tag 96
3.3.1.4. Domain Specificity 97
3.3.1.5. Analysis of CD4MAb-mediated inhibition of CD4-gp120 binding *in vitro* 98
3.3.2. Pseudovirus Inhibition Assay 99
3.3.2.1. Establishing working $TCID_{50}$ of pseudovirus 99

3.3.2.2. Preliminary Analysis of Pseudovirus Inhibition Assay 100
3.3.2.3. CD4MAb-mediated inhibition of HIV-1 pseudovirus replication 101
3.3.2.4. PBMC Assay (See Appendix D) 104
3.4. DISCUSSION 105
CHAPTER 4: CONCLUSION 108
REFERENCES 111
APPENDICES 126
APPENDIX A 127
a. For Bacterial Transformation/Culture/Plating: 127
b. For Agarose Gel Electrophoresis: 128
c. For SDS-PAGE: 128
d. For Coomassie Blue Staining and Western Blots 129
e. For Protein Isolation 130
g. For Tricine SDS-PAGE 132
h. For Mammalian Cell Cultures 133
APPENDIX B: Protocols 134
b. Plasmid extraction/Mini-Prep. (GenElute™ Plasmid Miniprep Kit, Sigma-Aldrich). 136
c. Isolation and purification of DNA (High Pure PCR product purification kit, Roche®) 137
APPENDIX C: Diagrams, Tables and Graphs 138
a) Amino acid sequence alignment of D1 (m1.1) and D2 (WT) relative to 2dCD4. 138
b) In silico derived-data of D1(m1.1)and D2 (WT) relative to 2dCD4. 139
c) Ramachandran Plots 141
d) Far-UV CD Voltage/Wavelength 142
e) Viral Inhibition with serum m79 142

f) Previous Expression of individual domains 1 and 2 of CD4 143
g) Restriction Analysis 145
APPENDIX D: PBMC-based IFN-G Stimulation Assay 146
a. Material and Methods 146
i. PBMC cell isolation 146
ii. PBMC culture and stimulation 146
iii. Assessment of supernatant inhibition of INF-γ 147
iv. INF-γ detection 148
a. Results 148
i. Preliminary analysis of inhibitory effects of CD4MAb1-40 on T-Cell activation 149
APPENDIX E: Analysis of CD4MAb-mediated inhibition of CD4-gp120 binding *in vitro*.. 152
APPENDIX F: TCID50 Calculation 153
APPENDIX G: ETHIC WAIVER 154

LIST OF FIGURES

Figure 1: Diagram of HIV particle (copied from http://www.niaid.nih.gov/factsheets/graphics/howhiv.jpg).....19

Figure 2: Molecular Structure of the first 2 N-terminal domains of Human CD4 (2dCD4) (PDB ID: 1CDJ) (Wu et al., 1996)..... 12

Figure 3: Schematic representation of the organisation of the β-strands in D1 and D2 (Taken from (Ryu et al., 1990)..... 34

Figure 4a: Diagrammatic representation of the crystal structure of core gp120 (from Kwong et al, 1998, PDB 1GC1)..... 36

Figure 5: *In silico* analysis of D1 (PDB ID: 1CDJ; Swiss-PDB Viewer v. 4.04.)..... 53

Figure 6: *In silico* analysis of D2 (PDB ID: 1CDJ; Swiss-PDB Viewer v. 4.04.)..... 55

Figure 7: Western Blot of D1 and D2..... 56

Figure 8: Protein Solubility Analysis of D1 and D2..... 57

Figure 9: Protein Washes..... 58

Figure 10: Reduced (DTT+) and non-reduced (DTT-) gels of D1 (m1.1) and D2..... 60

Figure 11: Reduced (DTT+) and non- reduced (DTT-) gels of 2dCD4 variants (WT, D1A, D2A, CΔA). Copied from (Cerutti et al., 2014). 60

Figure 12: Mt310 binding affinity to D1 (m1.1) and D2..... 62

Figure 13: Far-UV CD Analysis..... 63

Figure 14: Gp120 Binding of CD4 variants..... 65

Figure 15: Depiction of MHCII..... 75

Figure 16: Crystal structure of the MHCII-CD4 interaction, from Wang et al., 2001 (PDB 1JL4) 77

Figure 17: Crystal structure of CD4, MHCII and TCR complex, from Yin et al., 2012 (PDB 3T0E) 78

Figure 18: Immunological Synapse 79

Figure 19: Crystal Structure of the Ibalizumab Fab Fragment bound to 2dCD4, from Freeman et al., 2010 (PBD: 3O2D). 83

Figure 20: Preliminary Trial of Supernatant 1 against 2dCD4-WT (at 570nm readout)..... 92

Figure 21: Binding of hybridoma supernatant against 2dCD4 variants (450 nm readout)..... 94
Figure 22: Binding of hybridoma supernatant against 4dCD4 variants (450 nm readout)..... 95
Figure 23: Binding of hybridoma supernatants to irrelevant hexahistidine-tagged gp41..... 96
Figure 24: Domain Specificity of MAbs in the hybridoma supernatants 97
Figure 25: CD4MAb-mediated inhibition of CD4-gp120 binding in vitro. 99
Figure 26: Preliminary Viral Assay 100
Figure 27: Preliminary Analysis of CD4MAb-mediated inhibition of HIV-1 pseudovirus replication 101
Figure 28: CD4MAb-mediated inhibition of HIV-1 replication..... 104
Figure 29: Ramachandran Plots of D1 (m1.1) and D2. 141
Figure 30: CD-Analysis (V/nm) 142
Figure 31: Preliminary Analysis of CD4MAb-mediated inhibition of HIV-1 pseudovirus replication 142
Figure 33: Restriction Analysis of 4dCD4-Wt and 4dCD4-D2A in pET15b vector..... 145
Figure 34: Preliminary detection of INF- γ produced by PBMCs 149
Figure 35: Preliminary Analysis of Inhibitory effects of CD4MAb1-40 on T-Cell activation .. 151

LIST OF TABLES

Table 1: Description of CD4 variants (and abbreviations) used in this study 42
Table 2: In silico derived-data of D1(m1.1) 139
Table 3: In silico derived-data of D2 (Wt)..... 140
Table 4: Previous Expression of individual domains 1 and 2 of CD4..... 144
Table 5: *In vitro gp120 binding inhibition assay*..... 153

RECURRING ABBREVIATIONS

2dCD4: Two-domain CD4, consisting of D1 and D2

4dCD4: Four-domain CD4, consisting of D1, D2, D3 and D4

AIDS: Acquired Immunodeficiency Syndrome

BSA: Bovine Serum Albumin

CD4: Full-length 4-domain CD4 (Cluster of Differentiation 4)

Cys: Cysteine (amino acid)

D1, D2, D3, D4: Domains (Individual) 1, 2, 3, and 4 of CD4

D1 (m1.1): Mutant D1 (L5I, A55V, I76P, L96I and F98L) (Chen et al., 2011)

D2 (WT): Wild-type D2

DTT: Dithiothreitol

Env: HIV envelope

Far-UV CD: Far-UV Circular Dichroism

GSSG: Glutathione disulphide

HIV: Human Immunodeficiency Virus

IPTG: Isopropyl β-D-1-thiogalactopyranoside

LB: Luria-Broth

PBS: Phosphate Buffered Saline

sCD4: Solubilised recombinant CD4

SDS-PAGE: Sodium Dodecyl Sulphate PolyAcrylamide Gel Electrophoresis

T-TBS: Tween-Tris-buffered Saline

CHAPTER 1:
INTRODUCTION

1.1. INTRODUCTION

1.1.1. Epidemiology

According to the World Health Organisation, nearing the end of 2013, approximately 36 million people globally were infected with the **Human Immunodeficiency Virus** (HIV) (WHO_Media_Centre, 2014). The official report from the UNAIDS (2013) estimated that approximately 35.3 million [32.2– 38.8] individuals were living with the disease. The number of new HIV infections in 2012 was 2.3 million [1.9 – 2.7], which represented a 33% decrease in the incidence since the turn of the millennium. This corresponds to the improved accessibility to antiretroviral (ARV) therapy in the low- and middle-income countries (World_Health_Organisation, 2013). As a result, a decrease in the number of **Acquired Immunodeficiency Syndrome** (AIDS)-related deaths from 2.3 million [2.1– 2.5] in 2005, to 1.6 million [1.6– 1.9] at the end of 2012, was observed. In spite of the optimistic figures, HIV/AIDS remains the leading cause of death worldwide by an infectious disease (World_Health_Organization, 2014).

The prevalence of HIV/AIDS remains very high globally (World_Health_Organisation, 2013). The global burden of the disease is however unequally distributed. As reported in the 2013 UNAIDS Global Report, the Sub-Saharan African region, representing only 12% of the world's population, bears approximately 70% of the population infected with HIV. By the end of 2012, it was estimated that Sub-Saharan Africa was comprised of 25 million [23.5 – 26.6] people living with HIV, with an annual incidence of 1.6 million [1.4 – 1.8] and AIDS-related death tending to 1.2 million [1.1 – 1.3].

Nevertheless, as from 2004 – 2005, sub-Saharan Africa, amongst other low income countries, witnessed a significant decrease in AIDS-related deaths. With reduced new infections and greater access to ARV therapy, the mortality due to HIV/AIDS declined by over 50% from 2004 – 2012. For example, following introduction of ARVs in the public health system in KwaZulu-Natal (South Africa) in 2003, the adult life expectancy of the population cohort under observation (over 101,000 individuals) was increased from 49.2 to 60.5 years by 2011 (Bor et al., 2013). Behavioural changes towards safe sex (Gregson et al., 2006), voluntary medical male

circumcision (Bailey et al., 2007, Auvert et al., 2005) and most importantly, increased accessibility to treatment and ARV drugs, enlist some of the few factors that have certainly contributed towards the reversal of the trend.

1.1.2. Basics of HIV

1.1.2.1. Pathophysiology of HIV and AIDS

Infection with HIV is the cause of AIDS. The disease is characterised by the interference with the normal function, and the eventual ablation of the immune system. More specifically, the canonical hallmark of HIV/AIDS is the gradual destruction of the CD4+ T-cell population – the main HIV host cell (Douek et al., 2003). Following primary infection with HIV, the high viral load and significant reduction of peripheral blood T-cell counts correlate with an acute symptomatic phase. With restoration of the T-cell population and the maturation of an HIV-targeting immune response within the following few weeks, the virus is remarkably cleared from the peripheral blood. The period of low viraemia, during which there is the establishment of a viral reservoir, is an asymptomatic or chronic phase, with the dynamics of viral load and T-cell count determining the outcomes. Throughout, the trending decrease in peripheral T-cell count and increase in viraemia translates into the disease progression to AIDS. As defined by the WHO's clinical staging, with the CD4+ counts falling below 350 cell/µL, the progression of HIV infection becomes increasingly associated with the array of AIDS-related afflictions (World_Health_Organisation, 2007).

In the immuno-compromised state the infected person is at open risk to a multitude of severe and chronic opportunistic infections and diseases (Holmes et al., 2003). In 1981, when the first cases of AIDS were being reported in homosexual men and intravenous drug abusers in the U.S., the patients presented with a form of pneumonia caused by *Pneumocystis carinii*, a fungal infection which typically affects only severely immuno-compromised individuals (Gottlieb, 2006). Tuberculosis, caused primarily by *Mycobacterium tuberculosis*, is heavily associated with HIV/AIDS, particularly in developing countries like South Africa (Corbett et al., 2003). As well as increasing the risks of developing the disease, the positive HIV/AIDS status significantly

contributes to the reactivation of latent tuberculosis (McShane, 2005), and rapid disease progression (Daley et al., 1992). The African continent is faced with a worsening dual disease burden as nearly 93 % of new TB cases occurred in patients with an underlying HIV infection (World_Health_Organisation, 2011). Additionally, the HIV/AIDS condition is marked with increased susceptibility to *Salmonella* enteritis and acute diarrhoea, pneumococcal infections, cryptococcal meningitis, oral and oesophageal candidiasis, herpes zoster and cytomegalovirus infections (Holmes et al., 2003). Malaria, yet another Africa-biased burden, indicates poor and severe prognosis in HIV immunosuppressed patients (Grimwade et al., 2004). In fact, population studies in Kenya have shown that regular malaria infections results in repeated in increases viral loads in HIV-infected patients, which is likely to contribute to the spread of HIV (Abu-Raddad et al., 2006). Karposi's Sarcoma and Non-Hodgkin Lymphoma, as well as several non-AIDS defining cancers, further contribute to the extensive list of diseases associated with HIV/AIDS (Frisch et al., 2001).

1.1.2.2. Viral Classification and Diversity

HIV is a member of the *Lentivirus* genus and part of the *Retroviridae* family. HIV is one of the most genetically diverse species. Screening samples that were collected between the years 2000 – 2007 from across the globe illustrates its extreme diversity (Hemelaar et al., 2006, Hemelaar et al., 2011). The HIV type 1 (HIV-1) strain can be categorised into four genetic groups: M (major), O (outlier), N (non-M, non-O) and P. Subsequently, the M-group, primarily responsible for the AIDS epidemic, can be re-classified into 9 subtypes (A – D, F – H, J and K). However, it is interesting to note that subtype C corresponds to almost 50 % of the global distribution, and nearly exclusively all of Sub-Saharan HIV-1 infections. Within a single subtype, genetic diversity can range between 15 – 20 %, whilst between the subtypes, the corresponding figure is 25 – 35 %. Worsening the scenario, as result of genomic intermingling between subtypes, 19 recombinant forms of the virus have been identified during the survey and to date, 72 circulating recombinant forms (CRFs) have been identified (http://www.hiv.lanl.gov). Nevertheless, HIV-1, as opposed to the rarer HIV-2 which remains confined to West Africa, is the predominant strain responsible for the pandemic (McCutchan, 2006).

1.1.2.3. Viral Genome and Structure

The genetic composition and morphology of HIV-1 has been extensively studied. HIV consists of two copies of positive-strand RNA. The relatively short genome (~10 kb), capped by LTRs (Long Terminal Repeats), can be divided into three main segments encoding key proteins: the structural components; *gag* (encoding the p24, p17, p7, p6, p2 and p1), *pol* (encoding the viral enzymes protease, reverse-transcriptase, RNAse H and integrase), and *env*, the gp120-gp41 envelope precursor gp160 (Ratner et al., 1985). Also present are regulatory (*tat* and *rev*) and accessory protein encoding genes (*nef*, *vif*, *vpu*, and *vpr*). As described from electron micrographs, the typical viral particle is spherical and approximately 145±25 nm in diameter (Briggs et al., 2003). It consists of a shortened electron dense cone-shaped core (capsid) surrounded by a host derived lipid bilayer. The lipid bilayer is studded with about 70 – 80 "spikes", consisting of knobs connected to the membrane by stalks (Gelderblom et al., 1987). Respectively, the knobs and the stalks represent trimeric gp120 and gp41 (Ozel et al., 1988). These, as described later, play vital roles in viral entry into its host cell. The most external layer of the core, made up of matrix protein (p17), is associated with the inner side of the bilayer. Capsid protein (p24), arranged as rings of hexamers, forms the capsid. The capsid encapsulates the two RNA copies. Binding tightly to the RNA, the nucleocapsid protein (p7) is important for the stabilisation of the RNA and viral assembly (Dawson and Yu, 1998). Localised within the capsid are the enzymes reverse-transcriptase, integrase and protease, critical for viral replication. Additionally, the capsid encloses several accessory proteins (Vpu,Vif, Vpr and Nef) which are involved in a multitude of roles that ensure viral survival, replication and maturation (Malim and Emerman, 2008).

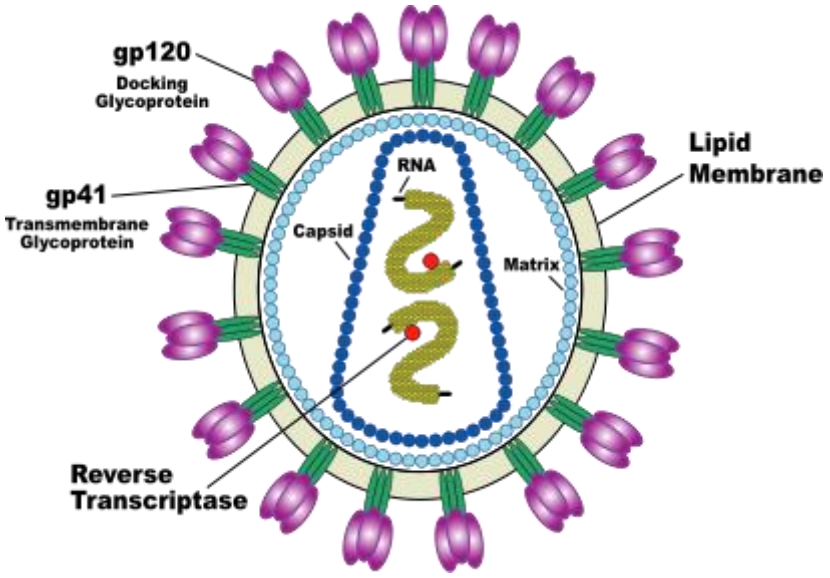

Figure 1: Diagram of HIV particle (copied from http://www.niaid.nih.gov/factsheets/graphics/howhiv.jpg)

1.1.2.4. Life-Cycle and Replication

HIV infection begins with the attachment of the viral envelope glycoprotein gp120 to host cell CD4 receptors, and subsequent interaction between gp120 and host cell co-receptors (CCR5 or CXCR4). As discussed more extensively in the following section, a series of events involving the viral envelope – host cell receptors' interaction lead to viral entry into the host cell. Within the cytoplasm, following the dismantling of the virion core, viral reverse transcriptase (RT) reverse transcribes and converts the viral RNA into linear double-stranded cDNA (Sarafianos et al., 2009). Assisted by integrase, the proviral cDNA is transported into the nucleus, and is inserted into gene-rich regions of the host genome (Schroder et al., 2002). Initially transcribed along with host transcription events, the gradual accumulation of accessory protein Tat (Trans-Activator of Transcription) directs the intensive transcription of the viral DNA (Debaisieux et al., 2012). Subverting the host cell transcription and translation machinery, all the viral proteins and genomic RNA are produced. Throughout, accessory proteins participate in a number of tasks that ensure the survival and assembly of the virion particle. A function of Vpu (Viral protein U) involves the formation of conductive ion pores on the host cell surface membrane to favour viral release and budding (Schubert et al., 1996). Viral proteases cleave the Gag-Pol polypeptide into

its functional components, and therefore participate in the finalisation of the mature virion (Nicholson et al., 1995).

After integration of viral DNA into the host cell genome, HIV is capable of entering the so called 'latent' state, a state of viral dormancy during which active viral replication is interrupted (Siliciano and Greene, 2011) Following immune activation by antigen-presenting cells, a small number of activated CD4+ T-cells revert to the resting (Go) state, and persist as long-lived memory cells. HIV contained within memory cells in the form of stably integrated DNA escapes canonical humoral and cell-based immune surveillance mechanisms, and these provide an important reservoir that sustains the emergence of viral quasi-species (Chun et al., 1997, Chun et al., 1995, Spina et al., 1997)

1.1.2.5. Viral Entry

The first step of HIV infection of host cells involves the attachment of the viral envelope gp120 to its primary receptor, CD4. As correctly presumed from early electron microscopy studies, "knob on stalk" structures coating the virion are the envelope glycoproteins gp120-gp41 trimeric heterodimers (Ozel et al., 1988, Gelderblom et al., 1987). With recent cryo-electron tomography analysis, the arrangement of trimeric gp120-gp41 heterodimers with the surface glycoprotein gp120 attaching non-covalently to the membrane spanning glycoprotein gp41 was reinforced (Liu et al., 2008, White et al., 2010). The structure of gp120 consists of five constant (C1-C5) and five variable regions (V1-V5) (Kwong et al., 1998). The core structure of gp120 (lacking V1 – V3), folding into a globular structure, comprises 25 β-strands, 5 α-helices and 10 loop segments. The overall structure is considered as an inner and outer domain, linked by a four-stranded "bridging sheet". The depression located at the interface of the two domains with the bridging sheet forming the CD4 binding site. Closer inspection of the binding site indicates two cavities into which the CD4 molecule inserts. The placement of CD4 into its binding site consequently leads to the occlusion of the gp120 binding site by Phe^{43} of CD4, which critically assists in stabilising the CD4-gp120 interaction.

Following the binding of the CD4 to its corresponding binding site, the gp120 undergoes conformational changes leading to exposure of several conserved sites on the gp120 termed CD4-induced binding sites (CD4i), including the highly-conserved co-receptor binding site (either CCR5 or CXCR4) (Rizzuto et al., 1998). Conformational changes occurring in CD4 as well, lead to the approach and re-orientation of the gp120 co-receptor binding site to its target (Yachou and Sekaly, 1999). The protruding N-terminus and extracellular loops of the transmembranal co-receptor procure the contact points for the gp120 interaction (Lee et al., 1999a). Additionally, the negatively charged nature of the N-terminus of the coreceptor is suspected to participate in electrostatic interactions with the positively charged residues of the V3 loop of gp120 (Kwong et al., 1998).

The core structure of gp41 consists of a bundle of three α-helical strands organised as a trimeric rod (Weissenhorn et al., 1997). From proximal to distal of the viral membrane, each of the strands in turn contains a regular α-helix and leucine zipper-like region. Capping the extremity of the latter, are the fusion domains. Upon co-receptor binding, conformational changes induced in the gp120 exposes the gp41. HIV entry at this stage is suggested to follow a similar mechanism as that of the "spring-loaded" fusion in *Influenza* (Carr and Kim, 1993). The fusion domains of the gp41 are extended towards the host cell membrane where contacts are made. Subsequently, the α-helices and leucine zipper-like domains complex to each other and form a six-helix bundle. In the process, as the result of the overall contraction of the structure the viral and host membranes are brought close to each other. Several such gp41 interactions eventually lead to the fusion of membranes, and hence the formation of fusion pores. The viral core can therefore access the host cell cytoplasm.

1.1.3. Current Antiretroviral Treatment and Prevention Strategies

1.1.3.1. Approved Anti-HIV Drugs

The multistage life-cycle of HIV offers a number of targets for drug-induced disruption. Since Zidovudine, the first antiretroviral drug approved for HIV treatment in 1987, at least 25 other anti-HIV drugs have been approved for clinical use (De Clercq, 2009, AIDSinfo, 2014).

The different drugs operate by various modes of actions. Several of them inhibit the normal functioning of viral reverse transcriptase (RT). These are consequently re-categorised as nucleoside RT inhibitors (NRTIs), nucleotide RT inhibitors (NtRTIs) and non-nucleoside (NNRTIs). NRTIs (zidovudine, didanosine, zalcitabine, stavudine, lamivudine, abacavir and emtricitabine) and NtRTIs (tenofovir), when converted to the active forms, essentially act as competitive inhibitors of dideoxynucleotides, the building blocks of viral DNA. The use of the analogues results in the premature termination in the elongation of the viral DNA. The NNRTIs (nevirapine, delavirdine, efavirenz and etravirine) bind to a non-catalytic site, which consequently due to an allosteric effect, leads to the inactivation of RT. As expected, integrase inhibitors (INIs; raltegravir, elvitegravir) and protease inhibitors (PIs; saquinavir, ritonavir, indinavir, nelfinavir, amprenavir, lopinavir, atazanavir, fosamprenavir, tipranavir and darunavir) target the corresponding enzymes. The fusion inhibitor Enfuvirtide, that blocks viral entry by interfering with the functionality of gp41, provides another mechanism of viral inhibition (Matthews et al., 2004).

Maraviroc is CCR5-specific antagonist which inhibits infection of CCR5-dependent (R5) viruses (Dorr et al., 2005). Functional and structural studies of CCR5 chemokine receptor in complex with Maraviroc provided further evidence of the role of the drug as a viral fusion inhibitor (Dorr et al., 2005, Tan et al., 2013). It is being suggested the small molecule Maraviroc, acting as a non-competitive inhibitor, binds to a region of CCR5 that is distinct from the binding site of viral gp120 (Garcia-Perez et al., 2011, Tan et al., 2013). Thus, Maraviroc is of particular interest in this project as it provides a certain proof of concept in finding an equivalent antibody against (the host factor) CD4, which is non-toxic and capable of inhibiting HIV infection.

1.1.3.2. Antibody Development against HIV

HIV vaccine research has focused extensively on raising antibodies against exposed, structurally conserved epitopes on the envelope glycoprotein. A key research tactic (reverse vaccinology) involves the identification of broadly neutralising antibodies (bNAbs) that can inhibit conserved functional epitopes of the viral envelope glycoprotein across all of the clinically relevant HIV strains (Trkola et al., 1995). The epitope of IgG1b12, the first bNAb to be recognised (Burton et

al., 1994, Burton et al., 1991), was found to overlap the CD4 binding site on gp120 (Roben et al., 1994). As visualised from the crystal structure of b12, a protein loop of the antibody (termed CDRH3) is capable of occupying the depths of the CD4 binding site (Saphire et al., 2001). Another bNAb, 2G12 recognises a carbohydrate-enriched region on the outer surface of gp120 (Calarese et al., 2005). The 447 – 52D monoclonal antibody targets the GPGR residues of the gp120 V3 loop (Stanfield et al., 2004). By contrast, the antibody 2F5 targets a conserved epitope on the gp41 (Muster et al., 1993). Further anti-gp41 monoclonal antibodies such as Z13 and 4E10 have been generated and characterized (Zwick et al., 2001). Exposure of CD4i epitopes provides additional binding targets for antibodies. The crystal structure of the Fab fragment of the 17b antibody in conjunction to CD4-bound gp120, showed that its binding site on gp120 is located on the bridging sheet and V1 – V2 loops (Kwong et al., 1998). The region closely corresponds to the co-receptor binding site. *In vivo* experiments involving passive immunisation with several of such antibodies, have provided strong evidence that the correct anti-HIV antibody present in sufficient quantity would be able to protect against HIV infection (Shibata et al., 1999, Gauduin et al., 1997, Mascola et al., 2000).

Within the last five years, there has been an explosion in the number of newly identified bNAbs (Eroshkin et al., 2014). PG9 and PG16, two somatically-related bNAbs which target V1 – V3 region of g120, were recognised from an infected individual and could neutralise 70 – 80% of viral isolates (Walker et al., 2009, Doores and Burton, 2010). VRC01, acting as a CD4 mimic, binds to the CD4bs of gp120 and thus sterically restricts viral attachment to CD4 (Zhou et al., 2010). The PGT group of antibodies, similarly to 2G12, targets glycans of gp120 (Pejchal et al., 2011). BNAbs develop in a HIV-infected individual (Richman et al., 2003, Doria-Rose et al., 2009), and thus thanks to the advancement of high-throughput screening technology, these could be identified. As well as identifying new bNAbs, high-throughput screening, coupled with sequencing and mathematical models, are being used to understand the development of the antibodies (Simek et al., 2009, Sather et al., 2009, Wu et al., 2011, Doria-Rose et al., 2010). By regression of the somatic hypermutation pathway, it would be possible to identify the HIV immunogen that elicited the bNAb. Thus, such studies would assist in the rationale vaccine design (Stamatatos et al., 2009).

1.1.3.3. The Problems with Antibody-Based HIV Treatments

It has been nearly 30 years since the discovery of HIV/AIDS and yet, no efficient vaccine has been developed. Several reasons, pertaining to viral biology, the immune system, and the interplay of the two, have been described for the failure. An excellent review which by D. R. Burton *et al*.(2012) provides the extensive details on issues relating to HIV vaccine development (Burton et al., 2012a). Here, a brief overview of the main problems associated with the development of vaccines and antibody treatments against HIV shall be described.

1.1.3.3.1. HIV Diversity and Rapid Mutation Rates

As mentioned previously, HIV is extremely diverse. The different HIV strains, subtypes and CRFs, display variable immunogenicities, pathogenesis and transmission characteristics. Consequently, this poses major obstacles in the diagnostics, prognostics, and most importantly, vaccine and drug development (Boutwell et al., 2010). The highly imprecise nature of the reverse transcriptase (RT) is considered as a main cause of such diversity (Korber et al., 2001). Coupled with a rapid replication rate, from a single homogenous HIV population following infection, a wide-distribution of genetically varied quasispecies arises. A study involving the monitoring of the C2 – V5 region of gp120 during the course of HIV infection, exemplified such divergence and diversification of a founder HIV population, to the point that there was the establishment of CXCR4 co-receptor-dependent HIV population (Shankarappa et al., 1999). In fact, it is being shown that most HIV clinical infections occur due a single founder virus (Keele et al., 2008, Salazar-Gonzalez et al., 2008). Ultra-deep sequencing provided further evidence of viral diversification which arises from a single virus within the only few weeks following infection (Fischer et al., 2010). It can be theorised that under the selective pressure of the immune system, micro-evolution pushes HIV towards resistant strains (Wolinsky et al., 1996). For instance, by tracking the changes in the genome of HIV during early infection in patients, it was observed that low neutralising antibody titres allowed for selection and escape of HIV resistant strains (Bar et al., 2012). Similarly, neutralising antibodies produced by HIV-infected patients drove the emergence of resistant strains for as long as 10 years after of initial infection (Chaillon et al.,

2012). Such mutations, translated as amino acid changes in the viral envelope, imply that critical epitopes can subsequently go unrecognised by cellular and humoral immune responses.

1.1.3.3.2. Inaccessible Neutralizing Epitopes on the Envelope Glycoprotein

Another important mechanism of immune evasion involves the inaccessibility of neutralising epitopes on Env (Johnson and Desrosiers, 2002). Several such epitopes remain buried at the core of the viral envelope and are only exposed transiently during the course of viral entry as a result of induced conformational changes. Whilst antibodies are produced in HIV-infected patients, these generally however target the exposed variable regions, rather than the conserved, recessed regions on gp120, leading to very restricted strain-specific neutralisation (Burton et al., 2012b). Furthermore, the heavily glycosylated variable loops of gp120, often blamed for concealing the more conserved regions (Poignard et al., 2001, Johnson and Desrosiers, 2002), are therefore a reason for the inability to develop efficient bNAbs. It is estimated that 50 % of the gp120-gp41 molecular weight is attributed to the associated carbohydrates. In effect, the viral envelope is coated with a dense "glycan shield" that blocks antibody interaction with underlying epitopes (Wei et al., 2003). It is interesting to note that the CD4-binding site of gp120 lacks oligosaccharides (Kwong et al., 1998). It is however protected by the shielding variable loops, which in addition, are glycosylated. Artificially altering the positions or removal of the oligosaccharides of the V1 or V3 loop dramatically increased the sensitivity of the virus to antibody neutralisation (Back et al., 1994, Overbaugh and Rudensey, 1992, Koch et al., 2003). Certain antibodies, such as 2G12, however, can actually recognise and bind to the carbohydrates on gp120 (Calarese et al., 2003). More recently, the PGT group of antibodies could bind directly to the glycans and many within this group are capable of potent, cross-clade neutralisation (Pejchal et al., 2011). Nevertheless, it has been shown that the glycan layer is not static, but changes throughout the course of viral infection (Overbaugh and Rudensey, 1992, Moore et al., 2012, Wei et al., 2003). To illustrate this, a study demonstrated that within 6 months of infection, a shift in the position of a critical glycan molecule on gp120 resulted in HIV resistance to PGT128 (Moore et al., 2012).

1.1.3.3.3. The Envelope Glycoprotein as an Immune Decoy

Many vaccine studies have focused their attention on monomeric forms of recombinant gp120. A large number of antibodies binding to gp120 have been generated in small animals, non-human primates as well as humans, but very few, if any, have a neutralising effect against clinically relevant HIV. One of the reasons for this is the existence of two "faces" on gp120: termed the 'neutralising' and 'non-neutralising' face (Moore and Sodroski, 1996). As their name suggests, the neutralizing face contains conserved epitopes which could elicit bNAbs, while no known bNAb epitopes exist on the non-neutralizing face. Further studies eventually lead to the conclusion that the neutralising and non-neutralising characteristics of gp120 relate to the positioning of its faces in the native state (Poignard et al., 2001, Johnson and Desrosiers, 2002). Considering that the gp120-gp41 heterodimer exists as a trimeric structure in the native state (Liu et al., 2008) it is now known that the neutralising face represents the exposed surface of the viral envelope, whereas the non-neutralising face represents the surface hidden within the trimer. Based on gp120 dissociation after co-receptor binding and the establishment of the gp41 fusion-hook, it is interesting to note that both the neutralising and non-neutralising faces are exposed (Parren et al., 1997). Hereafter, any antibodies directed towards the shed gp120 will unlikely target the conserved bNAb epitopes on the virion, since the conformations and exposed sites are different. Thus, the shed gp120 acts as an immune decoy, and these antigenic baits provide another mechanism of HIV escape from neutralising antibodies.

1.1.3.3.4. Extensive Somatic Hyper-mutation

With increasing usage of high-throughput antibody screening and sequencing approaches, a number of novel bNAbs have been identified in HIV-infected individuals (Walker et al., 2009, Zhu et al., 2013, Johnson et al., 2009). However, these mature bNAbs only come to existence after extensive somatic hypermutation in some of the chronically infected HIV individuals (Haynes et al., 2012, Verkoczy et al., 2011). Understanding the development of the antibodies and recognising the immunogen precursor that elicited such response would be of immense help in rationale vaccine design (Simek et al., 2009, Sather et al., 2009, Wu et al., 2011, Doria-Rose et

al., 2010). However, directing guided evolution of the antibody remains a complex task due to the number of variables that affect somatic hyper-mutation evolution (Gray et al., 2009, Piantadosi et al., 2009, Sather et al., 2009). For instance, following an analysis of over a hundred patient sera against several clinical features, it was shown that neutralisation breadth correlated only with viraemia, and 20% of these sera could be qualified as bNABs (Doria-Rose et al., 2010). Elsewhere, it is indicated that additionally, the generation of potent bNABs is influenced by length of time since the patient was infected and the binding avidity of the early antibodies against viral envelope (Sather et al., 2009). Moreover, it has also been suggested the development of bNABs has to be triggered during early infection (Piantadosi et al., 2009). Taken together, a number of studies suggest that the generation of bNABs in a patient begins from an early unmutated germline antibody with strong affinity to CD4-binding site of viral envelope that goes through a lengthy and complex maturation process, whilst being continuously exposed to heterogeneous viral antigens (Zhou et al., 2010, Xiao et al., 2009, Wu et al., 2010, Wu et al., 2011, Kwong and Mascola, 2012, Liao et al., 2013). Recently, the evolution and structure determination of mature CD4-binding site CH103 antibody, which could neutralise about 55% of HIV-1 strains, provides critical information on the pathway for maturation and the structural characteristics that bNABs require (Liao et al., 2013).In the future, with more studies, it might be possible to indentify the exact requirements for the development of potent bNABs against HIV (Burton et al., 2012a).

1.1.4. Project objectives

Targeting the HIV envelope glycoprotein with vaccine induced neutralizing antibodies has remained a major focus of biomedical preventative HIV research. The identification of novel neutralising antibodies through the mass screening of HIV infected sera, has provided a recent boost of optimism in the field individuals (Walker et al., 2009, Zhu et al., 2013, Johnson et al., 2009). However, it still remains that with the evolving nature of HIV and due to the extensive degree of somatic hyper-mutation required for the generation of mature bNAb, the development of a successful HIV vaccine remains difficult. An alternate school of thought to overcome this issue and prevent viral entry involves targeting the host cell receptors and co-receptors that are

employed by the virus during entry. Accordingly, in this project we have generated a panel of monoclonal anti-CD4 antibodies that are capable of inhibiting HIV infection, and defined their binding specificities at the domain level.

In chapter 2, after a detailed description of CD4, we describe the generation of recombinant bacterially expressed individual domains 1 and 2 of CD4. We began by designing the expression cassettes encoding the respective domains and proceeded to express, purify and characterise purified proteins biochemically. Here, we showed that proteins were stable and exhibited correct disulphide pairing. In chapter 3, using the purified individual domains of CD4 as part of ELISA assays, we were able to define the domain-specificities of a panel of anti-CD4 monoclonal antibody-containing hybridoma supernatants. We then confirmed the antiviral properties of the hybridoma supernatants *in vitro* using recombinant gp120, and finally, in cell culture using pseudovirus inhibition assays.

CHAPTER 2:
THE CD4 RECEPTOR

2.1. INTRODUCTION

Human CD4 plays a canonical role in the infection of HIV as the primary receptor for the viral surface glycoprotein gp120. Recent structural and biophysical data have suggested that CD4 plays a more active role in HIV entry than simply acting as a viral docking site. These data have revealed that CD4 is a dynamic and conformationally-active molecule that plays a major role in viral infection. In this chapter we introduce the structure, biophysics and basic biology of CD4, before describing the production of a panel of recombinant CD4 variants, which have been used as tools for generating novel candidate therapeutic monoclonal antibodies against HIV.

2.1.1. General Overview

The human T-cell surface glycoprotein cluster of differentiation 4 (CD4; previously T-cell surface antigen T4/Leu-3), is encoded by the CD4 gene, which is located on the forward strand of chromosome 12 (Ensembl Transcript ID: ENST00000011653). The 3114 base transcript is spliced into 10 exons, which upon translation produces a polypeptide of 485 amino acid residues (Ensembl Protein ID: ENSP00000011653). The polypeptide precursor has a molecular weight of 51,110.54 g/mol (~51 kDa), and an average residue weight of 111.595 g/mol. The unprocessed CD4 polypeptide contains a signal peptide (hydrophobic NH_2 – terminal domain, residues 1 – 25) while the mature CD4 polypeptide comprises residues 26 – 458. The actual polypeptide can be further divided into three regions: the extracellular (residues 26 – 396), transmembranal (residues 397 – 418), and cytoplasmic (residues 419 – 458) regions. Starting most distal from the cell surface membrane, the extracellular region contains four distinct domains: domain 1 (D1, residues 26 – 125), domain 2 (D2, residues 126 – 203), domain 3 (D3, residues 204 – 317) and domain 4 (D4, residues 318 – 374). Post-translational modifications include two lipidation sites (S-palmitoyl cysteine; Cys^{419}, Cys^{422}), two glycosylation sites (N-linked acetylglucosamine; Asn^{296}, Asn^{325}), and critically, as will be described in detail in subsequent sections, three potential disulphide linkages (Cys^{41} – Cys^{109}, Cys^{155} – $Cys^{184,}$ Cys^{328} – Cys^{370}). Following post-translational modifications, CD4 has a relative molecular weight of 55,000 g/mol (~55 kDa).

2.1.2. Function of CD4

Although canonically located on CD4+ T-cells (Maddon et al., 1985), the CD4 receptor is also present on dendritic cells (Patterson et al., 1995), macrophages (Lee et al., 1999b) and natural killer cells (Bernstein et al., 2006). The role of CD4 on non-T-cells remains largely unknown. However, recent evidence indicates that CD4 on non-T-cells are involved in roles other than the 'immunological synapse'. For instance, following ligation of CD4 on activated natural killer cells, CD4 has been shown to mediate the migration of the cells towards CD4-specific chemotactic factor IL-16, and induce cytokine expression (Bernstein et al., 2006).

Under normal physiology, the CD4 receptor located on T-cells, plays a fundamental role in the formation of the immunological synapse between the antigen presenting cells (APCs) and T-cells (Sweet et al., 1991, Bromley et al., 2001). During infection, as part of the innate immune response, APCs such as macrophages and dendritic cells phagocytose the invading pathogen. The phagocytosed material is digested intracellularly, with constituent proteins being cleaved to small peptides. These peptides associate with major histo-compatibility complex class II (MHCII) molecules, which are transported to the cell surface where the MHCII is embedded/inserted into the cell surface membrane. The MHCII thereby presents the peptide to circulating T-cells. T-cells bind to peptide-MHCII complexes via the T cell receptor (TCR), and recognise the peptide as foreign. This interaction and the resulting transduced signal is however weak. The immunological synapse is stabilised and transduced signal reinforced by the CD4, which binds to MHCII following the initial, kinetically 'loose' association between the TCR and MHCII. The co-stimulatory effect can be explained by the activation of tyrosine kinase $p56^{lck}$, an enzyme which is associated with the cytoplasmic domain of the CD4. The phosphorylation events initiated by the $p56^{lck}$ lead to a molecular cascade, which in turn ultimately results in activation of the T-cell and the release of immunostimulatory cytokines. Amongst their various targets, the cytokines activate β-cells into the production of antibodies, a defining feature of the adaptive immune response. For an extensive description on the role of CD4 T-cell in antigen recognition, the review by Merwe and Davis should be consulted (van der Merwe and Davis, 2003).

2.1.3. Structure of Extracellular CD4

The structure of the extracellular domain of CD4 has been extensively investigated. The crystal structure of the first two domains (2dCD4, Figure 2), which wholly contains the contact points for both MHCII and HIV-1 gp120, revealed a rod-shaped structure comprising two distinct but closely associated immunoglobulin-like domains linked by a flexible β-strand. (NOTE: Residue numbers are with reference to the 2dCD4 and NOT full length CD4) (Ryu et al., 1990, Wang et al., 1990). The surfaces of the relatively large solvent inaccessible interdomain regions are essentially hydrophobic.

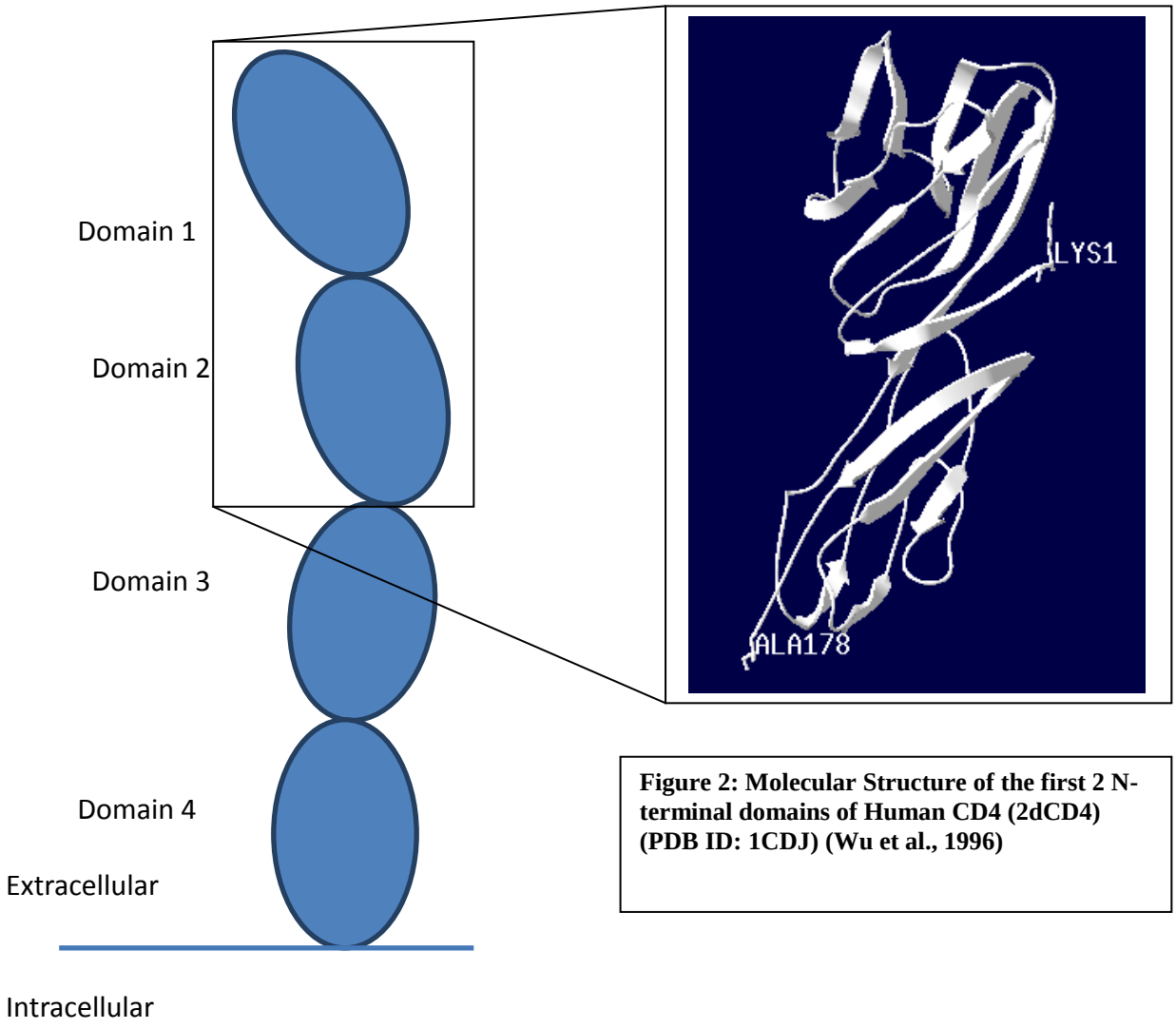

Figure 2: Molecular Structure of the first 2 N-terminal domains of Human CD4 (2dCD4) (PDB ID: 1CDJ) (Wu et al., 1996)

CD4 domain 1 (D1, residues 1 – 98) is made up of nine anti-parallel β-strands organised as a two β-sheet layer sandwich with Greek key topology (Ryu et al., 1990, Wang et al., 1990). In this way, D1 - and indeed all 4 extracellular domains of CD4 – are structurally homologous to variable immunoglobulin (IgV) domains, and the β-strands are defined accordingly: strands A, C, C', C", F and G form the one layer of the β-sheet sandwich, whilst strands B, D and E form the other layer (Figure 2). An extensive network of hydrogen bonds link the anti-parallel strands, which encapsulate a hydrophobic core. In D1, as for the typical IgV domain, the presence of the disulphide bond between Cys^{16} – Cys^{84} and the conserved Try^{28} (tryptophan) is noted. Conversely, there are two important differences in the structure of D1 and a typical IgV structure. Firstly, the C'C" loop of D1, corresponding to the complementarity-determining region 2 (CDR2) of antibodies is abnormally long. Secondly, the loops CC' and FG of D1, corresponding respectively to the CC' and CDR3, are on the other hand, shortened. This second difference correlates with the function of the loops in heavy- and light- chain (V_H - V_L) association, a feature which is relevant only for antibodies.

Domain 2 (D2), as a direct continuation of D1 from residues 99 – 173, is in turn made of seven anti-parallel β-strands (Ryu et al., 1990, Wang et al., 1990). The folding pattern of D2 follows a topology resembling that of constant immunoglobulin domain (IgC). Similarly, the strands of β-sheets are ascribed the same nomenclature. The strands A, B and E comprise one of the β-sheet sandwich layers, and strands C, C', F and G form the other (Figure 3). However, several striking differences are noted in D2 when contrasted to the typical IgC domain. The most apparent feature is the small size of D2 (75 residues), as opposed to the IgC or the other domains of CD4 (~100 residues). As a result, the lengths of the β-strands are considerably shorter. Another difference is that the C' strand of D2, corresponding to the D strand of IgC, is contained in the β-sheet that comprises of strands C, F and G. The D strand in the typical IgC is by contrast found in the β-sheet that includes itself (the D strand), E, B and A strands. In that regard, the hydrogen bond association between C' and C of D2 in the corresponding β-sheet layer resembles the IgV instead of IgC (Figure 2). Finally, a critical difference between D2 and the typical immunoglobulin-fold structure is the presence of respective intra- as opposed to inter sheet disulphide linkages. The disulphide bond formed by the residues Cys^{130} – Cys^{159} interlinks strands C and F of the same sheet. In subsequent sections, a more elaborate discussion of the nature, importance and possible functional implication of this disulphide bond will be discussed.

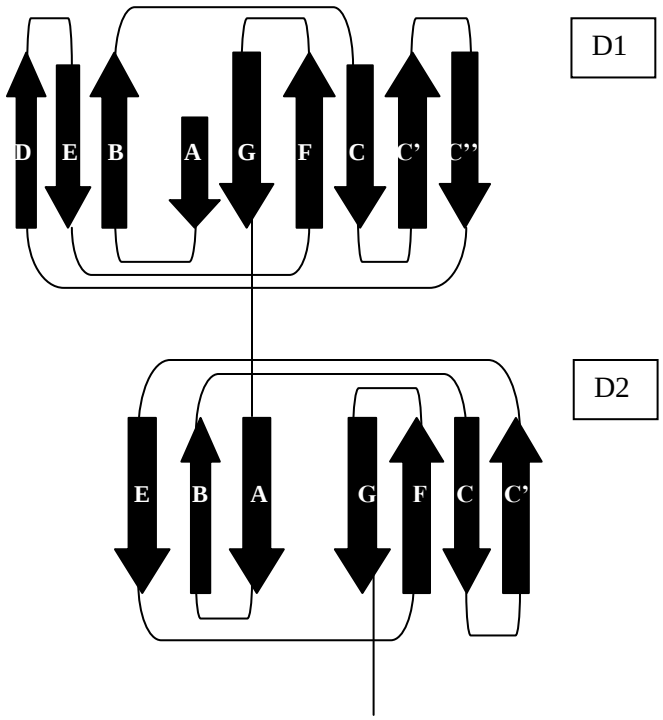

Figure 3: Schematic representation of the organisation of the β-strands in D1 and D2 (Taken from (Ryu et al., 1990)

Domain 1 (D1),

Domain 2 (D2),

Variable Immunoglobulin domain (V) and,

Constant Immunoglobulin domain (C)

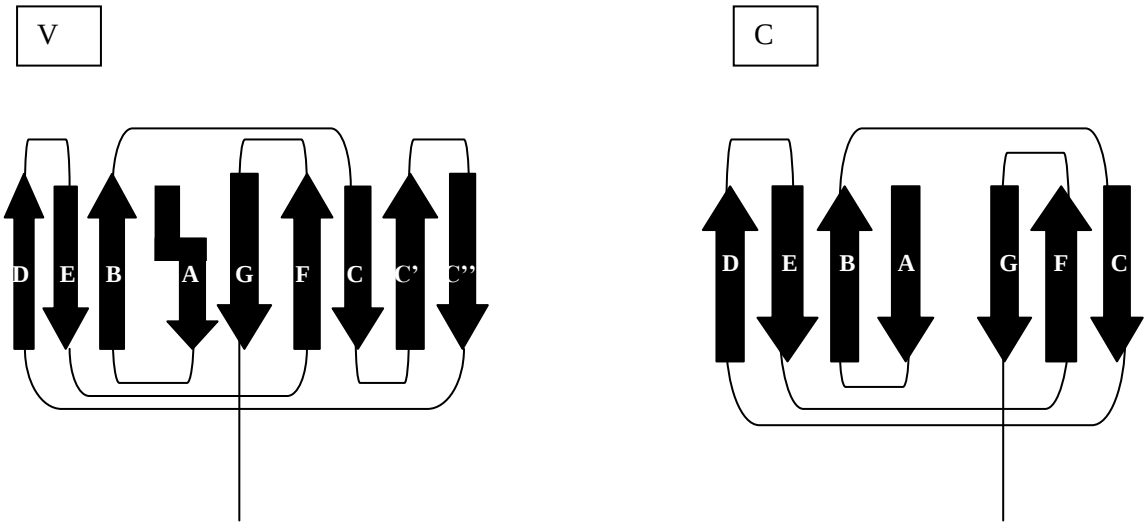

The crystal structure of full length sCD4 (1WIO) reveals an elongated, rod-like structure comprised of 4 distinct domains (Wu et al., 1997). As expected, a single strand, the direct continuation of strand G of D2 into strand A of D3, links the two domains. Similarly to the interface of D1 – D2, surfaces forming the D2 – D3 interface are solvent inaccessible and highly hydrophobic. Significantly, an obtuse angle of 140^{o} is observed between the D1D2 (domain 1, domain 2) and D3D4 (domain 3, domain 4). Such a wide angle is suggested to be related to junctional flexibility between D1D2 and D3D4.

2.1.4. The CD4-Gp120 Interaction

As the primary complex formed during contact between HIV and host target cells, the CD4-gp120 interaction has been studied extensively (Kwong et al., 1998). CD4 inserts into a depression in the gp120 formed at the interface of the inner and outer domains, with the bridging sheet on gp120 stretching in between (Figures 4a, b). The depression can be divided into two cavities. The larger of the two cavities (279 $Å^3$) fits the CC'C" strands of domain 1 of CD4, whereas the smaller cavity is occluded by the large ring structure of residue Phe^{43} (phenylalanine, position 43) of CD4. In general, there is good electrostatic complementarity between the contacting surfaces of CD4 and gp120, with the electro-positive apex of D1 fitting into the electro-negative cavity of gp120. Despite the relatively large surface area that is occupied during this interaction (742 $Å^2$ of CD4, 802 $Å^2$ of gp120), only 22 CD4 residues make direct contact with 26 gp120 residues. These interactions include stabilising Van der Waal's forces and hydrogen bonds. Residues 25 – 64 of CD4 provide the bulk of the binding surface on CD4 and interact with several segments of gp120. The most critical residues on CD4 are Phe^{43} and Arg^{59}. These are involved in a number of contacts with well-conserved residues of gp120: Asp^{368} (Aspartic acid, position 368), Glu^{370} (Glutamic Acid, position 370) and Trp^{427} (Tryptophan, position 427). To exemplify, 63 % of all of the bond interactions between CD4 and gp120 result from the short stretch of residues 40 – 48 (of the CC'C" strands of domain 1 of CD4). Furthermore, 23 % of these bond interactions between CD4 and gp120 arise due to Phe^{43}.

Presumably, sterically inhibiting those aforementioned critical residues would directly prevent the gp120-CD4 interaction.

Figure 4a

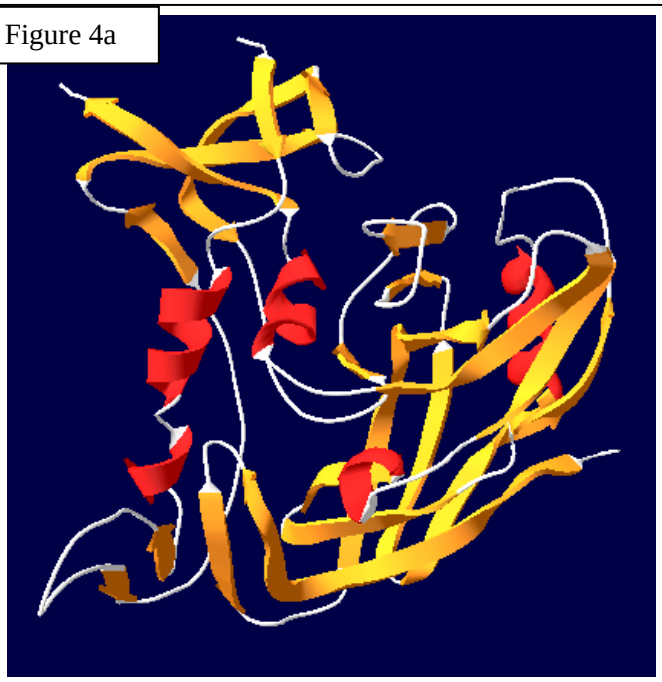

Figure 4b

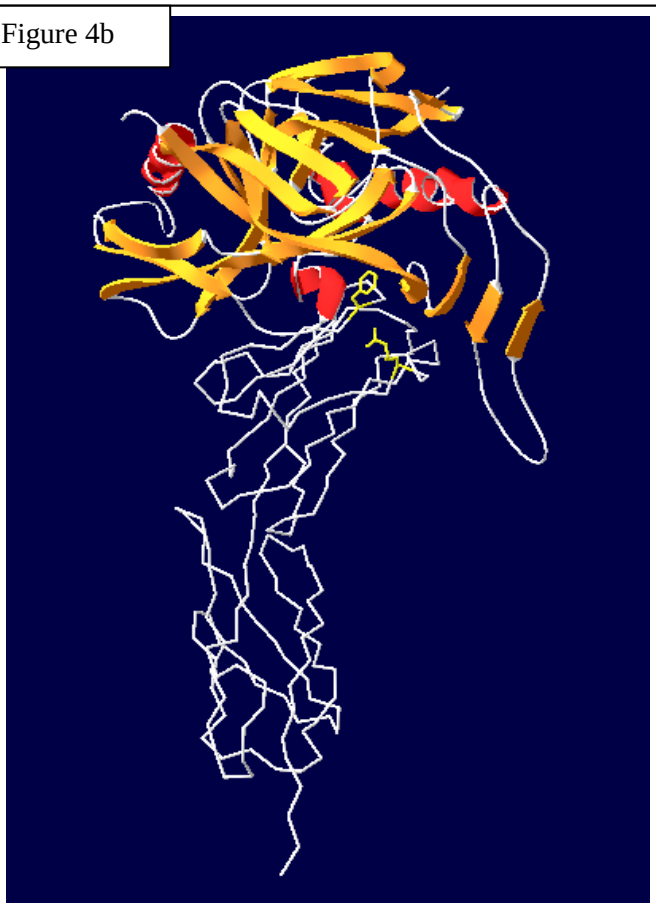

Figure 4a: Diagrammatic representation of the crystal structure of core gp120 (from Kwong et al, 1998, PDB 1GC1)

Figure 4b: Crystal structure of the gp120-2dCD4 complex shown in ribbon format. (PDB 1GC1)

D1 of CD4 fits into the larger pocket created by the inner and outer domains of gp120. Phe43 and Arg59 of CD4 (shown) are involved in the most critical contacts with gp120.

2.1.5. Conformational Changes in CD4

Upon comparison of the crystal structures of CD4 in the unbound (Ryu et al., 1990, Wang et al., 1990) and gp120 bound states (Kwong et al., 1998), CD4 did not seem to undergo conformational changes. In terms of thermodynamics, the CD4-gp120 interaction results in significantly large enthalpy and entropy changes (Myszka et al., 2000). This suggests that the majority of conformational changes that occur during CD4-gp120 binding occur on gp120. Such data coincide with the exposure of CD4-induced (CD4i) epitopes on the gp120 that are recognised preferentially by certain anti-gp120 antibodies (17b, 48d, A32) following gp120-CD4 complex formation (Wyatt et al., 1995).

However, it has been shown that just as with gp120, CD4 undergoes conformational changes upon gp120 binding (Denisova et al., 1997). Analogously, there is the exposure of previously concealed epitopes on CD4 that are recognised by anti-CD4 antibodies in the gp120-CD4 complex (Denisova et al., 1997). In order for the gp120 to make contact with the co-receptor, it has long been theorised that upon binding to gp120, CD4 must undergo considerable conformational change. A particularly interesting feature in that regard is the wide angle between the D1D2 and D3D4 (Wu et al., 1997). With a single strand connecting the two domains, a potentially large "jack-knife" rotation about the D2 – D3 junction could be possible (Ashish et al., 2008). It has therefore been proposed that the D2 – D3 junction acts as a hinge which serves to bring the entire virion closer to the host cell following CD4-gp120 binding. However, with the depiction of CD4 as a rigid molecule in X-ray crystallographic images of full length CD4 in the ligand-bound state, the "jack-knife" rotation about D2 – D3 remains questionable (Freeman et al., 2010). A more likely hinge region may be located at the base of the CD4, between D4 and the transmembranal portion of CD4. In support of this, deletion of the termed D4-TM (Transmembrane) was shown to reduce the capability of subsequent viral entry and fusion (Moir et al., 1996).

2.1.6. Redox Changes in CD4

A key aspect of the CD4 molecule that has been under investigation relates to dynamic redox changes incurred on resident CD4 disulphides. These redox changes are increasingly thought to represent a fundamentally important component of CD4 function, both with respect to its participation in T-cell activation and HIV entry.

2.1.6.1. The Role of Disulphide Bonds

The disulphide bond in proteins is a covalent bond between two cysteine residues. Under general circumstances, disulphide bonds are known to favour protein folding into the correct conformation. The presence of the disulphide bond lowers the entropy of the unfolded protein and thereby restricts folding towards the native form (Noiva, 1994, Thornton, 1981). Disulphides bonds are also canonically known to stabilise the structure of protein structure. For such roles, with the high bond energy associated, disulphide bonds were typically considered as stable and inert. In certain proteins however, disulphide bonds undergo cleavage and reformation as part of the normal physiology. These disulphide bonds, termed catalytic bonds, have long been identified as critical components of the function of thiol-disulphide oxidoreductases. The protein disulphide isomerase (PDI) involved in disulphide bond pairing during protein folding contains an alternating thiol-disulphide pair which allows corresponding disulphide bond formation or cleavage in substrate proteins (Sevier and Kaiser, 2002, Darby et al., 1994). Recent studies have put forward the possibility that another type of 'functional' disulphide bond, termed 'allosteric' disulphide bonds exists. Allosteric disulphide bonds are those which upon redox change are capable of initiating functionally important conformational changes in the protein (Chen and Hogg, 2006).

2.1.6.2. The Role of Disulphide Bonds in CD4

The disulphide bonds of cell surface receptors of lymphocytic populations have been shown to be susceptible to redox alterations depending on the cellular state. Activated lymphocytes, particularly B-cells, display significant increases in thiols (Lawrence et al., 1996). PDI, known to be secreted on the surfaces of B-cells (Tager et al., 1997), was effectively shown to participate in the reduction of the surface thiols (Lawrence et al., 1996).

To this end, CD4 itself has been shown to exist as both monomers and dimers on cell surfaces (Lynch et al., 2003, Matthias et al., 2002, Moldovan et al., 2002, Lynch et al., 1999), and redox exchanges involving the CD4 D2 disulphide is thought to play a critical role in regulating this isomerisation. The significance of disulphide-dependent CD4 oligomerisation is reflected by the observation that dimeric forms of CD4 are required for T-cell activation (Moldovan et al., 2002), and such dimeric forms of CD4 are linked by intermolecular disulphide bonds (Lynch et al., 1999). This suggests that active thiol-disulphide interchanges in the CD4 must occur in order to enable oligomerisation. Several reports, and most importantly from the four-domain CD4 crystal structure, suggested that the disulphide linkage arose from domain 4 of the CD4 (Lynch et al., 1999, Wu et al., 1997, Moldovan et al., 2002). More recent studies, however, have described the occurrence of the intermolecular disulphide bond between domain 2 cysteines of CD4 (Matthias et al., 2002).

2.1.6.3. Redox Changes in CD4 and HIV infection

It was also observed that lymphocytes, namely CD4+ T-cell and CD19+ B-cell populations that were derived from HIV infected patients exhibited a marked increase in reduced cell surface thiols (Lawrence et al., 1996). Whilst the over-expression of reduced thiols on the cell surface of HIV-infected lymphocytes could essentially be as a result of the activation of those cells, further studies revealed that the reduced state of thiols has critical significance in viral infectivity. Reduced, monomeric forms of CD4 have been shown to be the preferred state of the receptor for HIV entry (Matthias et al., 2010). The predominant explanation for this observation is that CD4 occurs in a conformation that enhances viral entry. Although, the detailed intricacies of these

conformational changes are remain elusive, there is strong evidence that they arise from redox alterations in the disulphide bond of domain 2 of CD4 (Matthias et al., 2002, Cerutti et al., 2014).The importance of the state of the disulphide bond of CD4 for gp120 binding was most recently demonstrated in our laboratory using recombinant two-domain CD4 fragment 2 (Cerutti et al., 2014).

2.1.7. Project Objectives for this Chapter

CD4 appears to be a highly dynamic molecule whose state can have implications for both normal physiology and viral infectivity. For this part of the project, we generated the individual domains 1 (D1) and 2 (D2) of CD4. We began by designing the expression cassettes encoding the individual domains. Once generated, the codon optimised, histidine-tagged encoding cassettes were cloned into plasmid vector pET15b, which were then used to transform *E.coli* expression hosts. Once expression of the protein was optimised, the proteins were then extracted from the bacterial harvest. Upon confirming the insolubility of the proteins, chaotropic solubilisation buffer was used to complete protein extraction. Proteins were then isolated using Ni/NTA agarose and washed accordingly. Following elution, proteins were refolded extensively. Purified protein in PBS buffer was characterised using biophysical methods in order to provide an indication on structural integrity of the purified, refolded products. Reducing and non-reducing SDS-PAGE gels confirmed correctly formed disulphide bonds. Far-UV CD analysis indicated the integrity of the secondary structure of the proteins. Finally, we showed by means of ELISA that D1 could bind to recombinant gp120.

2.2. MATERIALS AND METHODS

For detailed recipes, please consult Appendix A.

2.2.1. Design of CD4 Variants Cassettes

The wild-type DNA sequence of the four-domain T-cell surface glycoprotein CD4 molecule (*Homo sapiens*) was obtained online from the UniProtKB/Swiss-Prot database (P01730). Based on a previous publication, mutant domain 1 of CD4, termed D1 (m1.1), the following amino substitution were introduced: L5I, A55V, I76P, L96I and F98L (Chen et al., 2011). Since no previous study exclusively described individual domain 2, wild-type D2 was selected as default. The mutant four-domain CD4, termed 4dCD4 (D2A), consisted of alanine mutations of cysteine residues Cys130 and Cys159 in domain 2. The 3D crystal structure of the entire four-domain extracellular (PDB ID: 1WIQ) and the two-domain CD4 fragment (PDB ID: 1CDJ) were obtained from the RCSB Protein Data Bank. The visualisation, assessment and comparison of the wild-type and mutant CD4 domains were carried out using the Swiss-PDB Viewer v. 4.04. The sequences of the two domains were generated and aligned against corresponding wild-type sequencing using the vector NTI® software. Start and stop codons capped the DNA sequences. In frame 6xHis fusion tags encoding sequences were added to the C-terminus of the CD4 variants. The D1 (m1.1) DNA cassette was encoded between *BspHI* (N-terminal) and *XhoI* (C-terminal) restriction sites; D2 (WT) between *NcoI* (N-terminal) and *XhoI* (C-terminal) restriction sites and the 4dCD4 variants between *XhoI* (N-terminal) and *XbaI* (C-terminal) restriction sites. The sequences of CD4 variants were codon optimised for bacterial (*E.coli*) expression. The required DNA cassettes were synthesised by GenART® (Regensburg, Germany) and delivered in the vehicle pMA vector. First distal two-domain CD4 variants (plasmid vector and purified protein), which had previously been expressed in our laboratory, were kindly provided by N. Cerutti. These included wild-type (2dCD4-Wt) and the following variants Cys/Ala variants: C16A/C84A, C130A/C159A and C16A/C84A/C130A/C159A. These were respectively termed 2dCD4 (D1A), 2dCD4 (D2A) and 2dCD4 (CΔA). All of the cassettes/proteins used in this study included a 6xHis fusion tag at the C-terminus (Table 1).

CD4 Cassettes	First cloned and produced by	Description
D1 (m1.1)	Chen et al. (2011)	Individual domain 1, C-terminal 6x His-tag, Stable mutant based on the work of Chen et al. (2011)
D2	Original work	Individual domain 2, wild-type, C-terminal 6x His-tag,
2dCD4(Wt)	Cerutti et al. (2014)	Distal two-domain CD4, wild-type, C-terminal 6x His-tag,
2dCD4(D1A)	Cerutti et al. (2014)	Distal two-domain CD4, C16A/C84A, C-terminal 6x His-tag,
2dCD4(D2A)	Cerutti et al. (2014)	Distal two-domain CD4, C130A/C159A, C-terminal 6x His-
2dCD4(CΔA)	Cerutti et al. (2014)	Distal two-domain CD4, C16A/C84A/C130A/C159A, C-terminal 6x His-tag
4dCD4(Wt)	Original work	Extracellular Four-domain CD4, Wild-type, C-terminal 6x His-tag
4dCD4(D2A)	Original work	Extracellular Four-domain CD4, C130A/C159A, C-terminal 6x His-tag

Table 1: Description of CD4 variants (and abbreviations) used in this study

2.2.2. Preparation of Competent *E. coli* DH5α and BL21

Derived from frozen glycerol stocks of *E.coli* DH5α or BL21* (Life Technologies, CA U.S.A), 5 µL of overnight starter cultures were used to inoculate 40 mL of Luria-Bertani (LB) Broth (1% w/v tryptone (Sigma-Aldrich, MO, U.S.A), 1% w/v yeast extract (Sigma-Aldrich, MO, U.S.A), 0.5% w/v NaCl (Sigma-Aldrich, MO, U.S.A)) in sterile 50 mL capped Falcon tubes. With caps tightly closed and tubes placed at a tilt, the samples were incubated on a rotary plate at 37^{o}C until the culture OD_{600} reached approximately 0.4±0.1. The cells were collected by centrifugation (800 g, 10 minutes). The cells were re-suspended in 10 mL of ice cold transformation buffer and incubated on ice for 20 minutes. The cells were collected again by centrifugation (450 g, 4^{o}C, 10 minutes) and re-suspended in 1 mL of fresh ice cold transformation buffer (100 mM $CaCl_2.2H_2O$

(Sigma-Aldrich, MO, U.S.A), 10 mM PIPES-HCl (Sigma-Aldrich, MO, U.S.A), 15% Glycerol (Sigma-Aldrich, MO, U.S.A), pH to 7.0 with NaOH). Aliquots (50 µL per microtube) of competent *E.coli* were stored at -80^{o}C.

2.2.3. Bacterial Cloning

Five microgram of each of the lyophilised plasmids pMA-D1 (m1.1), pMA- D2, pMA-4dCD4 (Wt) and pMA-4dCD4 (D2A) (Regensburg, Germany) were dissolved in 50 µL of high-quality Millipore® distilled water, respectively. The plasmids were correspondingly transformed into competent *E.coli* DH5α using a heat-shock bacterial transformation protocol. To the respective 50 µL aliquot of thawed *E.coli* in 1.5 mL capped microtubes, 50 - 100 ng of plasmid vector was added. The samples were mixed by pipetting and incubated on ice for 20 minutes. Heat-shock transformation was conducted by incubating the samples on a heating block at 42^{o}C for 90 seconds. The samples were incubated on ice for another two minutes. Transformed bacterial suspension was then plated onto ampicillin-containing (100 µg/ml) Luria-Bertani (LB) agar (1% w/v Tryptone (Sigma-Aldrich, MO, U.S.A), 1% w/v Yeast Extract (Sigma-Aldrich, MO, U.S.A), 0.5% w/v NaCl (Sigma-Aldrich, MO, U.S.A), 1.5% w/v agar (Sigma-Aldrich, MO, U.S.A)) plates. The plates were incubated overnight at 37^{o}C. Plates with colonies were sealed and stored at 4^{o}C.

2.2.4. Plasmid Extraction

One colony of transformed *E.coli* DH5α was picked and inoculated into 4 mL of ampicillin-containing (100 µg/mL) LB broth (LB) in sterile capped 5 mL tubes. The LB was incubated overnight on a rotary plate at 37^{o}C. Plasmid extraction was conducted from 4 mL aliquots of the overnight culture using a plasmid extraction kit (GenElute^{TM} Plasmid Miniprep Kit, Sigma-Aldrich, MO, U.S.A), according to the manufacturer's instructions (Appendix B.b.). The plasmids were eluted in 100 µL of elution buffer. The concentration and purity of the eluted

plasmids were assessed by UV-spectrophotometry and agarose gel electrophoresis (1% agarose, 1x Tris-Acetate EDTA (TAE) buffer; Appendix A.a.iii.). Purified plasmids were stored at -20^{o}C.

2.2.5. Molecular Cloning of DNA Cassettes into Host Expression Vectors

CD4-encoding DNA cassettes optimised for expression in bacterial were subcloned into pET-15b (Novagen/Merck, Darmstadt, Germany) expression vectors.

All enzymes and buffers used during restriction digestion were from ThermoScientific^{TM}, Fermentas Life Science (MA, U.S.A). Purified pET15b, pMA-D1 (m1.1) and pMA-D2 (WT) plasmid vectors were digested using *Ncol/XhoI, BspHI/XhoI* and *NcoI/XhoI* restriction enzymes, respectively. Purified pMA-4dCD4 (Wt) and pMA-4dCD4(D2A) plasmid vectors, as well as pET-15b, were digested using *XhoI* and *XbaI* restriction enzymes.

Restriction reactions consisted of 2.0 µg of plasmid, 8.0 µL of 10x FastDigest® buffer and 2.0 µL (20 U) of each enzyme, made up to a final volume of 80.0 µL with high-quality Millipore® distilled water. These were incubated at 37^{o}C for 1h on a heating block. Digestion reactions were stopped by adding 3.0 µL of green FastDigest® loading buffer. The restriction fragments were resolved by agarose electrophoresis.

The corresponding D1 (m1.1), D2 and 4dCD4-encoding cassettes, as well as digested pET15b, were isolated by cutting the band out from the gel. The DNA fragments were purified using a High Pure PCR product purification kit (Roche®, Germany) according to the manufacturer's instructions (see Appendix B,ii). The concentration and purity of the eluted DNA fragments were assessed by UV-spectrophotometry and agarose gel electrophoresis.

Ligation reactions comprising digested pET-15b and corresponding inserts in a 1:1 (insert:vector) molar ratio were set up. Control ligation mixes contained only the linearised vector without insert. Ligation reactions contained 1.0 u/µL of T4 DNA ligase (ThermoScientific^{TM}, MA, U.S.A), 2.0 µL of 10x ligation buffer (ThermoScientific^{TM}, MA, U.S.A) and were made up to 20.0 µL with pure water. The reaction mixes were incubated for 1h at 22^{o}C in a water bath. The ligase was deactivated by incubating the ligation mix for 5 minutes

at 70^{o}C on a heating block. Five microlitres of the reaction mix was added to 50.0 µL of competent *E.coli* DH5α and transformation was conducted using the standard heat-shock protocol. Transformed *E.coli* was plated onto ampicillin-containing (100 µg/mL) LB agar plates. The plates were incubated overnight at 37^{o}C. Plates carrying colonies were sealed and stored at 4^{o}C.

2.2.6. Restriction Enzyme Analysis, Molecular Screening and Isolation of Pet-15b-D1 (M1.1), Pet-15b-D2, Pet-4dcd4 (Wt) and Pet-4dcd4 (D2A)

Colonies from the corresponding overnight incubated plates were picked and inoculated into 4.0 mL of ampicillin-containing (100 µg/mL) LB broth in sterile 5.0 mL capped tubes. With caps loose and maintained at a tilt (for optimum aeration and stirring), the samples were incubated overnight at 37^{o}C with vigorous agitation. Plasmids were purified using a GenElute^{TM} Plasmid Miniprep Kit (Sigma-Aldrich, MO, U.S.A).The concentration and purity of eluted plasmids were assessed by UV-spectrophotometry and agarose gel electrophoresis.

Restriction mapping was then performed to identify recombinant plasmids with successfully ligated inserts. Samples of purified pET15b-D1 (m1.1) and pET15b-D2 (WT), as well as pET15b control vector, were linearised with *BamHI*, while the CD4 domain-encoding inserts were excised using *XbaI and EcoRI*. PET-4dCD4 (WT), pET-4dCD4 (D2A) and control pET15b were linearised with *XhoI*, and the inserts excised using *XhoI and XbaI*. In addition to the corresponding plasmid DNA (~100ng) and enzymes (5U per reaction), the reaction mixes included the 10x FastDigest® buffer. The samples were made up to 20.0 µL with pure water and incubated at 37^{o}C for 1h. The reaction was neutralised by the addition of 3.0 µL of green FastDigest® loading buffer. Agarose gel electrophoresis was conducted and DNA bands were visualised under UV transillumination (NB: For restriction analysis figure, please see appendix C.f.)

2.2.7. Bacterial Expression of CD4 variants

2.2.7.1. CD4 Expression

The recombinant plasmids containing the 1- and 4-domain CD4-encoding inserts optimised for expression in *E. coli* were transformed into *E. coli* BL21 using the standard heat-shock protocol. Transformed *E.coli* BL21 with their corresponding plasmids were picked and inoculated into 5.0 mL of ampicillin-containing (100 µg/ml) LB broth. The samples were incubated overnight at 37^{o}C with vigorous agitation. One millilitre of each culture was diluted into 100 mL of fresh ampicillin-containing LB broth in sterile 250 mL flasks (two flasks per inoculant). The loosely closed flasks were incubated on a rotary plate at 37^{o}C. Upon reaching an OD_{600} of 0.6-0.7, one of the flasks was transferred to a shaking incubator set to 20^{o}C, while the other was maintained at 37^{o}C. After overnight incubation, samples of bacterial cultures were collected and added to an equal volume of 2x SDS-PAGE loading buffer (0.125M tris-cl (Sigma-Aldrich, MO, U.S.A), 4% SDS (Sigma-Aldrich, MO, U.S.A), 20% v/v glycerol (Sigma-Aldrich, MO, U.S.A), 0.2 M DTT (Sigma-Aldrich, MO, U.S.A), 0.02% bromophenol blue (Sigma-Aldrich, MO, U.S.A), pH6.8). The samples were placed in boiling water for 10 minutes, vortexed and stored at -20^{o}C.

SDS-PAGE of samples was conducted (See Appendix B.a). Once resolved, the gel was allowed to equilibrate in transfer buffer (Appendix A) (20 min) and then transferred onto a nitrocellulose membrane (Hybond C, Amersham Bioscience, UK) by standard Western Blotting procedures. The membrane was incubated on a rotary plate in 10 mg/mL of Bovine Serum Albumen (BSA; Sigma-Aldrich, MO, U.S.A) in 1% Tris-Buffered Saline containing 0.05% Tween (Sigma-Aldrich, MO, U.S.A) (1% BSA T-TBS) for 1h at room temperature, washed twice with T-TBS (5 minutes per wash), incubated with an anti-His-HRP conjugated probe (ThermoScientific, MA, U.S.A) in T-TBS (1:2000) for 1h, and finally washed 4 times with T-TBS (10 minutes per wash). His-tagged CD4 proteins were detected by chemiluminescence using the SuperSignal West Pico substrate system (Thermo-Fisher, MA, U.S.A) on a Chemi-Doc imaging instrument (Bio-Rad, CA, U.S.A).

2.2.7.2. Protein Solubility Analysis

An overnight bacterial culture of *E.coli* BL21 expressing the relevant recombinant proteins was diluted (1:100) into 1 L (in 2L flasks) of ampicillin-containing (100 µg/mL) LB broth. The bacteria expressing D1 (m1.1) and D2 were incubated overnight at 37^{o}C on a rotary plate (vigorous stirring), whereas those expressing 4dCD4 were incubated at 20^{o}C. The cultures were centrifuged (4000g, 30min, 4^{o}C) to collect cells, the spent medium discarded, and the cell pellet re-suspended in 20 ml of 1x Phosphate Buffered Saline (PBS, 1/20th volume of culture) (Sigma-Aldrich, MO, U.S.A). Lysozyme (0.5mg/ml) (Sigma-Aldrich, MO, U.S.A) was added to re-suspended cells and the suspension was incubated on ice on a rotary plate with gentle shaking for 1h. The BL21 *E.coli* suspension was transferred to a 50.0 mL Falcon tubes, and the samples were snap-frozen in dry ice/acetone and thawed twice. The lysed bacterial cells were sonicated (HD3100, MS73, Bandelin Sonopuls, Berlin, Germany) a minimum of three times (4500 kJ per L; 1 minute, 80% amplitude, 1.0 s pulse on, 0.5 s pulse off), or until viscosity of lysates was reduced. The total cell fraction (TCF) was centrifuged (10000 g, 4^{o}C, 30 minutes) and the supernatant collected as the soluble fraction (sol). The cell pellet was re-suspended in 20 ml of solubilising buffer (8M Urea (VWR International), 50mM Glycine (Sigma-Aldrich, MO, U.S.A), 0.5 M NaCl (Sigma-Aldrich, MO, U.S.A), 20 mM Imidazole (Sigma-Aldrich, MO, U.S.A), 2 mM β-mercaptoethanol (Sigma-Aldrich, MO, U.S.A), pH 7.4) and incubated for 20 minutes at room temperature with vigorous agitation. The re-suspension was centrifuged (10000 g, 4^{o}C, 30 minutes), and the supernatant was collected as the insoluble fraction (Insol). Fifty microlitre of TCF, Sol and Insol were collected and boiled for 10 minutes with an equal volume of 2x loading buffer. Samples were stored at -20^{o}C and analysed by SDS-PAGE and Western Blotting as described previously.

2.2.7.3. Protein Isolation and Purification

Recombinant CD4 proteins were purified from the insoluble fractions by nickel-chelate affinity chromatography. Ni^{2+}-charged NTA beads (a gift from Dr W. Prinz) were added to the insoluble fractions extracted from the overnight cultures. The suspensions were incubated overnight with

stirring at 4°C. Overnight suspensions were transferred to centrifugation tubes and the beads were harvested (3200 g, 2min, 4°C). The supernatant was carefully decanted and discarded. The protein-bound beads were sequentially resuspended and washed by centrifugation (3200 g, 2min, 4°C) with 50.0 mL of wash buffers (8M Urea (VWR International), 50mM Glycine (Sigma-Aldrich, MO, U.S.A), 0.5 M NaCl (Sigma-Aldrich, MO, U.S.A), 2 mM β-mercaptoethanol (Sigma-Aldrich, MO, U.S.A), pH 7.4) of increasing imidazole concentration (for D1 and D2: 5x 20 mM, 5x 50 mM; for 4dCD4: 3x 20 mM, 3x 50 mM, 3x 75 mM). The His-tagged proteins were eluted with 10.0 – 20.0 mL (depending on the original volume of bacterial culture extracted from) of elution buffer (500 mM Imidazole). The purified proteins were analysed by standard SDS-PAGE procedures.

2.2.7.4. Protein Re-folding

The 2dCD4 re-folding protocol, previously developed in our laboratory to facilitate formation of canonical disulphide bonds in proteins expressed in E coli, involves slow dialysis in glutathione-containing buffers (Cerutti et al., 2014, Cerutti et al., 2010). Briefly, the insoluble proteins were extracted from inclusion bodies by solubilisation with strongly denaturing (8M urea) buffer. The extensive re-folding protocol allows the gradual removal of solubilisation buffer and its replacement with PBS at physiological pH of 7.4. The slow removal of denaturant, at cold temperature, is important to promote the renaturation and correct refolding of the protein into its native conformation, and to limit precipitation. Sucrose and glycine act as stabilisers, and enhance the refolding process, whilst also limiting precipitation (Tsumoto et al., 2003). Additionally, with the inclusion of glutathione and glutathione disulphide in the refolding buffer, an appropriate redox system is setup to encourage correct formation of disulphide bonds (Singh and Panda, 2005). The following references should be consulted for extensive reviews on protein refolding (Sorensen et al., 2003, Middelberg, 2002, Tsumoto et al., 2003, Singh and Panda, 2005).

The eluates were respectively placed into pre-wet dialysis tubes (MWCO 10,000, Thermo Scientific SnakeSkin™ Pleated Dialysis Tubing, MA, U.S.A). For three consecutive days, the purified proteins were sequentially dialysed overnight at 4°C with stirring in 1 L of pre-chilled

folding buffer A (50 mM Glycine (Sigma-Aldrich, MO, U.S.A), 10% Sucrose (Sigma-Aldrich, MO, U.S.A), 1 mM Glutathione (Sigma-Aldrich, MO, U.S.A), 1 mM Glutathione disulphide (Sigma-Aldrich, MO, U.S.A), 4 M Urea (VWR International), 1 mM EDTA, pH 9.6, 4^{o}C), folding buffer B (15 mM Na_2CO_3 (Sigma-Aldrich, MO, U.S.A), 35 mM $NaHCO_3$ (Sigma-Aldrich, MO, U.S.A), 10% Sucrose (Sigma-Aldrich, MO, U.S.A), 0.1 mM Glutathione (Sigma-Aldrich, MO, U.S.A), 0.01 mM Glutathione disulphide (Sigma-Aldrich, MO, U.S.A), 1 mM EDTA (Sigma-Aldrich, MO, U.S.A), pH 9.6, 4^{o}C) and 1x PBS. The two final rounds of dialysis, were carried out for 2 hours in each case in 1 L of pre-chilled 1x PBS. The dialysed solution was collected and centrifuged (3200 g, 4^{o}C, 2 min) to pellet any precipitate formed. The supernatant was decanted, syringe filtered (0.45 µm filter) and stored at 4^{o}C.

2.2.7.5. Protein Analysis

The purified proteins were concentrated to 0.5 – 1.0 mg/ml using a centrifugal filter unit (10 kDa cut-off, Amicon Ultra-15, Millipore-Merk, Darmstadt, Germany), and final concentrations determined using a BSA protein quantification kit (Thermo Scientific, Pierce Protein Research Products, MA, U.S.A) as per the manufacturer's instructions. The refolded, concentrated CD4 proteins were analysed by reducing- or non-reducing SDS-PAGE in the presence or absence of 50 mM Dithiothreitol (DTT) (Sigma-Aldrich, MO, U.S.A), respectively.

.

2.2.7.6. Assessing Functionality of Bacterial Expressed CD4 variants

a. D1 (m1.1) and 2dCD4 variants

In the case D1 (m1.1), a sandwich ELISA was used since gp120 binding to directly coated protein is hindered as it abuts the plate's surface. CD4 variants and gp120 were allowed to complex before being added to the plate wells that had been coated with capture antibody. Gp120 bound CD4 undergoes conformational changes such that there is the exposure of CD4-induced binding sites (CD4i). These can be probed using antibodies directed to CD4i epitopes such as the well-characterised 17b monoclonal antibody. The 17b monoclonal antibody was

obtained through the NIH AIDS Reagent Program, Division of AIDS, NIAID, NIH: HIV-1 gp120 monoclonal antibody (17b) from Dr James E. Robinson (Moore et al., 1993, Wyatt et al., 1995, Trkola et al., 1996, Sullivan et al., 1998, Wyatt et al., 1998, Kwong et al., 1998). The anti-gp120 capture antibody, D7324 (Aalto BioReagents Ltd, Dublin, Ireland or Cliniqa Inc., Fallbrook, CA, U.S.A) (1ug/ml in PBS, pH 7.4) allows the capture and orientation of gp120-CD4 complex that enhances the exposure of CD4i to the subsequent 17b antibody (Gram et al., 2002). Purified recombinant 2dCD4 variants (WT, D1A, D2A and CΔA) were a kind gift from Mrs. N. Cerutti. One hundred microlitres (100 µl) of D7324 antibody (Aarto, UK, 1ug/ml in PBS, pH 7.4) was added to wells of 96 well-plates (Flat-bottom/ MaxiSorp, Nunc®, Denmark). PBS blank controls were included. Overnight coating at 4^{o}C was allowed. The coating antibody was aspirated and 250 µl of blocking solution (1% BSA (Sigma-Aldrich, MO, U.S.A) in 1x Phosphate Buffer Saline (PBS, Sigma-Aldrich, MO, U.S.A) containing 0.05% Tween-20 (Sigma-Aldrich, MO, U.S.A) (1% BSA T-PBS) was added to wells. Blocking was allowed for 90 minutes. Serial dilutions of D1 (m1.1) and 2dCD4 variants in PBS were prepared, following which $gp120_{bal}$ in PBS was added. $Gp120_{bal}$ was obtained through the NIH AIDS Reagent Program, Division of AIDS, NIAID, NIH: HIV-1BaL gp120 from DAIDS, NIAID. Final concentration of mixes of 2dCD4 and $gp120_{bal}$ were respectively 1 – 0 µg/ml and 100 ng/ml. Samples were allowed to incubate for 1 hour at room temperature. Block solution was aspirated and 100 µl of sample mix was added to the wells in triplicates, as well as to the PBS control. Incubation of the samples in the plate was allowed for 1h. Plates were then washed 5x with 1x T-PBS. Primary monoclonal antibody, 17b in 1x T-PBS, was added to corresponding wells (100 µl) at 0.3 µg/ml in PBS-T. One hour incubation was allowed, after which plates were washed 5x with 1x T-PBS. Secondary goat anti-human HRP-linked antibody (GE Healthcare, UK) in 1x T-PBS was added to wells and incubation was allowed for 1h. Plates were washed five times with T-PBS. TMB Ultra Substrate (Thermo-Pierce, U.S.A) equilibrated to room temperature was added to all wells (100 µl). The plates were then incubated for 30 min respectively at 37^{o}C on a shaker. An equal volume of sulphuric acid (1 M) was added to the wells to stop the reaction. Absorbencies of wells were measured on a plate reader at both 450 nm and 570 nm (Bio-Rad Model 650 Microplate reader, CA, U.S.A; fast read, 450 nm measure filter, 37^{o}C).

b. 4dCD4-WT

In order to confirm the conformation and functionality of 4dCD4-WT derived from bacterial expression, the binding ability to $gp120_{bal}$ was addressed. Using 100 µL per well, the bacterial expressed 4dCD4-WT was coated at 1 µg/ml in 1x PBS into a 96-well plate (Flat-bottom/ MaxiSorp, Denmark) for 1h. Control wells were coated with 100 µL of 1x PBS. The coating solution was removed and 250 µL of blocking reagent (1% BSA in T-PBS) was added for 1h. Blocking buffer was removed and 100 µL of $gp120_{bal}$ (500 – 7.8125 ng/ml in T-PBS) were added to wells for 1h. The gp120 was removed and wells were washed 5x with T-PBS. The 2G12 antibody at 100 µL at 0.1ug/mL was added to wells for 1 hour. Primary antibody was removed and wells were washed 5 times with T-PBS. Secondary anti-human goat HRP-linked antibody was added to wells and incubation for 1h allowed. Wells were washed 5 times with T-PBS before 100 µL of TMB-Ultra substrate (Thermo-Pierce, U.S.A) was added. Plate was incubated for 20 min at $37^{o}C$ on a rotary plate. Sulphuric acid, 100 µL at 1 M, was added to wells to quench the reaction. The absorbance values for all the wells were determined using a plate reader (Fast read, 450 nm measure filter, $37^{o}C$; Bio-Rad Model 650 Microplate reader; CA, U.S.A).

2.3. RESULTS

2.3.1. *In silico* analysis of CD4 variants

The published crystal structures of CD4 and the extracted domains variants were visualised using DeepView/Swiss-PDBViewer (Swiss Institute of BioInformatics, v4.0.4). References from previous authors who have successfully expressed of D1 and D2, and how were they expressed, is provided in Appendix C.f.

2.3.1.1. D1

The first domain of CD4 (D1) comprises residues 1 - 98 (Figure 6) and displays typical immunoglobulin topology, consisting of nine anti-parallel β-strands arranged as a two-layered β-sheet sandwich. A hydrophobic core is encapsulated within D1 whilst hydrophilic residues are localised at the surface. Extensive hydrogen bonds between the strands stabilise the structure. The disulphide bond between Cys^{16} – Cys^{84} links the two sandwich sheets. In contrast to 2dCD4 or full length sCD4, the first attempts at expression and purification of soluble WT D1 were unsuccessful (Chen et al., 2011, Sharma et al., 2005, Saha et al., 2011). The lack of D2 and the exposure of the highly hydrophobic D1 surface to the aqueous *in vitro* environment are often considered as the main reason for this. Accordingly, Chen *et al.* reported the CD4 domain variant designated D1 (m1.1), which contains the following substitutions: L5I, A55V, I76P, L96I and F98L (Chen et al., 2011). Upon isolation, D1 (m1.1) occurs as a highly soluble, monomeric protein, which acquires the native CD4 D1 fold and binds recombinant gp120 with high affinity (Chen et al., 2011). These mutations involve the replacement of residues having large hydrophobic side chains to ones with smaller, but still hydrophobic, side chains. Contrasting wild-type (WT) and mutant D1 (m1.1), it was seen that the mutations were mainly located on the D1/D2 interface. The interface of D1 and D2 consists of a largely hydrophobic surface formed by amino acids in each domain. A reduction in the hydrophobicity of the surface of mutant D1 can therefore improve the protein stability and limit aggregation whilst exposed to aqueous

solvent. Additionally, the substitution of isoleucine to proline at position 76 could also enhance the stability of D1 by firmly "kinking" the backbone of the polypeptide against the overall domain (MacArthur and Thornton, 1991).

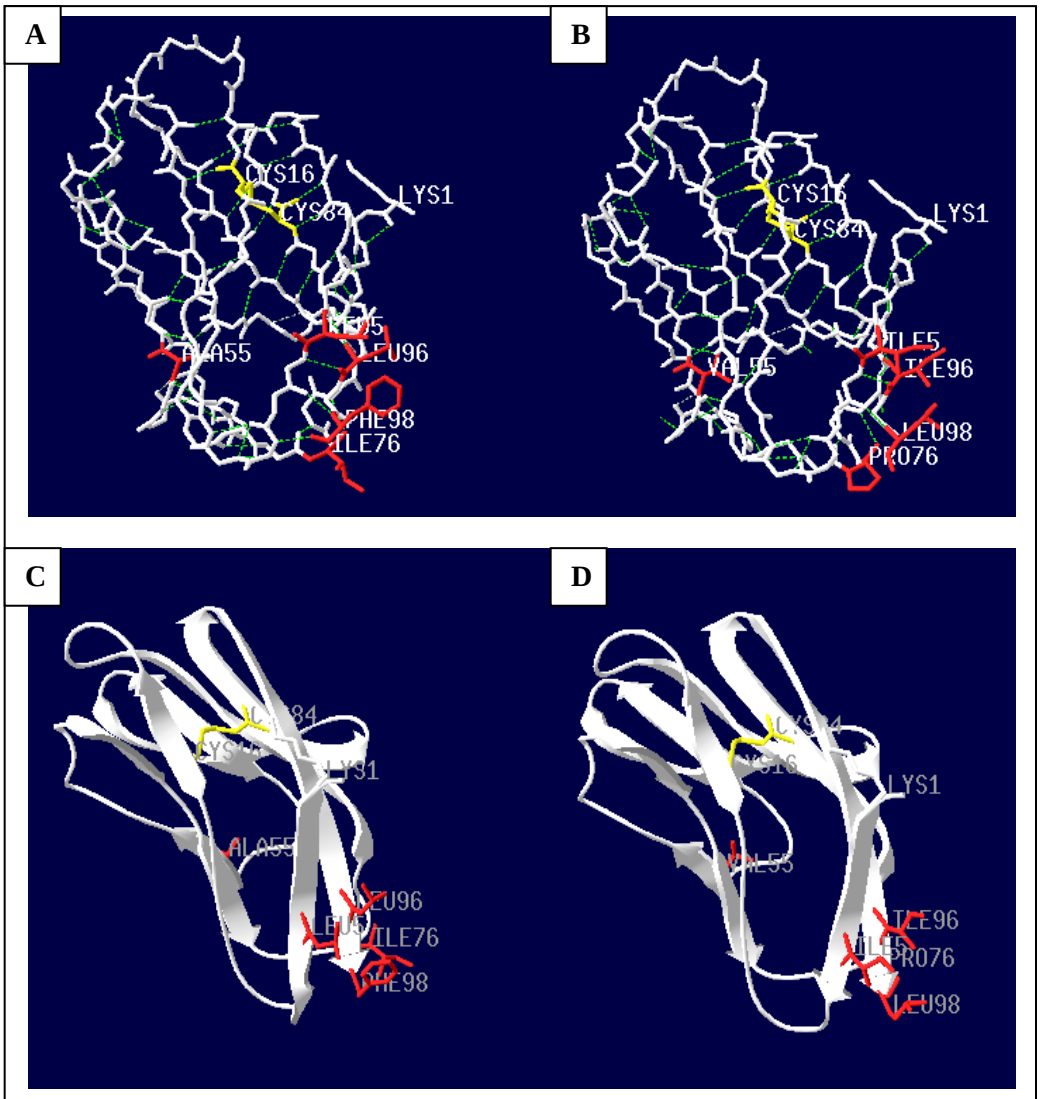

Figure 5: *In silico* analysis of D1 (PDB ID: 1CDJ; Swiss-PDB Viewer v. 4.04.).

3D backbone trace of wild-type (A) and mutant D1 (m1.1) (B), showing hydrogen bonds between strands (green lines) is depicted. Red residues indicate the mutated amino acids. Yellow residues show the disulphide Cys^{16} – Cys^{84} bond. For a simplified view, the ribbon diagrams of wild-type (C) and mutant D1 (m1.1) (D) are shown as well. N- and C- termini are denoted by Lys^{1} and Phe^{98}, respectively.

2.3.1.2. D2

The structure of the second N-terminal CD4 domain (D2) comprises residues 99 – 178, (Figure 7). CD4 D2 is directly linked to D1 via a β-strand on the C-terminus of D1. The topology of D2, consisting of seven anti-parallel β-strands organised into a two sheet-sandwich, is analogous to the constant immunoglobulin domain. Extensive hydrogen bonding arises between the β-strands. As for D1, hydrophobic residues are localised at the core of D2 whereas hydrophilic ones are exposed at the surface. The surfaces of D2 at the interface of D1 and D3 bear hydrophobic patches which abut against the respective domains (Wu et al., 1997, Ryu et al., 1990). Based on the fact that the 2dCD4 has been successfully expressed in previous work and in our laboratory, it was reasoned that the hydrophobic surface of D2 adjoining D3 would not have a deleterious impact on the stability or solubility of a recombinant domain 2 mini-protein. Since no previous work has described the expression of recombinant D2 in detail, the influence of the exposure of the surface D2 that directs towards D1 on the solubility and re-folding of the protein is unknown. While it is possible that the exposure of this hydrophobic patch to the aqueous *in vitro* environment could result in protein misfolding or protein aggregation that may compromise the ability to produce correctly folded recombinant forms of D2, we reasoned that the extensive hydrogen bonding network between the β-strands in D2 could facilitate folding into the native β-barrel-like structure, and the decision was made to assess the feasibility of producing a recombinant, natively folded CD4 D2 protein empirically.

The structure of D2 is atypical in comparison to CD4 domains 1, 3 and 4 or the conventional constant immunoglobulin domain topology. In particular, D2 is shorter by approximately 25 residues than the conventional Ig domains (which normally comprise approximately 100 amino acid residues). Another striking feature is that the D2 disulphide bond (Cys^{130} – Cys^{159}) links β-strands within the same sheet (as opposed to strands across sheets typical of the Ig-fold). Moreover, the C_α - C_α distance between the cysteine residues of D1 and D2 was found to be respectively 6.38 Å and 3.84 Å. The shorter bond length between the D2 cysteines is believed to increase the torsional strain on this disulphide bond (Wu et al., 1997, Ryu et al., 1990), that is suggestive to enable its facile reduction.

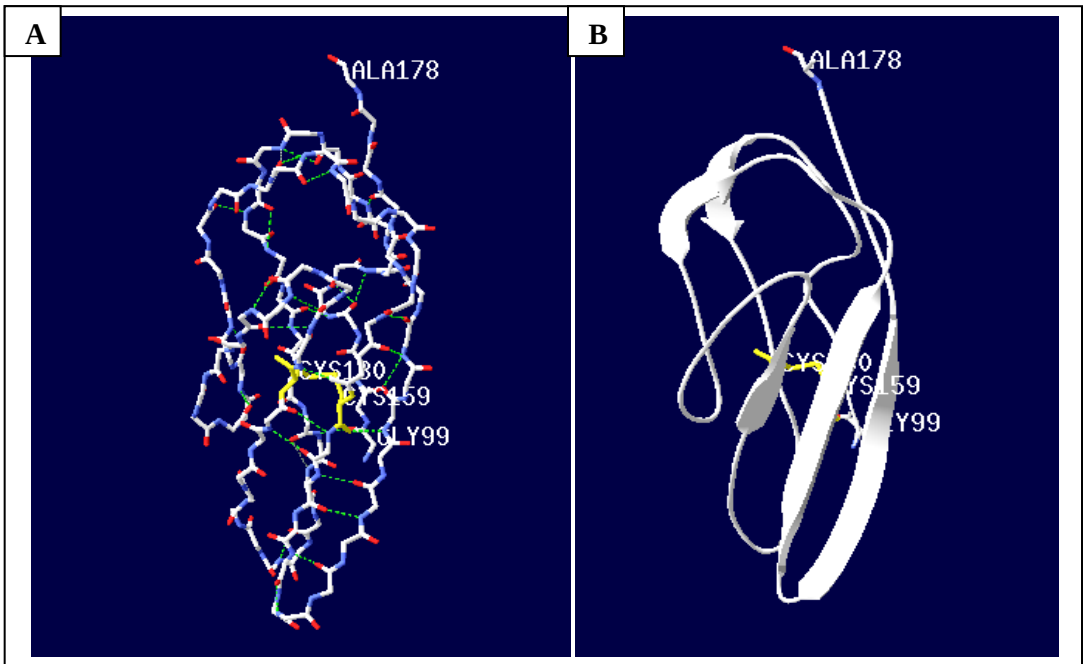

Figure 6: *In silico* analysis of D2 (PDB ID: 1CDJ; Swiss-PDB Viewer v. 4.04.)

3D backbone trace of wild-type (A), showing hydrogen bonds between strands (green lines) is depicted. Red residues indicate the mutated amino acids. Red and blue indicate oxygen of carboxyl and nitrogen of imino groups. Yellow residues show the disulphide Cys130 – Cys159 bond. For a simplified view, the ribbon diagram of wild-type D2 (B) is shown as well. N- and C-termini are denoted by Gly99 and Ala178, respectively.

2.3.2. Protein Expression Studies

2.3.2.1. IPTG Induction and Temperature Optimisation for Protein Expression

DNA cassettes encoding full-length (4-domain) CD4 (sCD4) and CD4 domains 1 (D1 (m1.1) and 2 (D2) were codon-optimized for expression in E coli and synthesised by Geneart (Regensburg, Germany). These were sub-cloned into the prokaryotic expression vector pET15b (Novagen/Merck, Darmstadt, Germany). Cassettes encoding 2dCD4 (wild-type and mutants) were synthesized and cloned into pET15b previously by others in our laboratory (Cerutti et al., 2010). Following transformation of *E .coli* BL21 with the indicated expression vectors, SDS-PAGE and Western blots revealed optimum yields of recombinant D1 (m1.1) and D2 in the whole cell lysates following overnight incubation of the cultures at 37^{o}C cultures (Figure 8). D1

(m1.1) and D2 migrated electrophoretically to positions consistent with their respective molecular weights (~12.4 kDa and 10.4 kDa). Pre-purified 2dCD4 (~22 kDa), was used as a control. The amount of protein present increased gradually with time and reached maximum yields following overnight incubation. Addition of IPTG at 1 mM had no apparent added effect on the yield of protein in either case. This is attributable to the "leakiness" of the T7 promoter under which expression of heterologous proteins is controlled in pET15b. The expression of recombinant proteins was significantly affected by temperature. At 37^{o} C, expression was highly stimulated in either case. On the other hand, expression of proteins at 20^{o} C was significantly reduced.

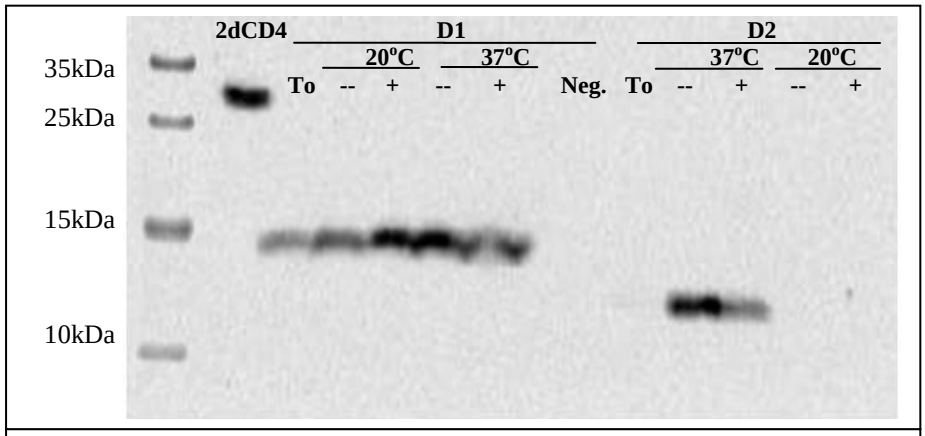

Figure 7: Western Blot of D1 and D2

Anti-His antibody probed Western blots showed that His-tagged D1 and D2 were effectively being expressed in *E. coli* BL21 whole cell lysate that was derived from overnight cultures. Reflecting on their corresponding molecular weights, the 2dCD4 control (~22kDa), D1 (~12kDa) and D2 (~10kDa) localised at different positions. Repeated experiments indicated that the maximum amount of protein was obtained after overnight culture. Whilst IPTG had no effect on the expression of the recombinant proteins, the higher temperature (37^{o}C) was stimulatory. Expression of proteins at the lower temperature (20^{o}C) was almost negligible in the case of D2. Neg.: Negative control, T_0: T_0 sample, +: IPTG included, --: IPTG-free.

2.3.2.2. Protein Solubility analysis

SDS-PAGE and Western blots of the soluble and insoluble cellular fractions revealed the D1 (m1.1) and D2 was localised almost exclusively in an insoluble fraction (Figure 9). Being in the

insoluble fraction, it is highly probable that the recombinant proteins were localised in the host bacteria as inclusion bodies. The exposure of the hydrophobic surfaces that abut the D1/D2 interface could be a strong factor influencing the insoluble nature of D1 (m1.1) and D2.

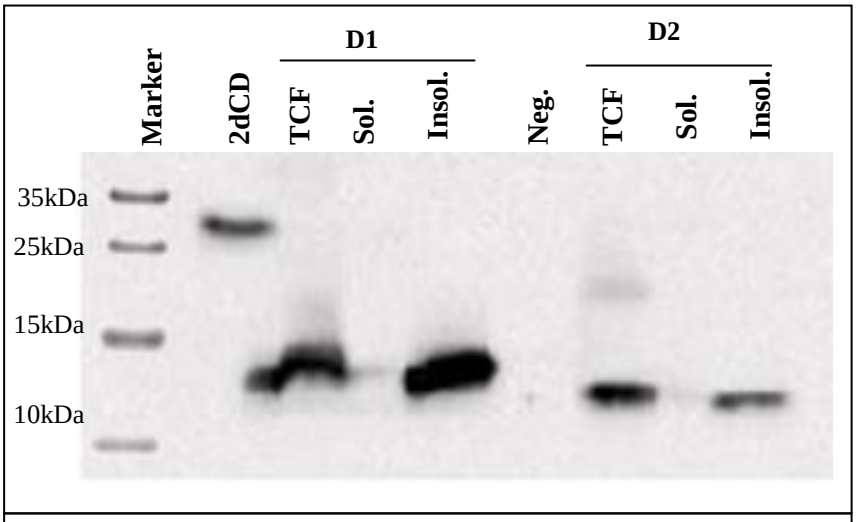

Figure 8: Protein Solubility Analysis of D1 and D2

Anti-His antibody probed Western blots show that the His-tagged D1 and D2 were effectively being expressed in the insoluble cellular fraction.

Neg: Negative control, 2dCD4: two-domain CD4/positive control, TCF: Total Cell Fraction, Sol.: Soluble Cell Fraction, Insol.: Insoluble cell Fraction

2.3.2.3. Protein Isolation and Purification

Following optimization of D1 (m1.1) and D2 expression, and confirmation that these proteins localized almost exclusively in the insoluble fraction, the recombinant proteins were purified by

Ni^{2+}-chelate chromatography following chaotropic extraction from inclusion bodies. SDS-PAGE analysis of the purified products showed that these were purified to near homogeneity (Figure 10).

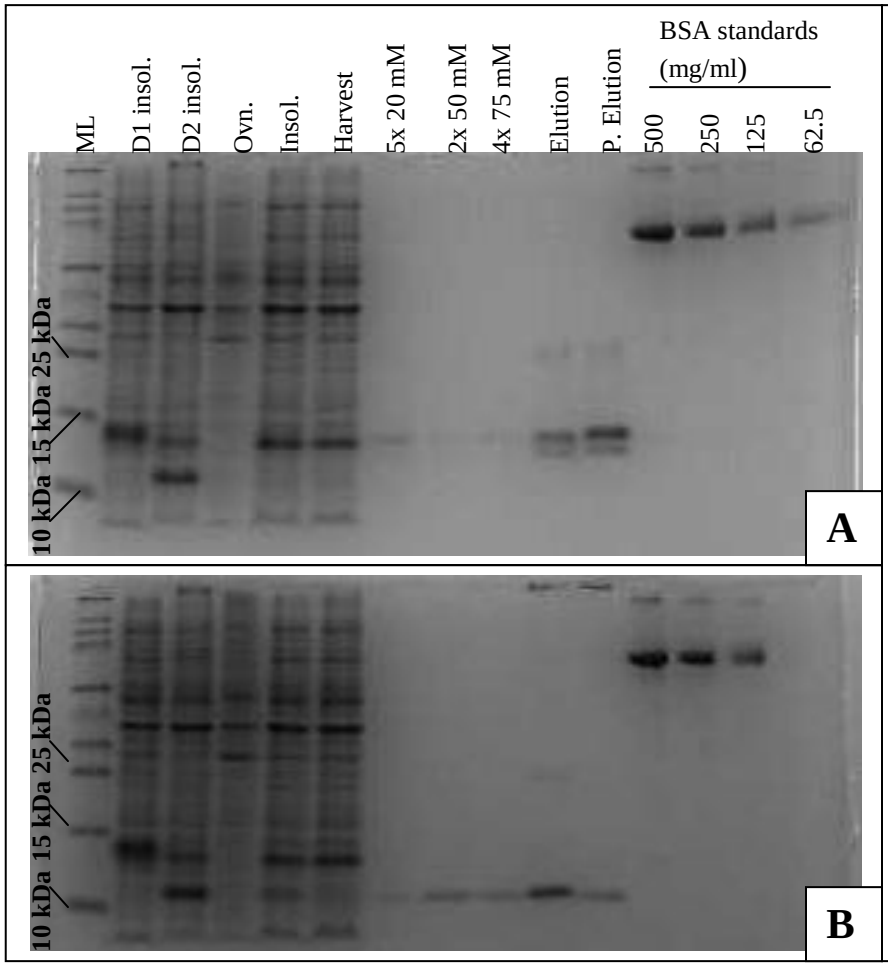

Figure 9: Protein Washes

Coomassie Blue stained SDS-PAGE (15 % polyacrylamide Tricine gel) **A**: D1; **B**: D2,

ML: Molecular weight ladder (BR spectra Multicolour Protein Ladder, ThermoScientific™, MA, U.S.A); **D1/D2 Insol.:** Insoluble cell fractions of D1 and D2 as positive controls; **Ovn:** Sample from overnight, upscaled culture; **Insol.:** Insoluble cell fraction; **Harvest:** supernatant sample from first bead harvest; **P.Elution:** Sample from previous eluate.

2.3.3. Protein Analysis: Structural

2.3.3.1. SDS PAGE Gels

Following denaturing, affinity purification of D1 (m1.1) and D2, the proteins were folded via an oxidative refolding protocol to facilitate formation of the canonical CD4 D1 and D2 disulphide bonds. The refolded proteins were analysed in the first instance by conventional standard SDS-PAGE gel electrophoresis followed by Coomassie Blue staining. However, improving the resolution of separated bands was deemed necessary for D1 (m1.1) and D2, and Tricine polyacrylamide gel electrophoresis was subsequently used for further analysis of these refolded proteins. In order to gain insights into whether disulphide bonds had been established in D1 (m1.1) and D2 following refolding, the purified proteins were analysed by reducing- and non-reducing SDS-PAGE. By default, the loading buffer used contains DTT which reduces disulphide bonds. The elimination of disulphide bonds in the presence of SDS allows the protein to completely unfold. In general, unfolded proteins have a greater hydrodynamic volume than their folded counterparts, and the former thus migrate with higher apparent molecular weight during electrophoresis. The upper bands in DTT-treated samples therefore represent the slower moving, fully denatured, disulphide-free proteins. Lower bands represent the proteins which have not been reduced.

Upon comparison with the non-reducing gel, D1 (m1.1) produces the expected increase in apparent molecular weight when disulphide bonds were reduced (Figure 11). In contrast, DTT-treatment of D2 resulted in the occurrence of an isomer with a lower apparent molecular weight. It could thus be reasonably speculated that reduction of the D2 disulphide gives rise to a more condensed CD4 domain 2 structure. This unusual consequence of disulphide reduction may, in turn, represent an important component of the biological function of CD4.

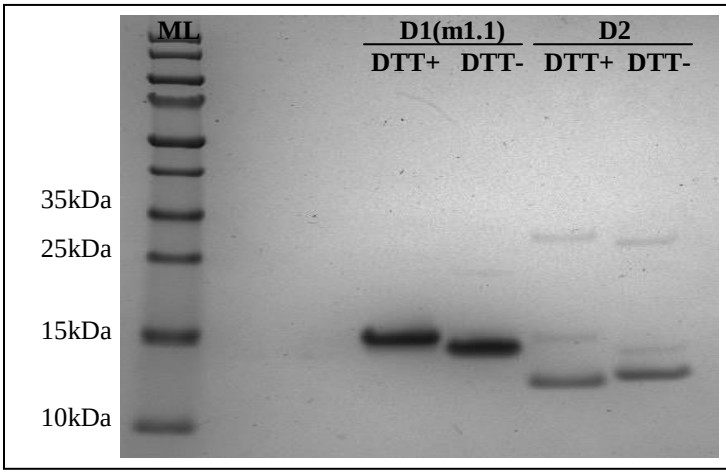

Figure 10: Reduced (DTT+) and non-reduced (DTT-) gels of D1 (m1.1) and D2.

Reduced D1 (m1.1), produced a single band at the expected higher apparent molecular weight. Reduced D2 however resulted in a band with lower apparent molecular weight as compared to the non-reduced sample. This unusual feature is indicative of the occurrence of a more compact structure in D2 when the disulphide bond in D2 is reduced.

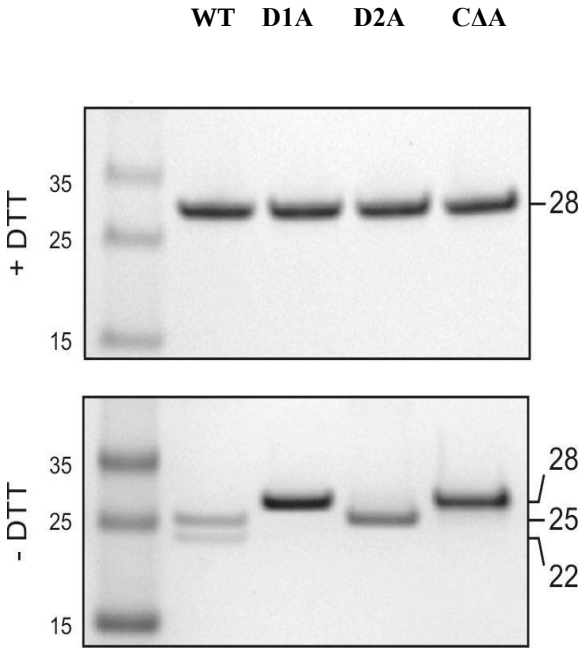

Figure 11: Reduced (DTT+) and non-reduced (DTT-) gels of 2dCD4 variants (WT, D1A, D2A, CΔA). Copied from (Cerutti et al., 2014).

Reduction of 2dCD4 variants resulted in localisation of variants at a single molecular weight corresponding to that of NR CΔA. With the exception of D1A which remained unchanged, NR WT and D2A displayed lower apparent molecular weight as compared to reduced samples. Dimeric bands in WT, corresponding to all disulphide being formed and reduced D2 disulphide bond, represent the two redox state in which the protein exists.

2.3.4. Protein Analysis: Low resolution Structure/Function analysis

As mentioned, D1 (m1.1) is based upon previously published work (Chen et al., 2011). Chen and colleagues showed that the stabilising mutation inserted into D1 (m1.1) allowed its purification following expression in *E coli*, and that this protein had native structure, bound to HIV-1 gp120, and competitively inhibited CD4-gp120 binding.

2.3.4.1. Analysis of interaction between D1 (m1.1) and D2 and a CD4 antibody (Mt310)

To assess the integrity of the D1 and D2 proteins purified in our laboratory, we performed an ELISA assay to check whether the CD4 domain proteins were reactive with a well-established monoclonal anti-CD4 antibody (mt310) whose conformational epitope is known to reside in CD4 domain 1 (Healey et al., 1990a, Qin L., 2001, Helling et al., 2015). D1 (m1.1) and D2 were coated onto the ELISA plate and probed using mt310. ELISA analysis revealed that D1 (m1.1) was recognised by D1-specific antibody mt310 (Fig. 13), while D2, serving as a control, displayed only low intensity non-specific recognition. We could not at this point gain insights into the structural integrity of D2 in terms of antibody recognition, as D2-specific antibodies are not commercially available. Later in Chapter 2, we however provide evidence that D2 - recognisable by supernatants from hybridoma cell lines generated following immunization of mice with a native 2dCD4 – has native structure.

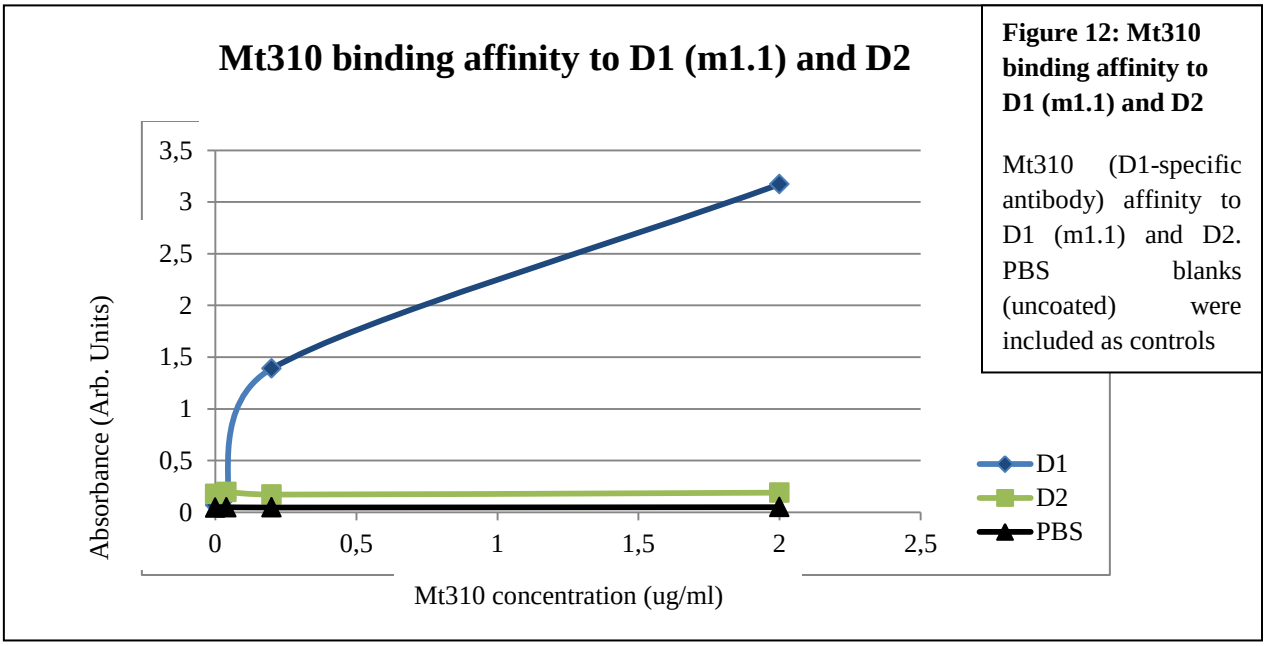

Figure 12: Mt310 binding affinity to D1 (m1.1) and D2

Mt310 (D1-specific antibody) affinity to D1 (m1.1) and D2. PBS blanks (uncoated) were included as controls

2.3.4.2. Far-Field CD Analysis of D1 (m1.1) and D2

To obtain insights in the nature of the secondary structures formed in D1 (m1.1) and D2, far-field circular dichroism was performed (Figure 14). Incomprehensible, flat spectra or CD spectra with a significant negative trough between 195 – 200 nm - characteristics of misfolded, disordered or denatured proteins (Sreerama et al., 2000, Wu et al., 1992) - were not observed. Instead, both proteins had spectra that were consistent with the presence of significant β-sheet secondary structure, suggesting that these domains are able to acquire Ig-fold-like structures when expressed independently of the adjoining domains (Figure 14).

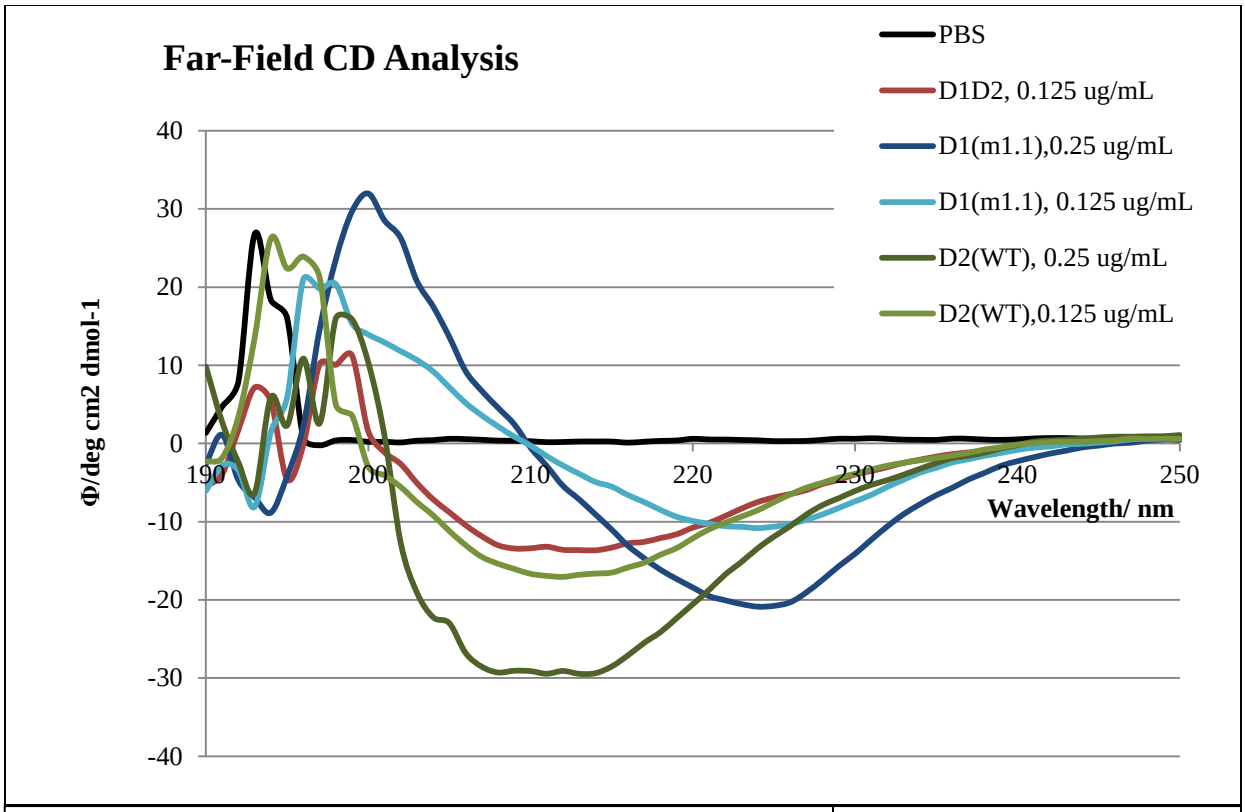

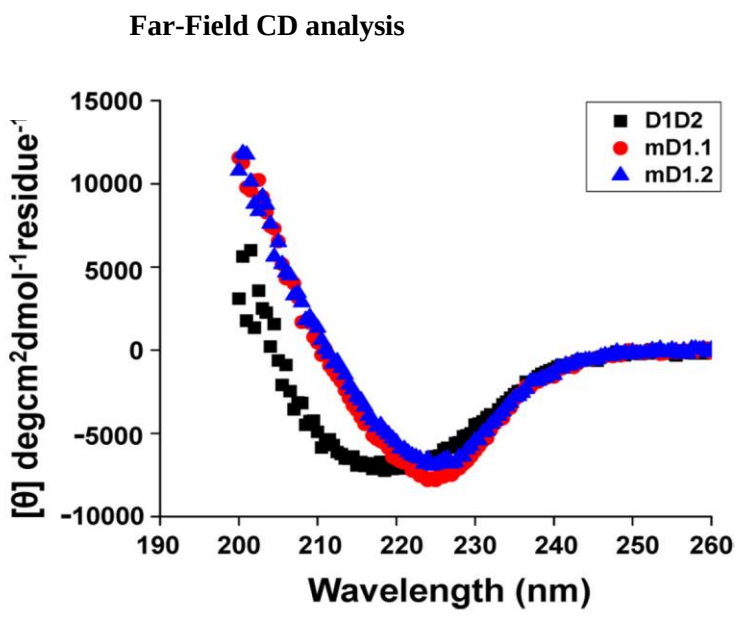

Figure 13: Far-UV CD Analysis

The top figure depicts the far-field CD curve profiles of D1 and D2 at two different concentrations. The signature profile of D2 is observed to closely follow that of reference 2dCD4. Relative to 2dCD4, a shift of the minima towards the right was observed for D1 (from ~214 – ~225 nm). The signature profile of D1 was consistent with data obtained from previous work (left, (Chen et al., 2011).

For voltage versus wavelength plots, see appendix C. d.

The D2 spectrum closely followed that of 2dCD4, and almost overlapped when at equal concentration. Noticeably, with a peak and trough at respectively ~195 nm and ~214 nm, D2 produced a profile which tends to resemble that of a the typical β-strand enriched Fab fragment of γ-immunoglobulin G (Doi and Jirgensons, 1970). This observation correlates with the structure of D2, which as predicted from *in silico* visualisation, Ramachandran plot (see Appendix D) and X-ray crystallography (Ryu et al., 1990), assumes an immunoglobulin topology with abundant β-strands. CD spectra of purified D1 (m1.1) were consistent with the original work on this protein published by Chen and colleagues (Chen et al., 2011) (Figure 14), with the peak and trough profile of a typical β-strand enriched protein observed at approximately 225 nm. However, relative to the 2dCD4 reference, the trough was shifted to the right, with minima at approximately 225 nm. This observation, also consistent in the original work, could be explained by the occurrence of α-helices/loops in D1 which was predicted by the Ramachandran plot (see Appendix C.d).

2.3.4.3. Gp120 Binding Ability of CD4 variants

The functionality of D1 (m1.1) was confirmed by demonstrating robust binding to gp120 along with several other CD4 variants (Figure 15). It was observed that all CD4 variants, with the exception of the 2dCD4-CAΔ, bound gp120. Since both 2dCD4-D1A and 2dCD4-D2A bind gp120, at least one of the disulphide bonds is required for the preservation of the gp120 binding site.

As described by Chen and al., attributable to its small size and higher solubility, D1 (m1.1) had significantly greater affinity for gp120 as compared to two-domain CD4 variants (Chen et al., 2011). Comparison of equimolar amounts of D1 (m1.1) to 2dCD4 variants (mass ratio D1 to 2dCD4 is approx. 1:2) in our experiments served to confirm the observation.

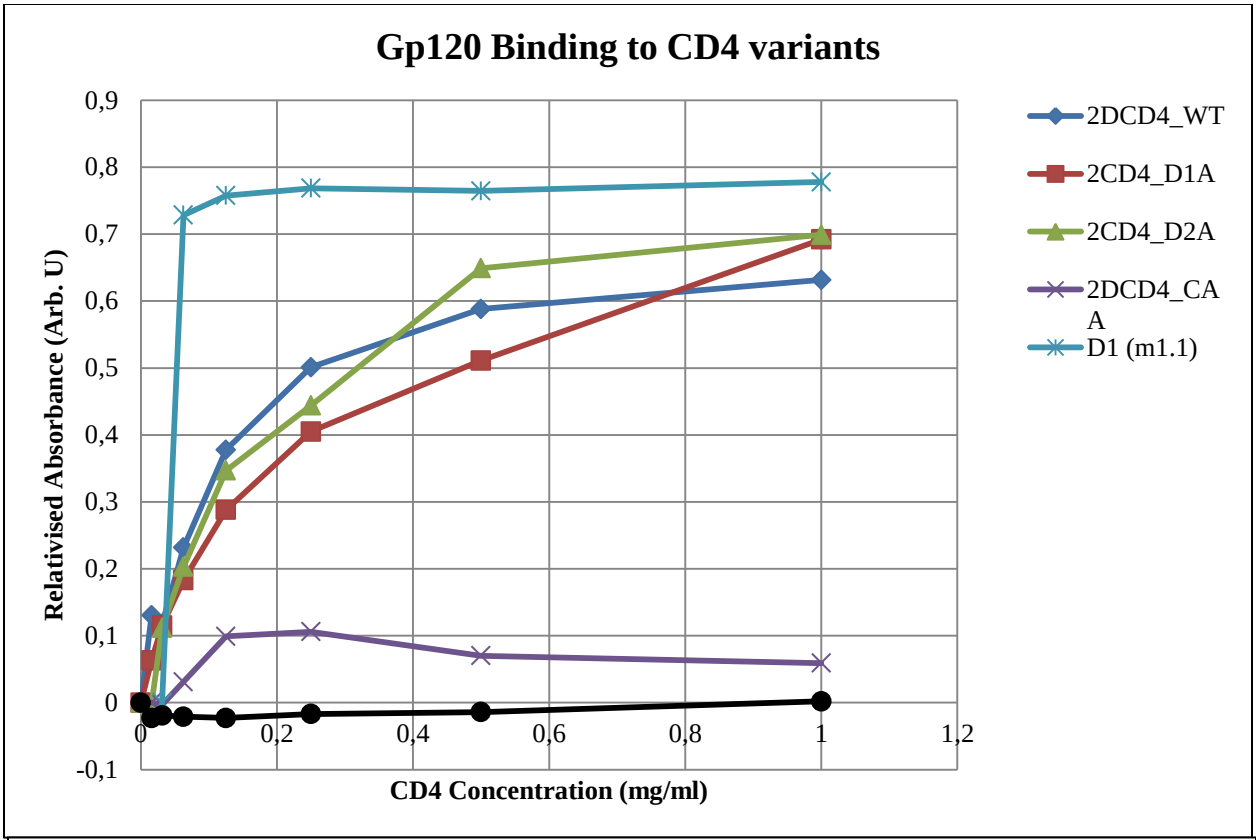

Figure 14: Gp120 Binding of CD4 variants

Gp120 binding to CD4 variants confirm their functionality. Gp120 bound to CD4 undergoes conformational changes that reveal the CD4i epitopes. CD4i can be probed subsequently using the 17b monoclonal antibody, and hence confirms the gp120-CD4 complex. With the exception of 2dCD4-CAΔ, all of the variants allowed for gp120 binding. As defined by Chen et al. (2011), mutant D1 (m1.1) showed high binding to gp120.

2.4. DISCUSSION

The focus of the first part of this study was to express and characterise individual single domains CD4 D1 and D2. These were successfully expressed in bacterial host cells. As described from previous work, initial attempts to express wild-type D1 were unproductive (Chen et al., 2011, Sharma et al., 2005, Chao et al., 1989). The exposure of the hydrophobic surface which normally abuts D2 in the native state (Ryu et al., 1990), is considered the primary factor leading to poor solubilisation and heavy aggregation of D1. Based on previous work (Chen et al., 2011), a mutant D1 (m1.1) with substituted residues at the D1/D2 interface was stably expressed, thus the same protein was expressed in this study. D2 has also been expressed previously (Matthias et al., 2010). While the potential for a recombinant D2 to be poorly soluble was acknowledged, considering that 2dCD4-WT is readily purified in native, soluble form despite exposure of the D2 surface which abuts D3, it was reasoned that the production of a native, soluble form of CD4 D2 would be possible.

In this study however, C-terminal His-tagged D1 (m1.1) and D2 (WT) were expressed in transformed *E.coli* BL21 cell cultures that were incubated overnight with vigorous stirring at 37^{o}C. Overexpression of certain recombinant proteins in *E.coli* can interfere with bacterial metabolism and result in either bacteriostatic or bacteriocidal effects. Abundant expression of either D1 (m1.1) or D2 (WT) in *E.coli* did not have any such negative effects. Localisation of both of the recombinant proteins in the insoluble cellular fraction suggested that both proteins were sequestered in inclusion bodies. Following solubilisation and extensive refolding, the reducing/non-reducing SDS-PAGE and far-field CD analyses indicated that the purified, refolded recombinant CD4 D1 and D2 proteins contained oxidized disulphide bonds and native β-sheeted secondary structures.

Stable and soluble D1 could only be obtained after the introduction of amino acid changes located at the interface of D1/D2 (Chen et al., 2011, Sharma et al., 2005, Saha et al., 2011). This indicates that there exist strong interactions between D1 and D2 in native CD4 or recombinant two-domain 2dCD4. The presence of the large hydrophobic patches at the D1/D2 interface implies hydrophobic interactions and Van-der-Waals' forces contribute mainly to the

maintenance of the structure of D1 in the native state (Ryu et al., 1990). Based on the solvent accessible surface area calculations, five critical residues on D1 that interact strongly with D2 were identified in a previous study (Sharma et al., 2005). The residues, all located at the D1/D2 interface, possessed hydrophobic side chains (V3, L5, I76, L96 and F98). Mutation of the residues to either threonine or alanine served to reduce the hydrophobicity of the D1 surface and therefore eliminate its dependence on D2. Although this version of mutant D1 was successfully expressed and purified in soluble form, biophysical characterisation revealed that the protein did not mimic the natively folded structure: the protein had poor stability at physiological pH (7.4), a three-fold lower affinity for gp120 in comparison to recombinant 2dCD4 and a far-UV CD sprectra indicative of short irregular β-strands. The reference study (Chen et al, 2011) on which the recombinant CD4 domain 1 protein (CD4-D1 (m1.1) used in this study is based, showed that this mutant folded more readily into the native state. As shown in this study by SDS-PAGE and CD analyses, D1 (m1.1) was highly soluble and had stable β-sheeted secondary structure at pH 7.4. Previous studies on D1 (m1.1) showed that this protein was able to bind to both soluble gp120 and MHCII expressing human B-cells, and interfere with HIV infection (Chen et al., 2011). In addition to confirming the robust binding of D1 (m1.1) to recombinant gp120, in this study it was further shown that D1 (m1.1) binds specifically to the monoclonal anti-CD4 antibody mt310, whose epitope is contained wholly within the first domain of CD4. Taken together, these tests further confirmed the structural and functional integrity of D1 (m1.1) purified in this study. The critical residues that had to be mutated to facilitate purification of a soluble CD4 domain 1 protein were established after an intense screen of a large D1 mutant library. D1 (m1.1) was selected from this library based on its stability, solubility and cross-reactivity against different HIV envelopes, and is thus likely to resemble the native structure of CD4 domain 1 as it occurs in the context of the full-length protein. The sites of mutation in D1 (m1.1) (L5I, A55V, I76P, L96I and F98L) overlapped with those from the above mentioned study. Minimising the influence of the largely hydrophobic residues remained the dominant strategy. The mutation to proline could contribute additionally by "kinking" and locally stabilising the polypeptide backbone against the overall globular domain (MacArthur and Thornton, 1991).

Previous studies considered the expression and purification of soluble histidine-tagged D1 from the periplasm of *E.coli* and from the supernatant of mammalian cell cultures (Chen et al., 2011).

Individual wild-type D2 was efficiently expressed, purified and refolded, and the preservation of native CD4 secondary structure was strongly indicated from the CD analyses. Whilst the preliminary studies conducted in this chapter suggested that D2 had attained native β-sheeted secondary structure, further compelling evidence for this would be confirmed by the work described in Chapter 3, which demonstrated that D2 was a target for CD4-specific antibodies. The yield of refolded D2 however, compared to D1 (m1.1), was lower. The exposure of the hydrophobic patch of D2 that normally touches D1 could certainly be the main factor leading to a relatively large amount of protein precipitation observed during the refolding process. Introducing stabilising mutations to improve the solubility and yield of D2 could be considered in the future. However, this would imply the risk of compromising the integrity of the structure and disrupting potential antibody epitopes.

Previous studies have described the use of the *E. coli* expression system for the expression and purification of mutant D1 as insoluble inclusion bodies (Sharma et al., 2005, Saha et al., 2011). Although the use of commercially available recombinant *E.coli* expressed was mentioned (Matthias et al. 2010), the eleborate details for its expression and purification were not described. Whilst the use of mammalian cell culture for recombinant protein expression provides the ideal microenvironment for protein folding and includes post-translation modification, it remains a costly and tedious task. Our laboratory, with much experience with recombinant protein expression in *E.coli*, demonstrated that mutant D1(m1.1) and D2 could be produced in high yields from inclusion bodies, and subsequently purified following solubilisation and extensive refolding process. Aside from the disulphide bonds, domain 1 of CD4 does not include any other post-translation modification (glycosylation, lipidation…). With the established in-house GSH-GSSG containing refolding protocol, and as indicated by SDS-PAGE gels, correct disulphide pairing could be confirmed D1(m1.1) and D2. Furthermore, with the CD- and binding studies that were conducted in this study, the maintenance structural and functional integrity of the recombinant protein is suggested.

The disulphide-reducing and non-reducing treatments followed by SDS-PAGE analysis of D1 (m1.1) and D2 provided insights into the formation of disulphide bonds in D1 and D2. Attention was however focused on the peculiar behaviour of D2. As opposed to D1 (m1.1), treatment with disulphide reducing agent led to the observation of an isomer which migrated faster than the

unreduced form. As evidenced from D1 (m1.1), the expectation was that the fully denatured and disulphide reduced protein resolves at a higher apparent molecular weight due to increased hydrodynamic volume, and proportionally lower electrophoretic mobility.

The structure of D2, and in particular its Cys^{130} – Cys^{159} disulphide link, is contrary to the other CD4 domains or the typical immunoglobulin topology. Rather than inter-bridging the two β-sheets, the disulphide bond links strands within the same sheet (Ryu et al., 1990). Thus, as compared to D1, the C_α - C_α distance between cysteine residues in D2 is usually short (3.84 Å vs. 6.38 Å). Moreover, the orientation of the disulphide bond in D2 is right handed and has high dihedral strain energy (Matthias et al., 2002). High dihedral strain energy coincides with ease in reduction of the bond (Katz and Kossiakoff, 1986). Explaining the unusual behaviour of D2 to disulphide reduction is difficult without further analyses. Investigating the effect of thioredoxin, a redox protein that has been shown to assist in the reduction disulphide bonds of D2 in native CD4 (Matthias et al., 2002, Cerutti et al., 2014), is an area of ongoing research in our laboratory. Further assessment of the individual D2 domain would not only provide further evidence on structural integrity, but also provide insights on the functional role played by the disulphide bond.

Without further investigations, accounting for the presence of the unusual conformation of reduced D2 can be tentatively suggested. The formation of a more condensed structure as a result of the direct or consequent effect of disulphide reduction could be speculated. Rather than acting as a molecular tether that prevents uncoiling of the protein, the disulphide bond could instead act as a separating ‘pillar’ which prevents the collapse of the structure into a more condensed form. The observed high strain energies associated with the disulphide bond in D2 (Matthias et al., 2002, Katz and Kossiakoff, 1986), could in fact be a reflection of the compression of the bond. Alternatively, as a consequence of denaturation and disulphide reduction, as yet undefined interactions in D2 could lead to the occurrence of a more condensed structure, a phenomenon which may represent an important component of the biological function of CD4.

In addition to stabilizing protein structures or acting as catalytic sites for mediating thiol-disulphide interchange reactions, redox active thiol-disulphide elements can induce conformational changes which affect the function of the protein (Schmidt et al., 2006). An intricate understanding of the biochemistry of the disulphide bonds is crucial as they were shown

to be redox active in native CD4 in CD4-expressing cells in culture (Matthias et al., 2002). The presence of free thiols in CD4 on the cell surface of activated T-cells was furthermore demonstrated. Secreted upon activation of the T-cell (Rubartelli et al., 1992), thioredoxin localises at the surface membrane (Wollman et al., 1997) and modulates the disulphide reduction. Interestingly, only the disulphide bond of D2, but not those of D1 and D4, was reduced. In another study which puts forward the domain-swapped CD4 dimer model, the ability of cell-surface CD4 to form dimers due to disulphide cross-linking between D2 domains is described (Maekawa et al., 2006). In the same instance, the elimination of disulphide bonds and prevention of the formation of dimers, were found to critically hinder binding of CD4 to MHCII (Maekawa et al., 2006). Therefore, it can be proposed that activated T-cells secrete thioredoxin which mediates the cleavage of intramolecular disulphide bonds within D2 before intermolecular CD4 linkages can occur (Cerutti et al., 2014). However, it should be stressed such dimers were formed following drastic conformational changes in D2 which led to the swapping of domains (Maekawa et al., 2006).

It was shown that the redox state of the disulphide bond in D2 affected gp120 binding and HIV entry (Matthias et al., 2002, Matthias et al., 2010, Cerutti et al., 2014). In this study, we also attempted to confirm the importance of the redox state of disulphide bonds in recombinant 2dCD4 in terms of gp120 binding. As described in previous sections, 2dCD4 variants were available in our laboratory (Cerutti et al., 2014), and included wild-type (2dCD4-Wt) and the following variants Cys/Ala variants: C16A/C84A, C130A/C159A and C16A/C84A/C130A/C159A. These were respectively termed 2dCD4 (D1A), 2dCD4 (D2A) and 2dCD4 (CΔA). By means of ELISA, the ability of 2dCD4-Wt, -D1A, -D2A, but not -CΔA, to bind to gp120 was confirmed (Cerutti et al., 2014). This indicates that complete ablation of both disulphide bonds, or complete reduction of both disulphide bonds, does not allow for gp120 binding. Previous evidence of viral entry inhibition was demonstrated when either the dithiols of CD4 or the active site of thioredoxin were maintained in a reduced state by trivalent arsenic (Matthias et al., 2002). Trivalent arsenicals, known to react with thiols that are close to each other but not distant ones (Donoghue et al., 2000), prevented further modulation of the redox state of the dithiols. The later study by the same author however described the preference of HIV for disulphide reduced monomers of CD4 during viral entry (Matthias et al., 2010). Rather than chemically inhibiting the redox-activity of the D2 thiol-disulphide, mutants of CD4 with

cysteines of D2 replaced by alanine were expressed on T-cells. HIV infection of these host cells was remarkably enhanced. Taken together, these data underscore the importance of the thiol-disulphide interaction in CD4 D2 for HIV entry.

The next phase of this study involved the generation of a panel of novel anti-CD4 monoclonal antibodies as novel candidate anti-HIV therapies. We also attempted to verify whether such antibodies bound preferably to specific CD4 conformations. Recently, an antibody directed against HER3 (Human Epidermal Growth factor Receptor 3), a critical receptor that when overexpressed leads to oncogenesis, could lock HER3 into an inactive conformation (Garner et al., 2013). In the same analogy, we sought to verify whether certain anti-CD4 antibodies may mediate inhibitory effects by antagonizing specific conformations of CD4 that are required for viral entry.

CHAPTER 3:
ANTI-CD4 ANTIBODIES AS ALTERNATIVE HIV THERAPIES

3.1. INTRODUCTION

Whilst the need for eliciting efficient broadly neutralising antibody (bNAb) responses against HIV following vaccination remains critical, alternative forms of antiretroviral therapy exist. An alternative approach to the problem of viral escape that leads to drug resistance involves shielding the CD4 receptor against HIV by means of an anti-CD4 antibody. In this chapter, we introduce the concept of CD4-targeting monoclonal antibodies as a potential novel class of potent antiviral therapeutic ligand, using Ibalizumab, a recently developed monoclonal anti-CD4 antibody with broad and potent anti-HIV activity, as a prototypical example. We then describe the generation of a new panel of CD4-binding antibodies, and our preliminary data characterizing the domain and isomer specificities of these antibodies, along with their potential therapeutic efficacy in cell culture.

3.1.1. Anti-CD4 Antibodies against HIV

3.1.1.1. Early Development

As early as 1984, shortly after the identification of HIV virus as the aetiological agent of AIDS, it was recognised that the CD4 receptor is a critical requirement for HIV infection (Dalgleish et al., 1984). Faced with difficulties in finding a cure for HIV/AIDS by directly targeting the viral envelope glycoprotein, the idea of inhibiting viral entry by targeting CD4 quickly emerged (Sweet et al., 1991, Capon and Ward, 1989, Auffray et al., 1991). Early experimental anti-CD4 monoclonal antibodies provided very optimistic results in inhibiting viral entry (Healey et al., 1990b, Zeira et al., 1990). Subsequently, as well as developing new anti-CD4 antibodies with the view of inhibiting viral infection, the antiviral activities of existing anti-CD4 antibodies were investigated (Peterson and Seed, 1988). In one example, it was found that the well-established anti-CD4 antibody Leu3a, the epitope for which resides in CD4 domain 1, inhibited viral infection in monocytic cells (Zeira et al., 1990), consistent with the fact that Leu3a binds to an epitope on CD4 that overlaps with the gp120 recognition site. Two other anti-CD4 antibodies (Q425 and Q428), which bind to CD4 D3, were found to inhibit HIV infectivity despite allowing

gp120-CD4 binding (Healey et al., 1990). These antibodies most likely inhibit conformational changes that occur in the receptor complex after initial contact between CD4 and gp120 is made.

3.1.1.2. Immune Suppressive Effects

It is reasonable to suspect that the placement of an antibody on CD4 may compromise the natural role of the receptor in immune modulation. Before the notion of blocking HIV using anti-CD4 antibodies was acknowledged, such antibodies were predicted/known to interfere with immune function, and ultimately lead to T-cell depletion (Cobbold et al., 1984, Goronzy et al., 1986, Dalgleish et al., 1984). In parallel, anti-CD4 antibodies targeting the distal portion of CD4 domain 1 were verified as immune suppressive/modulating agents in the treatment of rheumatoid arthritis (Herzog et al., 1989), a disease that results from aberrant autoimmune responses. Upon treatment of patients with the antibodies, CD4 T-cell counts dropped drastically, but eventually, recovered to normal levels (Herzog et al., 1989). OKT4A, whose epitope was mapped onto domain 1 of CD4 (Peterson and Seed, 1988) is likely to cause viral inhibition by blocking the gp120 binding of CD4. However, once amongst the list of potential therapeutic anti-CD4 mAbs that could possibly inhibit HIV infection, it was soon found that OKT4A is in fact a potent immunosuppressant that can be used during organ transplantation procedures (Delmonico et al., 1993, Cosimi et al., 1990). OKT4A therefore binds to CD4 in a way that prevents the receptor from coupling to MHCII during formation of the CD4-MHCII-TCR antigen presentation complex. An alternate mechanism of immune suppression, as demonstrated whilst using the GK1.5 antibody that targets the analogous mouse CD4 receptor, suggests that a negative signal is transduced from CD4 to directly inhibit T-cell activation, irrespective of whether there is effective antigen presentation or not (Tite et al., 1986). In this scenario, immune suppression arises not directly due to T-cell depletion, but its dysfunction (Carteron et al., 1988). (Anderson et al., 1997)

3.1.2. Description of MHCII-TCR-CD4 interaction

3.1.2.1. MHCII

As far as the intricate interactions between CD4 and MHCII are concerned, it is important to be reminded of the general structure of MHCII (Figure 16). The cell surface molecule MHCII is a heterodimer, consisting of α- and β-monomers. Each monomer is made up of extracellular, transmembranal and cytoplasmic portions. The extracellular portion of each of the monomers is divided into two domains: with respect to the cell surface membrane of the APC (antigen presenting cell), α_1 and β_1 domains are most distal, while α_2 and β_2 are most proximal. The association of the α_1 and β_1 domains form the cusp into which the peptide that is being presented inserts. The α_2 and β_2 abut the unexposed domains of α_1 and β_1, and form the length of the extracellular portion of MHCII.

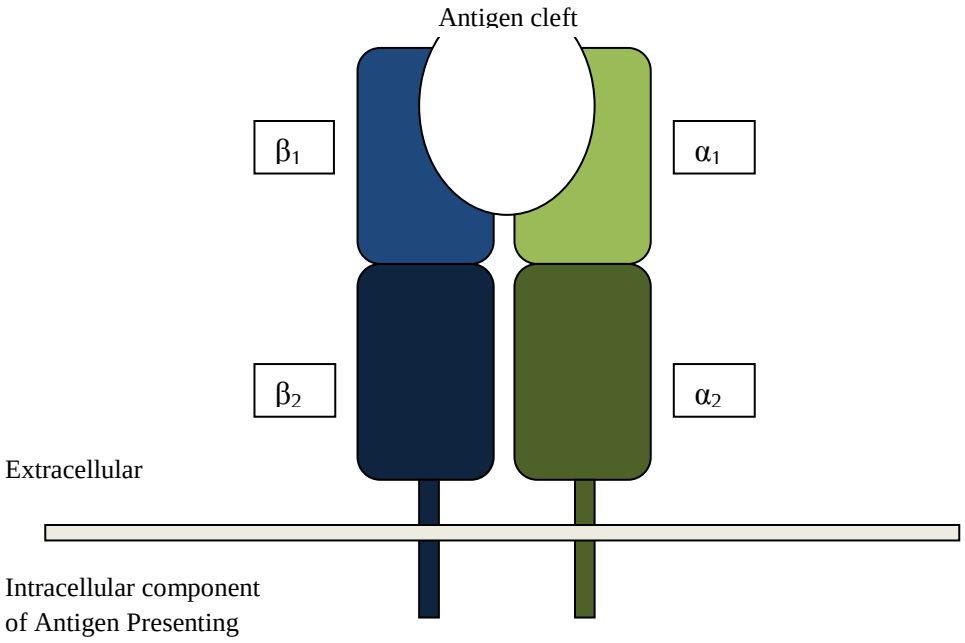

Figure 15: Depiction of MHCII

MHCII is a heterodimer, consisting of monomers α- and β. The α_1 and β_1 domains, which are most distal, form the cusp in which processed antigen is presented to the $CD4^+$T-Cell.

3.1.2.2. MHCII-CD4 interaction

In order to understand the implications in terms of immune suppression as a result of the placement of an antibody on CD4, an overview of the CD4 interaction in the immunological synapse is necessary. Depicting the elaborate interactions, the crystal structure of a two-domain CD4 (2dCD4) in association with MHCII (Wang et al., 2001) provides invaluable information on the potential sites on CD4 that if blocked, could lead to immunosuppressive effects.

The crystal structure of the 2dCD4 – MHCII complex shows the interaction of CD4 with the α_2 and β_2 domains of MHCII (Figure 17) (Wang et al., 2001). With respect to CD4, all direct contacts between the two molecules arise from D1. D2 is placed away from the interaction point and does not contribute to any contact. The portion of D1 comprising Phe^{43}, the C" strand, and the short α-helical segment between strand D and E defines the MHCII contact surface of CD4. Intriguingly, the observed interaction between CD4 and MHCII nearly resembles that between CD4 and gp120 (Kwong et al., 1998). This part of CD4 inserts into the cognate CD4-binding site on gp120. The Phe^{43} inserts into a conserved hydrophobic pocket formed between the α_2 and β_2 domains of MHCII. This interaction saliently resembles the interaction of CD4 with gp120, whereby the aromatic ring of Phe^{43} inserts into a hydrophobic pocket formed at the interface of the inner and outer domains. Besides Phe^{43}, other critical residues in the interaction between CD4 and MHCII include Lys^{35}, Lys^{46} and Arg^{59}, and the latter also plays a fundamentally important role in stabilizing the CD4-gp120 interaction. Seemingly, the near identical mimicry in the mechanisms by which CD4 binds to MHCII and to gp120, poses a major limitation to the generation of anti-CD4 antibodies. Whilst these can effectively inhibit HIV infection, they are likely to have immunosuppressive effects by preventing normal CD4 – MHCII interactions.

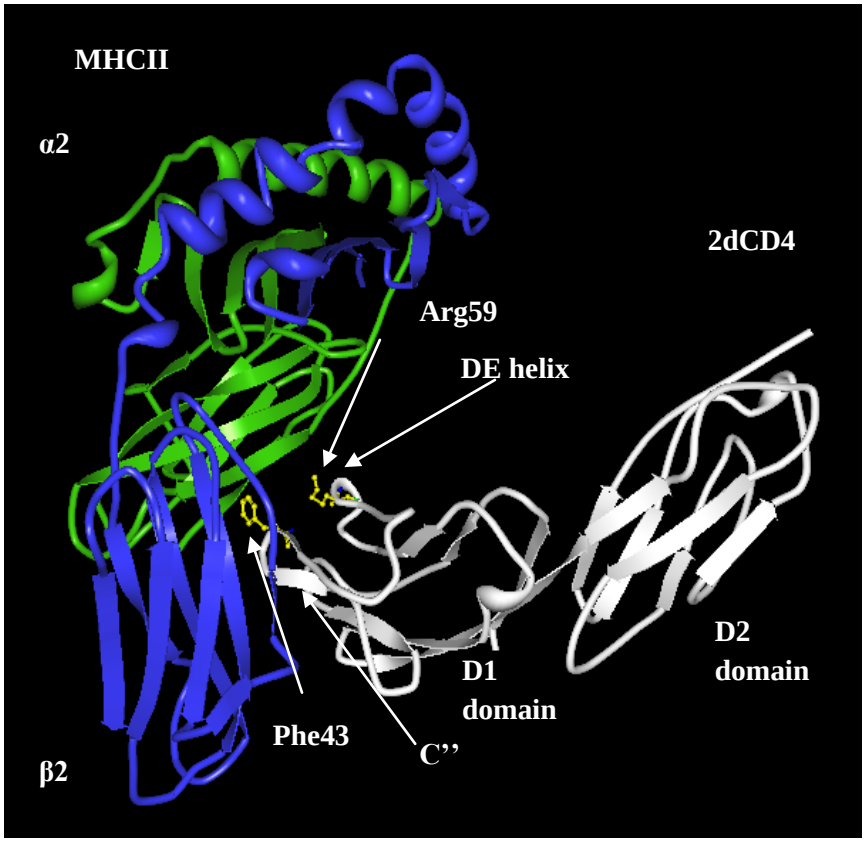

Figure 16: Crystal structure of the MHCII-CD4 interaction, from Wang et al., 2001 (PDB 1JL4)

Strictly the domain 1 of CD4 forms contact with MHCII at the junction of the α_1 and β_2. Interaction of D1 includes Phe^{43}, C'' strand, and the short α-helical segment between strand D and E.

Green: α2 domain of MHCII

Blue: β2 domain of MHCII

White: 2dCD4

3.1.2.3. MHCII-CD4-TCR Interaction

The crystal structure of the TCR-MHCII-CD4 complex procured the visualisation of the interaction (Figure 18, 19) (Yin et al., 2012). The complex forms a V-shaped structure. Extending from the apex, one of the arms of "V" is defined by the peptide-presenting MHCII bound to the distal domains of the TCR. The other arm is represented by the elongated four-domain CD4, which associates with the proximal portion of MHCII via its N-terminal domain 1. From this picture, if a horizontal line representing the cell surface membrane of the T-cell is drawn to complete the "V" into a triangle, the angles between TCR – horizontal, CD4 – horizontal, and CD4 – MHCII are 60^o, 70^o and 50^o, respectively. Despite not directly binding to the MHCII binding site of D1, the potential for anti-CD4 antibodies to impose physical constraints that prevent the formation of the triangular immunological synapse is appreciable. Logically, with widening of the triangular space from the apex to the imaginary T-cell surface membrane, it can be presumed that the degree of steric restriction lessens if an antibody is

directed towards the more proximal domains of CD4. A superimposition of the MHC-bound CD4 over unbound CD4 showed minimal angular variations between the domains (Wu et al., 1997). This is suggestive of the rigid nature of CD4, with flexibility only potentially occurring at the base of CD4 between D4 and the transmembrane domain (Moir et al., 1996). In this case, an antibody directed towards the most proximal domains (D3/D4) could interfere with the tilt required by CD4 to make contact with MHCII.

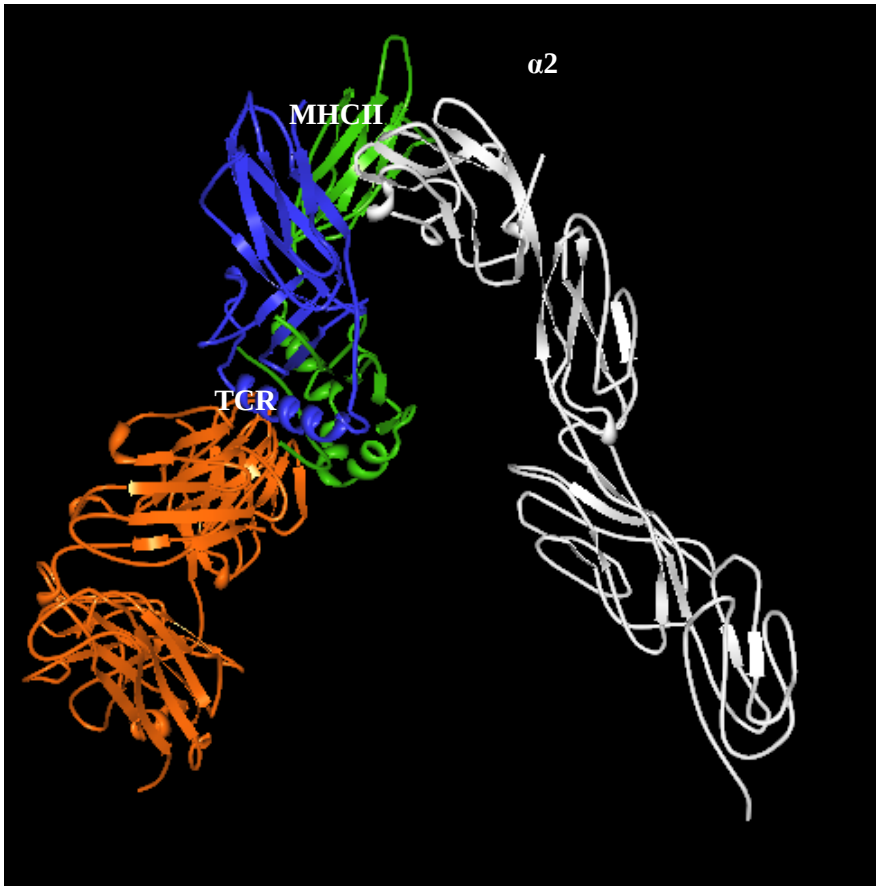

Figure 17: Crystal structure of CD4, MHCII and TCR complex, from Yin et al., 2012 (PDB 3T0E)

Green: α2 domain of MHCII; Blue: β2 domain of MHCII; White: 2dCD4; Orange: T-Cell Receptor

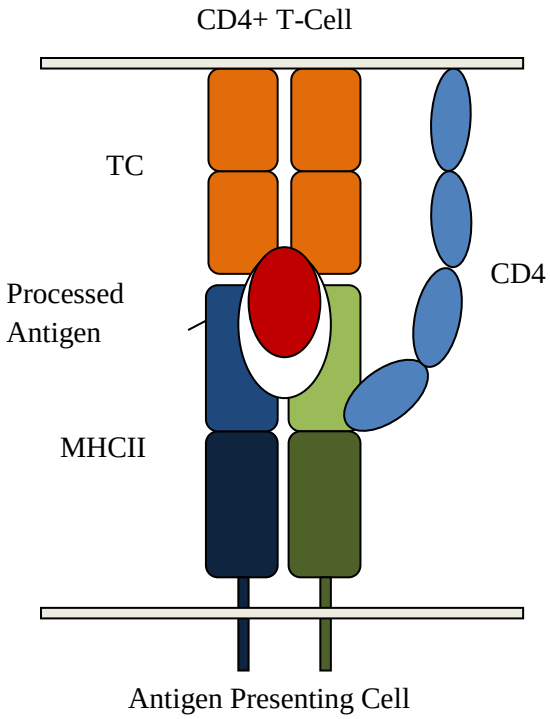

Figure 18: Immunological Synapse

Diagrammatic representation of the immunological synapse comprising the TCR-MHCI-CD4 complex. The elongated CD4 makes contact with MHCII as it presents the antigen to the TCR. This synergy allows the reinforcement of the transduction signal to initiate the T-cell response.

3.1.3. Ibalizumab: Model Anti-CD4 Antibody against HIV

3.1.3.1. Drug Discovery and Development

Out of one of the early experiments in the development of HIV-inhibitory anti-CD4 antibodies emerged the anti-CD4 murine monoclonal antibody 5A8 (Mu5A8 mAb) (Burkly et al., 1992) - the precursor to Ibalizumab. The epitope for Mu5A8 mAb, generated by immunising mice with CD4+ CHO cell transfectants, was mapped to domain 2 of CD4 and could potently hamper HIV infection. Most importantly, the antibody Mu5A8 was unique in that its antiviral effect was observed despite allowing for gp120-CD4 binding both in T-cells and sCD4 (Burkly et al., 1992, Moore et al., 1992). The antiviral effect, as indicated when observing the failure of Fab fragments of Mu5A8 to inhibit viral infection, was attributed to the ability of Mu5A8 to sterically block the conformational changes in either CD4 or gp120 required for viral entry following gp120-CD4 binding[1]. Upon further investigation however, a "hetero-antibody"

[1] Such effect was in fact an artifact arising from the limited number of viral strains used. See section 3.1.3.3

(antibody comprising of two different Fab) consisting of 5A8 and an irrelevant control Fab could not inhibit viral infection despite binding to CD4, as opposed to bivalent Mu5A8 (Burkly et al., 1992)[2]. This could suggest that steric constraints are insufficient to explain the inhibitory effect of this antibody. In fact, it was shown that upon incubation of sCD4 and Mu5A8 mAb with virus, as opposed to the domain 1 binding 6H10 antibody that caused gp120 dissociation, a ternary structure consisting of gp120-CD4-Mu5A8 can actually exist (Moore et al., 1992). As suggested, it is possible that Mu5A8 functions by blocking conformational changes in CD4 that are critical for viral entry.

Most importantly, shortly after its discovery, Mu5A8 mAb was tested *in vivo* and was found to have no immunosuppressive effects (Reimann et al., 1993). After the initial *in vitro* test confirming that Mu5A8 mAb was capable of binding to rhesus macaques CD4 with comparable affinity to that of human CD4, and could inhibit simian immunodeficiency virus (SIV) replication *in vitro,* Mu5A8 was administered intravenously into animals. CD4 T-cells were effectively coated by Mu5A8 and throughout the experiment, CD4+ cell numbers were maintained at normal physiological levels. The functionality of the cell-mediated and the humoral immune responses as a whole was confirmed by verifying proliferation of extracted peripheral blood mononuclear cells (PBMCs) and maintenance of the level of anti-tetanus toxoid antibodies. These promising results obviously were surprising as previous studies have described general ablation of the immune system in mice models treated with an anti-CD4 analogue antibody as result of CD4 T-cell clearance (Goronzy et al., 1986, Alters et al., 1990). In fact, upon administration of Mu5A8 in the monkeys, an almost immediate peak in circulating CD4+ T-cells was observed prior to a steady drop to adequate levels (Reimann et al., 1995, Reimann et al., 1993).

As expected, the study was extended to confirm actual viral clearance in non-human primates (Reimann et al., 1995). Rhesus macaques that had been chronically infected with SIV_{mac} displayed drastic decreases in provirus levels following Mu5A8 mAb treatment, as opposed to controls which received irrelevant antibody. Interestingly, viral clearance correlated to initial CD4+ T-cell levels: monkeys having higher levels of T-cells were able to eliminate SIV provirus

[2] Possible artefact as well. See section 3.1.3.3

much more rapidly. However, the functionality of the T-cells also drove the clearance of the Mu5A8 mAb due to the strong anti-murine response encountered, resulting in rapid clearance of the antibody (Reimann et al., 1993, Reimann et al., 1995). Hu5A8, a humanised form of Mu5A8, displaying much lower antigenicity, and was able to remain in circulation for weeks prior to viral detection and clearance (Reimann et al., 1997). Moreover, Hu5A8 maintained identical properties to the murine version in terms of binding affinity to human or monkey CD4, inhibition of both HIV and SIV, and non-immunosuppressive effects. From there, it was indicated that Hu5A8 would be tolerated in humans. Pharmaceutical grade Hu5A8 mAb was produced and used as part of an official good-laboratory practice pre-clinical trial demonstrated tolerability and safety of the antibody in chimpanzees (Boon et al., 2002).

Hu5A8, termed TNX-355, as antiviral therapy in the treatment HIV infected patients mirrored the optimistic results obtained from previous *in vitro* and non-human primate studies (Kuritzkes et al., 2004). Cohorts of HIV-1 infected patients (T-cell count >100 cells/mm^3, viraemia $\geq$ 5000 RNA copies/mL), treated with increasing amounts TNX-355 (0.3 – 25 mg/kg), showed significant dose-dependent decreases in HIV-1 plasma RNA, which were maintained as long as the CD4+ T-cells remained coated with TNX-355. CD4+ T-cell levels immediately peaked following treatment and no immunosuppressive effects were observed. TNX-355 was not immunogenic in humans, and was well-tolerated with minimal adverse effects. Under the current name Ibalizumab (TaiMed Biologics), respective decreases and increases in viraemia and CD4+ T-cells have been observed and verified, whilst safety and tolerance in both healthy and infected subjects of the drug was confirmed (Jacobson et al., 2009, Norris D, 2006, Khanlou H, 2011, TaiMed_Biologics_Inc, 2011).

3.1.3.2. Epitope Mapping of Ibalizumab

From the initial studies describing the discovery of the anti-CD4 antibody currently known as Ibalizumab, it was found by means of mutagenic expression of chimeric human/mouse CD4 molecules, that the antibody was directed towards the stretches of residues 121 – 124/ 127 – 134 in domain 2 of CD4 (Burkly et al., 1992). With the progression of Ibalizumab into phase II

human clinical trials, parallel studies sought to gain further insight on the mechanism of action of the mAb by refining the definition of its epitopes. Extending the use of mouse/human chimeric CD4 molecules, point mutations that were introduced into domains 1 and 2 were found to be important for Ibalizumab binding to CD4 (Song et al., 2010). These residues were located at the interface of CD4 domain 1 and 2. As well as being located in domain 2 (Leu^{96}, Pro^{121}, Pro^{122}, Gln^{163}), two of the 6 identified residues were found in domain 1 (Glu^{77}, Ser^{79}). While not directly involved in making contact with the antibody, certain of these residues may play a role in maintaining the conformation of Ibalizumab's binding epitope.

Recently, the crystal structure of the Fab fragment of 5A8/Ibalizumab bound to two domain CD4 (2dCD4) was solved (Figure 20) (Freeman et al., 2010). The overall picture depicted the binding of the Fab fragment to an epitope spanning D1 and D2. Consistent with the original mutagenesis-based epitope mapping studies (Burkly et al., 1992), Ibalizumab was found to interact primarily with residues 121 – 125 of the BC-loop of D2 through an extensive hydrogen bonding network. Additionally, structural analysis showed the insertion of the tip of the BC loop of CD4 D2 between the light and heavy chains of the CDR (complement determining region) of Ibalizumab, in which Pro^{122} makes extensive contact with the light-chain. The residues 164 – 165, located on the short FG loop of D2, were confirmed as further key contacts interacting with the heavy chain of Ibalizumab. Contacts in domain 1 were confirmed, with residues Ser^{79} and Glu^{77} in the EF loop interacting with the tip of the light-chain.

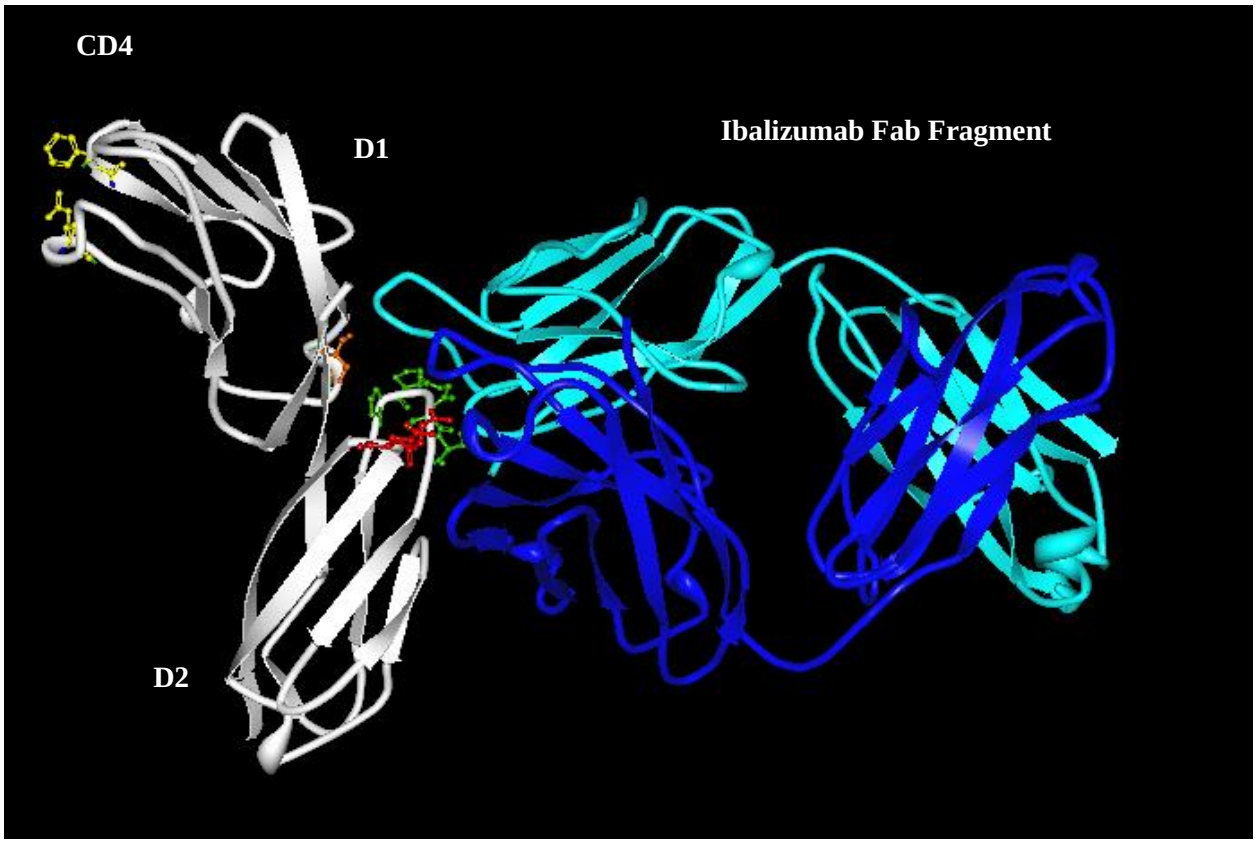

Figure 19: Crystal Structure of the Ibalizumab Fab Fragment bound to 2dCD4, from Freeman et al., 2010 (PBD: 3O2D).

Depiction shows interaction of the Fab Fragment with the BC-loop of D2 (Green). Other interactions with D2 include residues 164 and 165 of the FG loop (Red). Ser79 and Glu77 of D1 also seem to be involved in the interaction (Orange). It should be noted that Phe43 and Arg59 of D1 (Yellow), critical in gp120 and MHCII binding, are located distant and are not involved in the interaction.

H-chain of Fab: dark blue; L-chain of Fab: Light Blue

3.1.3.3. Mechanism of Action of Ibalizumab

The mechanism of action of Ibalizumab as a viral entry inhibitor and non-immunosuppressive agent is still poorly understood. From the recent crystal structure of the Ibalizumab Fab fragment coupled to 2dCD4, it is clear that the binding site of Ibalizumab on CD4 does not correspond to the binding site of gp120 or MHCII (Freeman et al., 2010). Consistent with this, Ibalizumab presence on CD4 does not prevent gp120 binding (Burkly et al., 1992, Moore et al., 1992). Several theories have been proposed to explain these favourable properties of Ibalizumab.

Firstly, based on preliminary work on Mu5A8, it was indicated that through the inability of Fab fragments to inhibit viral infection as opposed to IgG, steric restriction preventing post-binding events was at play (Burkly et al., 1992). However, new studies elaborating on the matter describe both the Fab fragment and IgG as capable of blocking viral infection, dependent on the viral strains tested (Freeman et al., 2010). Additionally, full-length bivalent Ibalizumab antibody, which showed equivalent ability to inhibit viral infection as a Fab fragment, was determined not to be absolutely required. The previous observations could therefore have been due to an artefact arising from the limited number of viral strains used (Moore et al., 1992, Burkly et al., 1992). Nevertheless, steric restriction of conformational events post gp120-CD4 binding may still be a valid explanation for those viral strains where the IgG form inhibits viral entry more effectively than the Fab fragment.

The second suggestion relates to the ability of Ibalizumab to either a) trigger conformational changes in the CD4 molecule that limit viral entry, or b) prevent subsequent conformational changes in CD4 that allow viral entry. Interestingly, it was observed that the binding of Ibalizumab to CD4 induced a flip in the peptide bond between Asn^{164} and Gln^{165} in domain 2 (Freeman et al., 2010). This resulted in only a local conformational change that led to the stabilisation of hydrogen bonds between the Fab fragment and the corresponding residues of CD4 domain 2. Such a change however, might be insufficient to explain the mechanism of viral entry inhibition.

Furthermore, major conformational changes are visualised in gp120 that is bound to CD4 (Kwong et al., 1998), whereby there is exposure of CD4-induced binding sites and gp41. No such drastic changes are observed in CD4 in the gp120-CD4 crystal structure, although inducible conformational changes in bound CD4 have been suggested (Denisova et al., 1997). As mentioned in the previous chapter, in order that CD4 bound virus might enter the host cell, the CD4 molecule needs to be able to drastically flex towards the T-cell surface membrane. The mechanism of this is still largely unknown (see chapter 1), but it is an intriguing possibility that Ibalizumab exerts its antiviral effects by inhibiting such changes in CD4.

Finally, studies by others and in our laboratory have shown that the redox state of thiol/disulphide bond Cys130-Cys159 of CD4 domain 2 plays a critical role in gp120-CD4 binding and viral entry (Matthias et al., 2002, Cerutti et al., 2014), and that significant

conformational differences exist between reduced and oxidised isoforms of CD4 (Cerutti et al., 2014). In particular, these studies have shown that HIV only binds efficiently to CD4 containing reduced D2 cysteines. It is thus notable that Cys125 is located within Ibalizumab's epitope and an intriguing possibility that Ibalizumab exerts its antiviral effects by interfering with the dynamic redox regulation of the CD4 D2 disulphide that is required for viral entry.

3.1.3.4. Resistance to Ibalizumab

During phase II clinical trials, Ibalizumab has shown considerable promise as a viral entry inhibitor in the treatment of HIV infection (Jacobson et al., 2009, Norris D, 2006, Khanlou H, 2011, TaiMed_Biologics_Inc, 2011). By binding to CD4 instead of the hypervariable regions on HIV gp120, Ibalizumab may provide a greater barrier to viral escape than ligands that are targeted to gp120. Nevertheless, viral resistance to Ibalizumab did eventually emerge in several of the pre-clinical and clinical trials mentioned above. SIV isolated from rhesus macaques before and after treatment with hu5A8 showed clear reduction in neutralisation sensitivity (Reimann et al., 2002), and reports from a phase II clinical trial described viral RNA in plasma increasing to baseline levels within about two months despite continuous Ibalizumab treatment (Jacobson et al., 2009). When tested *in vitro*, the isolated virus was effectively shown to have significantly reduced sensitivity to Ibalizumab. It was determined that resistance correlated to viral mutations entailing the loss of asparagine-linked glycosylation sites in the variable region 5 (V5) of gp120 (Toma et al., 2011, Pace et al., 2013). Resistance to Ibalizumab in patients is likely due to negative selection and propagation of the viral strains that naturally had the variation beforehand (Pace et al., 2013). The mechanism by which such mutations allow viral escape is still yet to be confirmed.

3.1.4. Project Objectives

Despite the demonstrable potential of anti-CD4 antibodies as alternative HIV therapies, Ibalizumab is currently the only acknowledged existing anti-CD4 antibody that inhibits viral

entry without resulting in immunosuppression. However, with resistance to Ibalizumab being reported, it is critical to begin looking for alternatives.

In this chapter, we sought to develop novel Ibalizumab-like anti-CD4 antibodies that could inhibit HIV whilst being non-immunosuppressive. Following the immunization of mice with recombinant mammalian 2dCD4, supernatants from a panel of 40 monoclonal antibody-generating hybridomas, were screened for such properties. Using the panel of recombinant CD4 variants described in Chapter 2, we determined firstly the domain specificities of the antibody supernatants. Due to the importance of the redox state of the disulphide bonds in CD4, we also attempted to verify whether antibodies had altered binding affinity for disulphide defective mutants. We then established the gp120 inhibition properties of the antibody supernatants *in vitro*. Finally, we then confirmed such observations using pseudovirion inhibition assays.

3.2. MATERIALS AND METHODS

For detailed recipes of standard buffers and solutions, please see Appendix A.

3.2.1. Generation of Monoclonal Anti-CD4 Antibodies Producing Hybridomas

The production of monoclonal anti-CD4 antibodies was outsourced to ProMab Biotechnology, Inc (California, U.S.A). Purified 2dCD4-WT (expressed in *E. coli*) was used to immunise BALB/C mice. Following immunisation, hybridoma selection and propagation, 1 ml samples of supernatants derived from 40 cultures were received and stored at -80˚C for further analyses. These 40 antibody-containing supernatants samples were selected by the manufacturer based on the strengths of their reactivities with 2dCD4, a number defined per contract prior to immunization. The hybridoma supernatants were designated CD4MAb1 – 40.

3.2.2. Detection of Anti-CD4 Antibodies in Hybridoma Supernatants

3.2.2.1. Screening against Recombinant Expressed 2dcd4 (WT)

A preliminary 'broad-screen' ELISA was conducted in order to confirm the presence of CD4-specific antibodies in 40 hybridoma supernatants received from ProMab Biotechnologies. In order to assess data statistically, triplicates of experimental wells were used. Using 100 µL per well, recombinant 2dCD4 (Wt) in 1 x PBS (Sigma-Aldrich, MO, U.S.A) was coated onto a 96-well plate (Flat-bottom/ MaxiSorp, Nunc®, Denmark) at 1.0, 0.5 and 0.2 µg/mL for 1h at room temperature. Control wells were coated with 100 µL of 1 x PBS. The coating solutions were removed and 250 µL of blocking reagent (1% BSA in T-PBS) (Sigma-Aldrich, MO, U.S.A) was added to each coated well, and the plate was incubated for 1 hour at room temperature. Blocking buffer was removed and 100 µL of each hybridoma supernatant (1:2 – 1:15625 dilutions in T-PBS) was added to 2dCD4-coated wells for 1 hour at room temperature. The supernatants were removed and wells washed 5 times with T-PBS. A goat anti-mouse HRP-linked antibody (100 µL at 1:2000 in PBS-T; GE Healthcare, UK) was added to each well and the plate was incubated

for 1 hour at room temperature. Wells were washed 5 times with T-PBS before the addition of 100 µL of TMB-Ultra chromogenic substrate (Thermo-Pierce, U.S.A). The plate was incubated for 20 minutes at 37^{o}C on a rotary plate (600 rpm). To stop the chromogenic reaction, 100 µl of sulphuric acid solution (2 M) was added to each well. The absorbencies of the wells at 570 nm (A_{570}) were determined using a plate reader (Fast read, 570/450 nm measure filter, 37^{o}C Bio-Rad Model 650 Microplate reader, CA, U.S.A).

3.2.2.2. Low-Resolution Epitope Mapping: Elucidation of CD4 Antibody Domain Specificities

Bacterially expressed D1 (m1.1), D2, 4dCD4-WT and 4dCD4-D2A, as well as 2dCD4 (WT), mutant 2dCD4 (D1A), mutant 2dCD4 (D2A) and mutant 2dCD4 (CΔA), were used to determine the domain specificities of each monoclonal antibody-containing hybridoma supernatant. In order to assess data statistically, triplicates of experimental wells were used. One hundred microlitres (100 µL) of each recombinant CD4 variant at 1.0 µg/mL in PBS was used to coat the wells of 96-well plates (Flat-bottom/ MaxiSorp, Nunc®., Denmark) for 1h at room temperature. In order to exclude the possibility that any of the antibodies were directed to a His-tag epitope (present on the C-terminus of the immunogen), a recombinant His-tagged gp41 protein, was additionally coated in parallel. Control wells (blanks) were coated with 100 µL of 1x PBS (Sigma-Aldrich, MO, U.S.A). Thereafter the plates were processed as described above to detect CD4-bound antibodies, with 100 µL of each supernatant (1:50 µg/ml in T-PBS) used in the first probing step.

3.2.2.3. CD4-Gp120 Binding Assay

An ELISA assay was used to verify whether the antibodies could potentially inhibit binding of gp120 to CD4 binding *in vitro*. In order to assess data statistically, triplicates of experimental wells were used. One hundred microlitres (100 ul) of 4dCD4 (WT) (1 µg/mL in 1x PBS) was coated onto 96-well plates (Flat-bottom/ MaxiSorp, Nunc®, Denmark) for 1h at room temperature. Control wells were coated with 100 µL of 1x PBS. The coating solutions were

removed and 250 µL of blocking reagent (1% BSA in T-PBS) (Sigma-Aldrich, MO, U.S.A) was added to each well. Plates were incubated overnight at 4^{o}C. The blocking reagent was removed and 50 µL of each supernatant (1:50, 1:500 1:5000 dilutions in T-PBS) were added to corresponding wells. Following a 1 hour incubation, 50 µL of recombinant HIV-1 $gp120_{bal}$ (400 ng/mL) in T-PBS was added to wells, which were incubated for a further 1 hour at room temperature. The wells were washed 5 times with T-PBS and 100 µL of the monoclonal anti-gp120 antibody 2G12 (0.1ug/ml) was incubated in each well for 1 hour. The following reagent (2G12) was obtained through the NIH AIDS Reagent Program, Division of AIDS, NIAID, NIH: HIV-1 gp120 Monoclonal Antibody (2G12) from Dr Hermann Katinger (Buchacher et al., 1994, Trkola et al., 1996, Mascola et al., 1999, Etemad-Moghadam et al., 1999, Crawford et al., 1999). Wells were washed 5 times with T-PBS and 100 µL of a secondary HRP-conjugated sheep anti-human antibody (GE HealthCare, UK) was added to wells. Following 1h incubation, the wells were washed 5 times with T-PBS before adding 100 µL of TMB-Ultra substrate (Thermo-Pierce, U.S.A). The plate was incubated for 20 min at 37^{o}C on a rotary plate (600 rpm), and 100 µl of sulphuric acid solution (2 M) was added to wells to stop the reaction. The absorbencies of the wells at 570 nm (A_{570}) were determined using a plate reader (Bio-Rad Model 650 Microplate reader; fast read, 570/450 nm measure filter, 37^{o}C).

3.2.3. HIV-1 Pseudovirion Inhibition Assay

3.2.3.1. Determination of Working Viral Dilution

The inhibitory effects of the anti-CD4 antibodies on HIV replication were assessed by an HIV-1 pseudovirion inhibition assay. ZM53M.PB12, SF162.LS and TZM-bl cells were kindly provided by Dr Mark Killick.

TZM-bl cells stably express large amounts of CD4 and CCR5 (NIH AIDS Reagent Program, Cat. 8129), making it a recommended cell-line for assessment of HIV infection *in vitro*. TZM-bl cells have also been genetically modified to allow for the detection of HIV infection and replication using luciferase as a reporter. During viral integration in the host DNA, the viral

promoter drives the overexpression the luciferase, which can be subsequently detected using luciferase detection methods.

ZM53M.PB12 (obtained from Drs E. Hunter and C. Derdeyn) and SF162.LS (obtained from Dr D. Monefiori, Laboratory for AIDS Vaccine R&D, Duke University Medical Center) were produced using $pSG3^{\Delta env}$ (Dr John C. Kappes and Xiaoyun Wu) backbone and complementing Env(gp160)-expressing plasmids. Throughout, as short handedness, we shall refer to ZM53M.PB12 and SF162.LS as ZM53 and SF162 respectively.

In 25 cm^2 Nunc culture flasks, TZM-bl cells were grown in growth media (DMEM; 10% FCS (Biochrom Heat Inactivated FCS, UK), 1x Glutamax, 100 units of Penicillin and 0.1 mg/ml of Streptomycin) (Sigma-Aldrich, MO, U.S.A) until they reached approximately 90% confluence. Cells were gently washed with 1 x PBS, trypsinized (0.05% Trypsin-EDTA) (Sigma-Aldrich, MO, U.S.A) and resuspended in growth media. Following counting with a haemocytometer and Trypan Blue (Gibco©, LifeTechnologies, CA, U.S.A), cells were seeded into a 96-well culture plate (ThermoScientific™ Nunc™ MicroWell™ 96-Well Microplate/ Nunclon™-D, Denmark) at 10^5 cells per well in 100 µL of media. The initial concentrations of ZM53 and SF162 were respectively 1.95 x 10^6 and 8.75 x 10^5 TCID50. In order to determine working concentrations of SF162 and ZM53 pseudovirions ($TCID_{50}$), a 10 X serial dilution of pseudovirus stocks (1:10 – 1:10000) was prepared in growth media supplemented with 80 µg/mL of DEAE-Dextran (Sigma-Aldrich, MO, U.S.A). Fifty microlitres of the diluted virus samples were added per well. Cell control wells received virus-free growth medium. Volumes of wells were made up to a total of 200 µL with growth media. Plates were incubated for 48 hours at 37°C/5% CO_2, following which the culture medium was aspirated and discarded. Wells were washed once with 1x PBS (Sigma-Aldrich, MO, U.S.A), one hundred microlitres (100 µL) of Glo-Lysis buffer (Promega, WI, U.S.A) was added per well and with occasional gentle rocking, and the plate was incubated for 5 minutes at room temperature. Fifty microlitres (50 µL) of the lysate was extracted per well and transferred to white luminometer plates (Promega, WI, U.S.A). An equal volume of reconstituted Bright-Glo™ Assay reagent (Promega, WI, U.S.A) was then added to the cell lysate and the reactions were incubated for a further 5 minutes at room temperature.

Luminescence was recorded using a luminometer (Veritas Microplate Luminometer, Promega, WI, U.S.A) calibrated for the Bright-Glo™ assay protocol.

3.2.3.2. Viral Assay

As described above, 10^5 of resuspended TZM-bl cells in 100 µL media were seeded per well of a 96-well culture plate (ThermoScientific™ Nunc™ MicroWell™ 96-Well Microplate/ Nunclon™-D, Denmark). In order to assess data statistically, triplicates of experimental wells were used. Concentrated hybridoma supernatants of samples were added to corresponding wells at a dilution of 1:15 in a total of 150 µL per well. Positive control anti-CD4 antibody (mt310) was added to final concentration of 1.33 µg/mL in 150 µL per well. A serum sample (M79) derived from rabbits immunized with a recombinant gp120-CD4 complex, which shows potent antiviral effects *in vitro,* was kindly provided by Dr Mark Killick. This would be used as positive control for comparison with the panel of CD4MAbs. Wells free of antibody/supernatant/serum served as negative controls. Plates were incubated for 2 h at 37°C/5% CO_2 to allow for anti-CD4 antibody binding, following which 50 µL of virus in DEAE-Dextran (Sigma-Aldrich, MO, U.S.A) supplemented media was added to experimental and viral control wells. Cell controls without virus were made to 200 µL with DEAE-supplemented media. The final dilutions of virus and DEAE-Dextran per 200 µL volume were respectively 1:500 (3900 TCID50 for ZM53; 1750 TCID50 for SF162) and 20 µg/mL (For TCID determination, see Appendix F). Plates were incubated for 48 h at 37°C/5% CO_2, and luciferase activity measured by the procedures described above.

3.3. RESULTS

3.3.1. Screening Supernatants

3.3.1.1. Preliminary Binding to 2dCD4-WT

One millilitre samples of supernatants derived from 40 hybridoma cell lines, which were generated from mice immunized with purified, native 2dCD4, were obtained from Promab Biotechnologies (Richmond, U.S.A). Screening ELISAs were then performed in order to characterize the binding specificities of antibodies in each of the 40 hybridoma supernatants. We first carried out a direct ELISA in which CD4MAb-1 was incubated on a 96-well microtiter plate that had been coated with purified wild-type 2dCD4. This approach confirmed that CD4MAb-1 bound recombinant 2dCD4 robustly (Figure 20). Probing and detection was conducted using anti-mouse secondary antibody linked to HRP. Increasing amounts of either 2dCD4-WT or concentration of supernatant resulted in increased binding. This approach established the optimal concentration ranges of the 2dCD4 coating solution and hybridoma supernatant dilution levels, and provided a platform for screening CD4Mab-2-40.

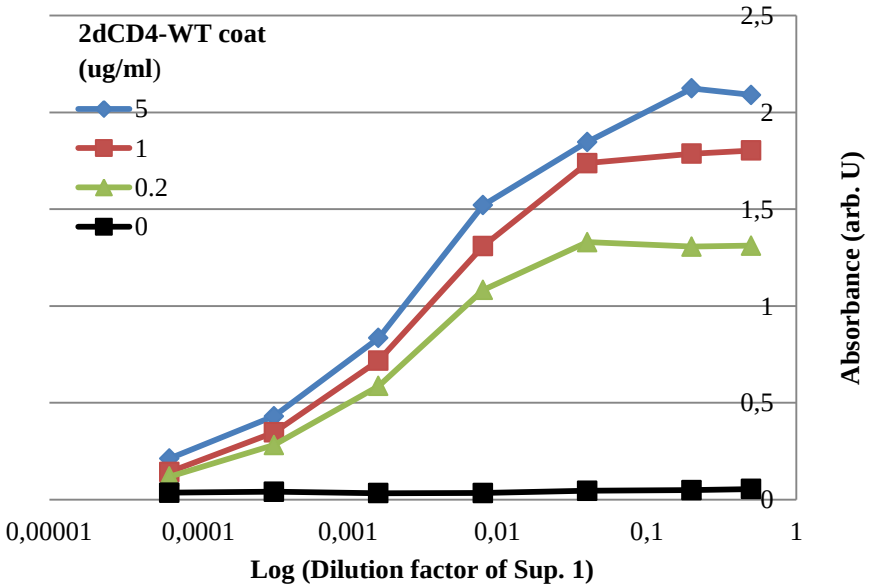

Figure 20: Preliminary Trial of Supernatant 1 against 2dCD4-WT (at 570nm readout)

It was observed that supernatant effectively bound to bacterially expressed 2dCD4-WT. Increasing either the amounts of CD4 coated in each well or the concentration of supernatant used allowed for increased binding.

3.3.1.2. Interaction of CD4-MAbs with Recombinant CD4 variants

We next sought to characterize the ability of the antibody clones to bind a range of CD4 variants, including 2dCD4 and 4dCD4. In each case both wild-type CD4s and variants containing Cys/Ala substitutions in domain 2 were used (2dCD4-Wt, 2dCD4-D2A, 4dCD4-WT and 4dCD4-D2A). Additionally, we also included the Cys/Ala substitution variant (2dCD4-CΔA) as a further control to validate the importance of the preservation of the disulphide bond in epitope recognition. This control includes the C130A/C159A mutation in domain 2, as well as the C16A/C84A mutation in domain 1. All 40 antibody clones bound with various levels of efficiency to the wild-type and Cys\Ala variants of both 2dCD4 (Figure 21a, b) and 4dCD4 (Figure 22a, b). Once again, due to unknown and variable antibody concentration in supernatants, characterization of the relative antibody-binding affinities of CD4MAbs at this stage was not possible. However, it was qualitatively evident that supernatants bind robustly to 2dCD4-WT and 2dCD4-D2A. Most samples had significantly reduced binding to the control 2dCD4-DΔA variant, suggesting that the epitopes to which these antibodies are directed are dependent on secondary or tertiary structural conformations. In contrast however, several D2-specific antibodies (22 – 36) were able to bind 2dCD4-DΔA, albeit at lower levels than to the WT and D2A variants. This suggests that the epitopes of these antibodies are not strictly conformation-dependent, and are likely to be comprised primarily of continuous linear amino acid sequences within the second domain of CD4.

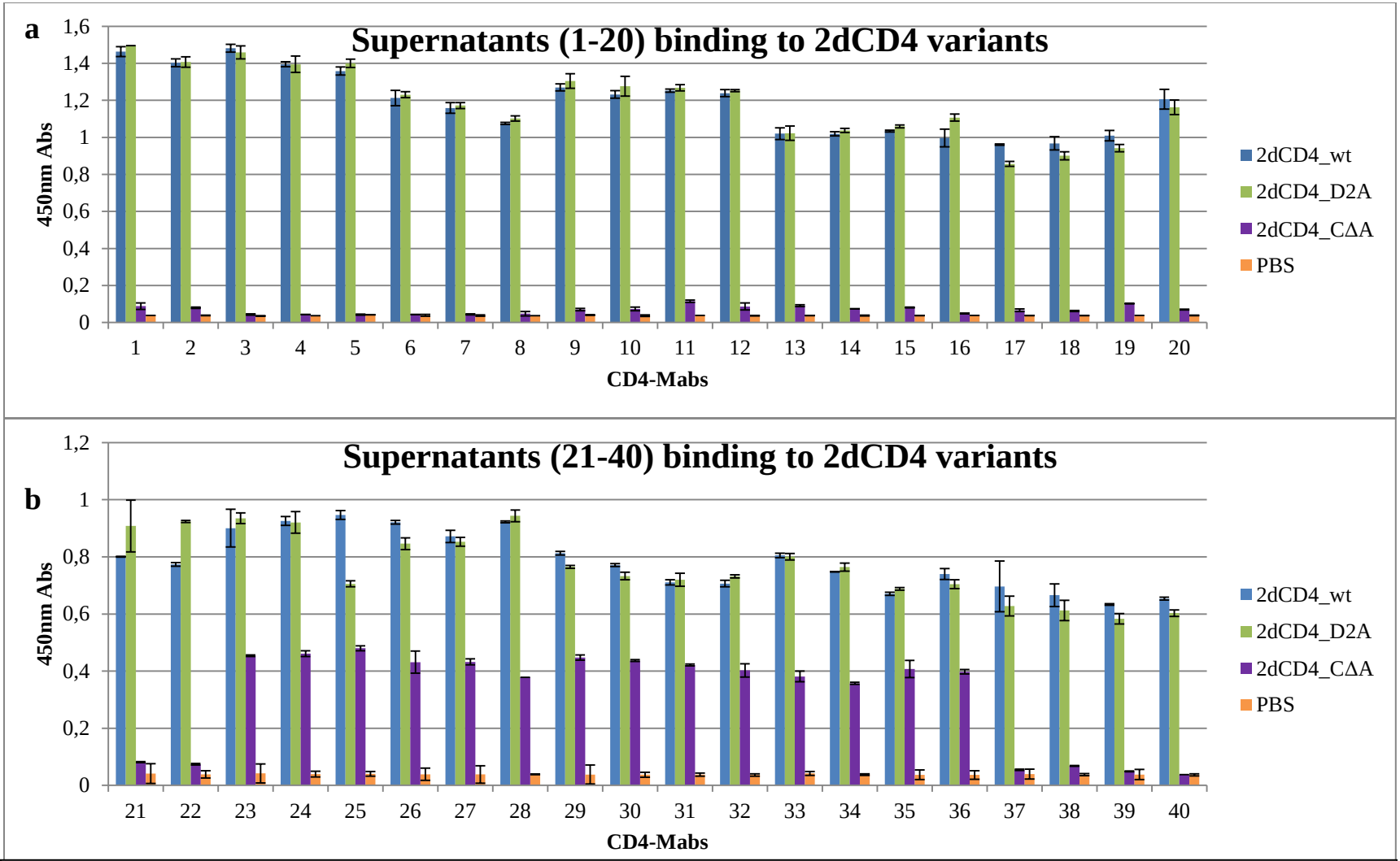

Figure 21: Binding of hybridoma supernatant against 2dCD4 variants (450 nm readout).

All CD4 variants, with the exception of 2dCD4-CΔA, allowed for binding. By approximately 50% less than with the other CD4 variants, supernatants 23 – 36 (D2-specific) could bind 2dCD4-CΔA. Triplicates of experimental data were used for calculating means; error bars represent standard deviation (μ±1sd).

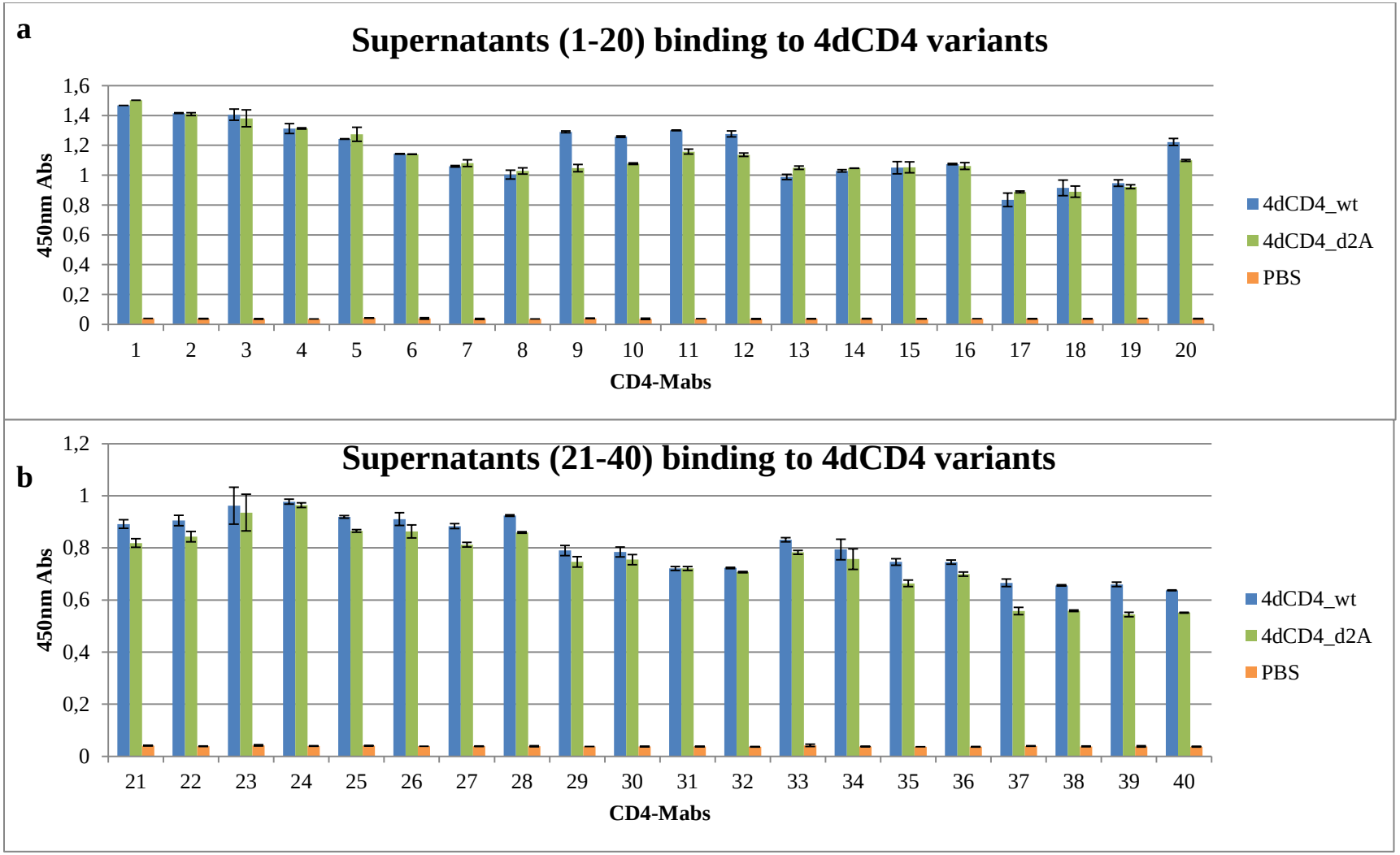

Figure 22: Binding of hybridoma supernatant against 4dCD4 variants (450 nm readout).

Both variants of 4dCD4 allowed for binding of the CD4-Mabs, with no significant difference whether against wild-type or mutant 4dCD4. Triplicates of experimental data were used for calculating means; error bars represent standard deviation (μ±1sd).

3.3.1.3. Binding towards Hexahistidine Tag

Before proceeding with further analyses, we determined whether supernatants had any affinity for the hexahistidine tag, since the immunogen used to raise the 40 hybridoma clones was a his-tagged recombinant 2dCD4, raising the possibility that a significant number of the antibody clones were directed towards a polyhistidine epitope. The use of an irrelevant hexahistidine tagged protein - 6xHis-gp41 produced by others in our laboratory coated on ELISA wells confirmed that none of the supernatants were directed towards the tag (Figure 24).

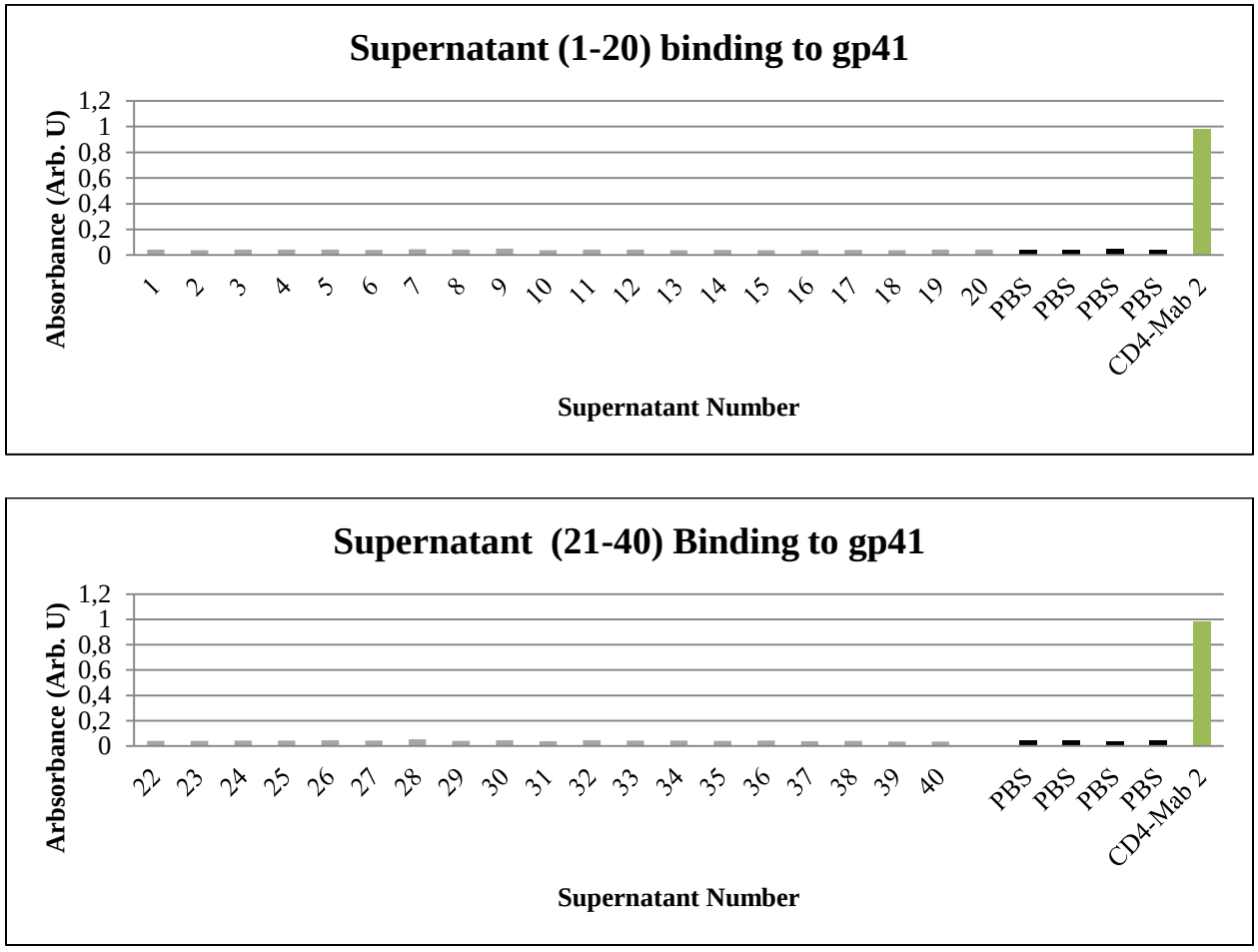

Figure 23: Binding of hybridoma supernatants to irrelevant hexahistidine-tagged gp41

Grey bars reflect the interactions between the indicated CD4-MAb and a 6XHis-tagged HIV gp41 protein. CD4-MAb 2 bound to coated 2dCD4 (shown in green) was used as a positive control to demonstrate antibody binding to non-histidine tag epitope.

3.3.1.4. Domain Specificity

We next sought to establish the domain specificities of CD4MAbs 1 – 40 by coating ELISA plates with CD4 D1 (m1.1) or D2 and probing these with each hybridoma supernatant (Figure 24). It was found that of the 40 supernatants tested, 24 were specific for D1, while the remaining 16 clones bound specifically to D2. Interpreting the binding affinity of supernatants relative to each other was difficult as the amount of antibody present in supernatant is likely to be highly variable. To do so accurately, antibody purification from supernatant and quantification would be necessary (beyond the scope of this study). Moreover, robust binding of a significant number of the CD4MAbs to D2 suggested that bacterially expressed D2 refolds into a structure that reconstitutes at least some of the native Ig-fold-like CD4 secondary structure.

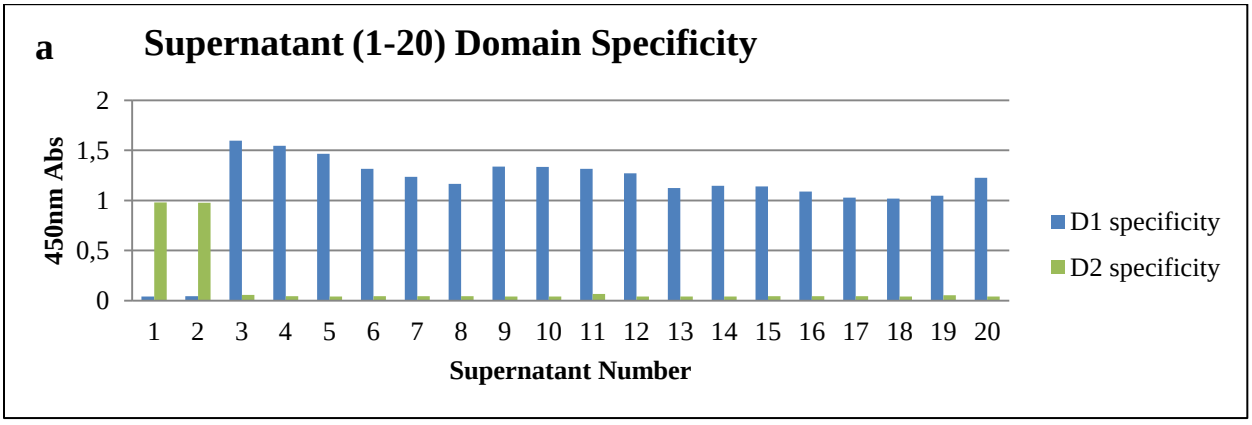

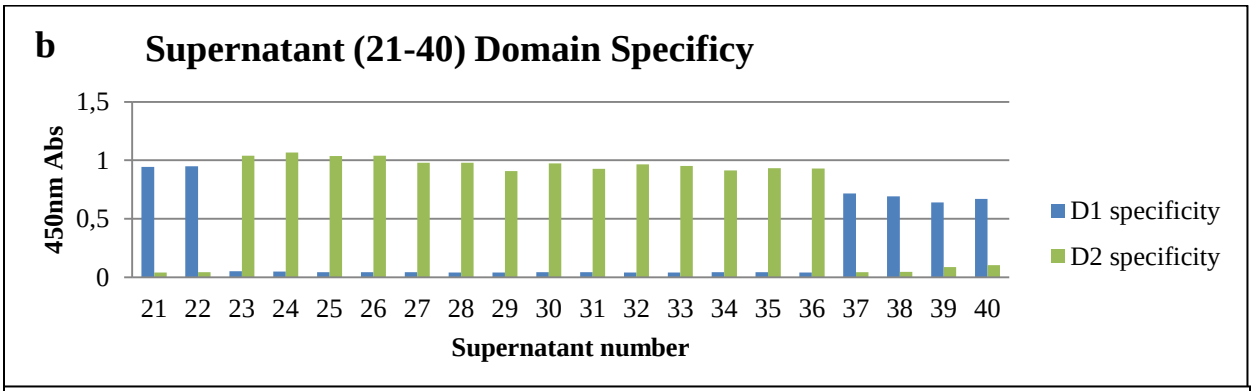

Figure 24: Domain Specificity of MAbs in the hybridoma supernatants

Coating ELISA plates with either D1 or D2 (1 µg/ml) followed by incubation with the indicated hybridoma supernatant (1:100) allowed for identification of domain specificity (in blue: D1; in green: D2). Due to the variability and unknown antibody concentration in supernatants, it was not possible to effectively compare binding affinities.

3.3.1.5. Analysis of CD4MAb-mediated inhibition of CD4-gp120 binding *in vitro*

After characterizing the binding specificities of the 40 anti-CD4 antibody clones, we next set out to establish to what extent each of these were able to block binding of gp120 to CD4. The ELISA plate was coated with 4dCD4-Wt in order to represent native physiological extracellular CD4. CD4-MAbs were then incubated with the coated 4dCD4-Wt in order to allow for binding. Gp120 was added to the wells, probed and detected. Whether the presence of the CD4-MAb bound to 4dCD4-Wt could inhibit gp120 binding was thus determined. It was found that all of the supernatants inhibited recombinant gp120 binding to 4dCD4-WT. For clarity of presentation, the results of four of the 40 CD4-MAbs (Figure 25) are shown in this chapter. The remaining 36 antibodies showed qualititatively similar levels of inhibition – these results are shown in Appendix E. At an antibody dilution of 1:10, all of the 40 antibody supernatants were capable of inhibiting gp120 binding, which was almost completely ablated. For every 10 fold dilution of the CD4-MAb, gp120 binding was roughly doubled. The epitopes of D1-specific mAbs present in the supernatants are likely to overlap with the gp120 binding site on CD4, while the inhibitory effects of the D2-specific mAbs on CD4-gp120 binding could be due to steric inhibition due to the antibodies' Fc portion. To confirm these suggestions, further characterisation is required (beyond the scope of this project). Studies have confirmed that Ibalizumab binding to CD4 does not prevent gp120 binding despite inhibiting subsequent viral entry. The mechanism of action of Ibalizumab is therefore suggested to involve the inhibition of a series of events that lead to viral entry following gp120-CD4 engagement. In contrast, the domain 2 specific Mabs identified in this study all prevented gp120 binding. Potentially, this indicates a novel class of D2-specific antibodies that could inhibit viral entry by directly preventing the gp120-CD4 interaction.

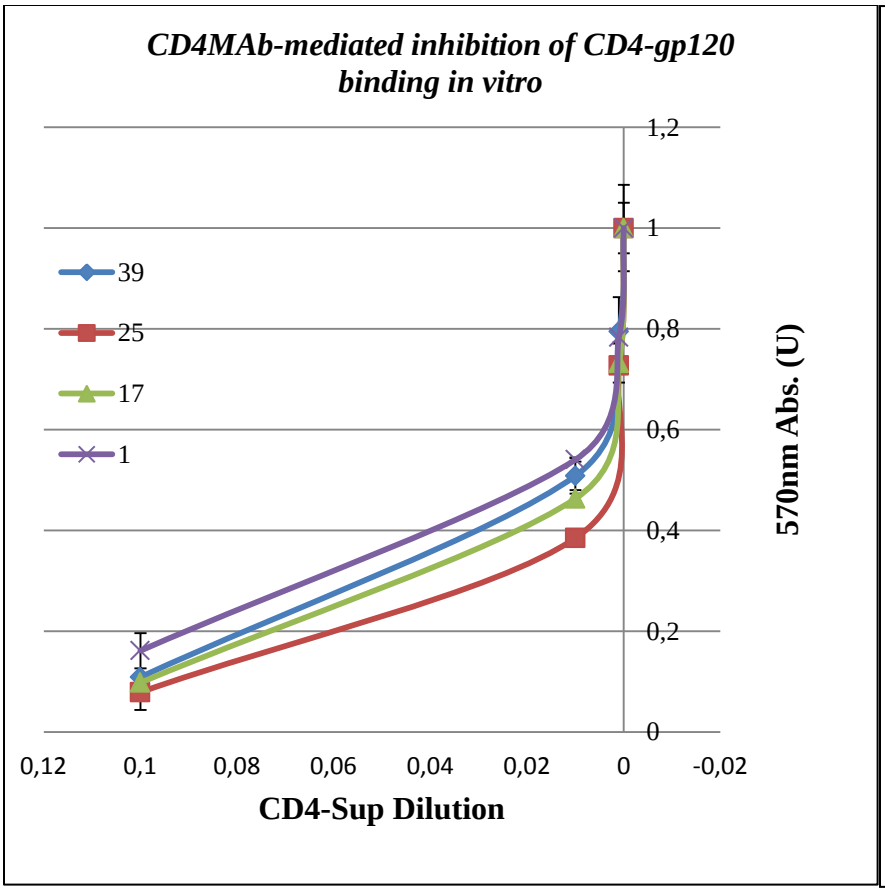

Figure 25: CD4MAb-mediated inhibition of CD4-gp120 binding in vitro.

Inhibition of gp120 (200 ng/ml) binding to 4dCD4-Wt following pre-incubation with CD4-Mab-containing supernatants at dilutions of 0.1, 0.01, 0.001 and negative control (PBS). Absorbance readings reflect the level of gp120 binding. The data has been normalised to the negative control. Supernatants 17 and 39 are D1-specific; 1 and 25 are D2-specific. Triplicates of experimental data were used for calculating means; error bars represent standard deviation (µ±1sd). For remaining CD4MAbs, consult Appendix E.

3.3.2. Pseudovirus Inhibition Assay

3.3.2.1. Establishing working $TCID_{50}$ of pseudovirus

Both ZM53 and SF162 pseudoviruses were capable of infecting TZM-bl cells. SF162 however had greater infectivity as compared to ZM53. This preliminary viral inhibition assay allowed for the determination of the working concentration of pseudovirus to be established (Figure 26). The working dilution of pseudovirus was established and selected to be 1:500, at which adequate luminescence (10^5 – 10^6 RLU) for observation was obtained. This represented 3900 TCID50 for ZM53 and 1750 TCID50 for SF162 (For further description of TCID50 calculation, see Appendix F).

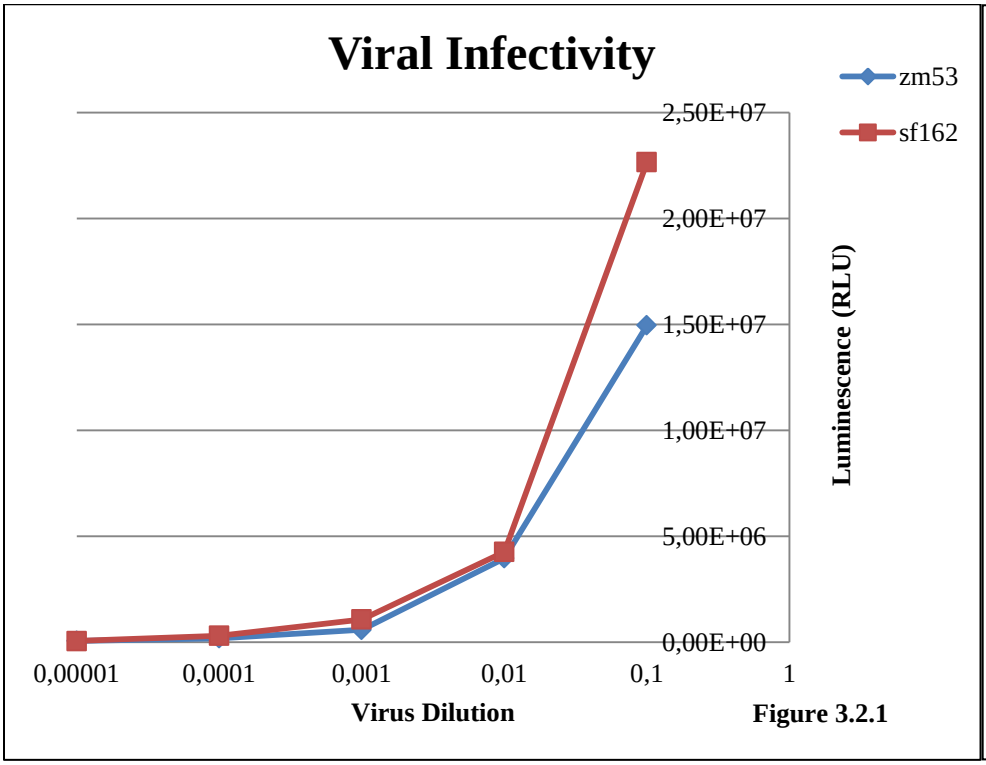

Figure 26: Preliminary Viral Assay

TZM-bl cells, plated out into 96-well culture plate (10^5 cells/well), were incubated with pseudovirus SF162 and ZM53 (Dilution range: 0.1 – 0). Viral infection and replication was confirmed and quantified using the luciferase reporter detection system.

3.3.2.2. Preliminary Analysis of Pseudovirus Inhibition Assay

At a concentration of 1ug/ml, mt310 showed potent inhibition of pseudoviral infection that was comparable to the cell control (Figure 27). The rabbit m79 serum, at 1:100 dilution, showed inhibition of viral infection, although to a lesser extent compared to mt310 (Figure 28). This pseudovirus inhibition assay would serve as the reference for further experiments dealing with the panel of CD4MAbs.

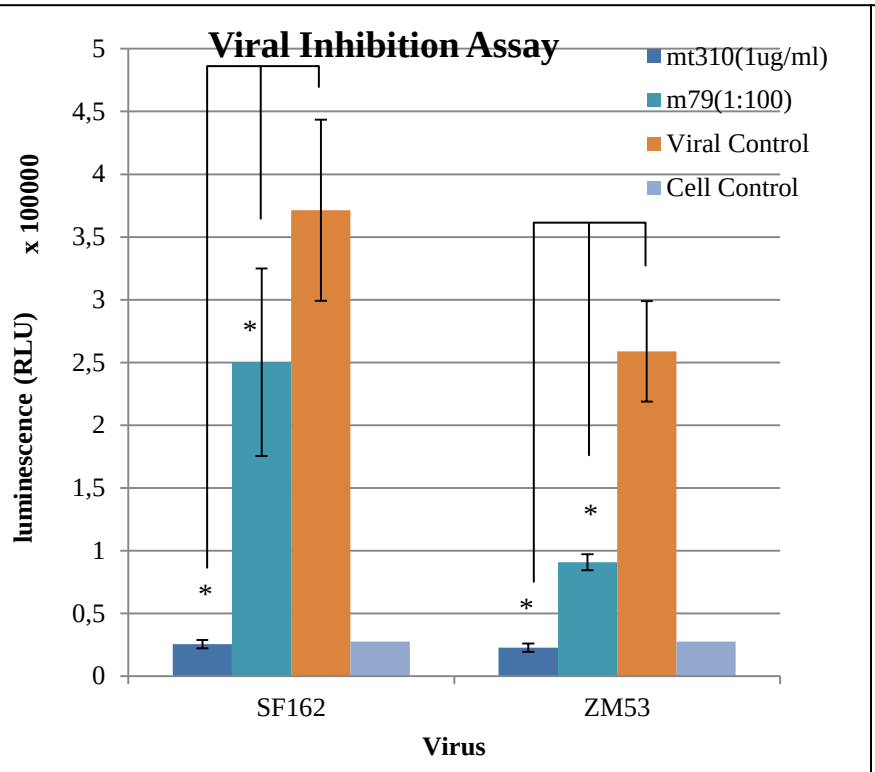

Figure 27: Preliminary Analysis of CD4MAb-mediated inhibition of HIV-1 pseudovirus replication

Serum m79, which was derived from a rabbit immunized with a gp120-CD4 complex, had shown significant viral inhibition against both SF162 and ZM53. Control mt310 antibody completely ablated viral infection. Triplicates of experimental data were used for calculating means; Error bars represent standard deviation (μ±1sd). * indicate significant reduction in viral infectivity relative to viral control (t-test, $p<0.05$)

3.3.2.3. CD4MAb-mediated inhibition of HIV-1 pseudovirus replication

The first attempts to demonstrate the inhibitory effects of the CD4-MAbs in pseudovirus inhibition assays failed to show any significant inhibition mediated by any of the 40 clones. Considering that these antibodies mediated robust inhibition of CD4-gp120 *in vitro*, the reasons for their inability to inhibit viral replication efficiently in cell culture is unclear. A strong possibility is that the concentration of the antibodies in the hybridoma supernatants is relatively low. We therefore decided to concentrate the hybridoma supernatants prior to setting up the pseudovirion inhibition assays, such that the concentrations used would be approximately 20-fold higher than those employed in the preliminary screening assay. Due to limited amount of supernatant we received (~ 1.0 mL), we limited ourselves to testing inhibitory effects on a single pseudovirus strain, ZM53. In this experiment, viral inhibition was observed in 22 of the 39 tested supernatants (supernatant 25 was compromised and had to be discarded) (Figure 28).

Effectively, all 40 supernantants could inhibit gp120 binding to CD4 in the ELISA. However only 12 of the CD4 supernatants showed significant ability to prevent viral infection and viral infection to varying degrees. A plausible explanation for this observation could be due the unknown, but certainly varying concentration of antibodies present in the supernatants. Supernatants having lower MAb concentration, whilst being able to inhibit gp120 binding to CD4 in the ELISA, could be insufficient to saturate CD4 molecules present on TZMBls in order cause observable reduction in the infection during the viral assay. Another explanation could be due to the occurrence of gp120-gp41 (gp140) trimers in the viral assay (Ozel et al., 1988), instead of recombinant monomeric gp120 which was present in the ELISA. As compared to monomeric gp120, native trimeric gp140 could bind to CD4 in such a way that it is not sterically hindered by the anti-CD4 – thus allowing viral entry and infection. It is also possible that mammalian expressed CD4 is functionally different to that CD4 expressed from bacteria when it concerns viral binding and entry. For instance, mammalian CD4 has glycosylated residues in domains 3 and 4 (Spellman et al., 1991), and these could reduce binding affinity of MAbs to the CD4 molecule by imposing steric constrains. Interestingly, CD4MAb-20 enhanced viral infection and therefore, it would be interesting to further characterise the antibody responsible for such observation.

It is difficult to interpret the relative inhibitory potencies of each antibody clone, and the above explanation the observed differences remains highly suggestive without further investigation. This study however positively identifies a panel of CD4-specific antibodies that have inhibitory effects on HIV replication, and provides a platform for further selection of specific antibody clones for further characterization and development. This will involve expansion of selected hybridoma cultures and purification/quantification of corresponding antibodies for detailed kinetic and anti-HIV activity analysis (not the scope of this project).

Figure 28

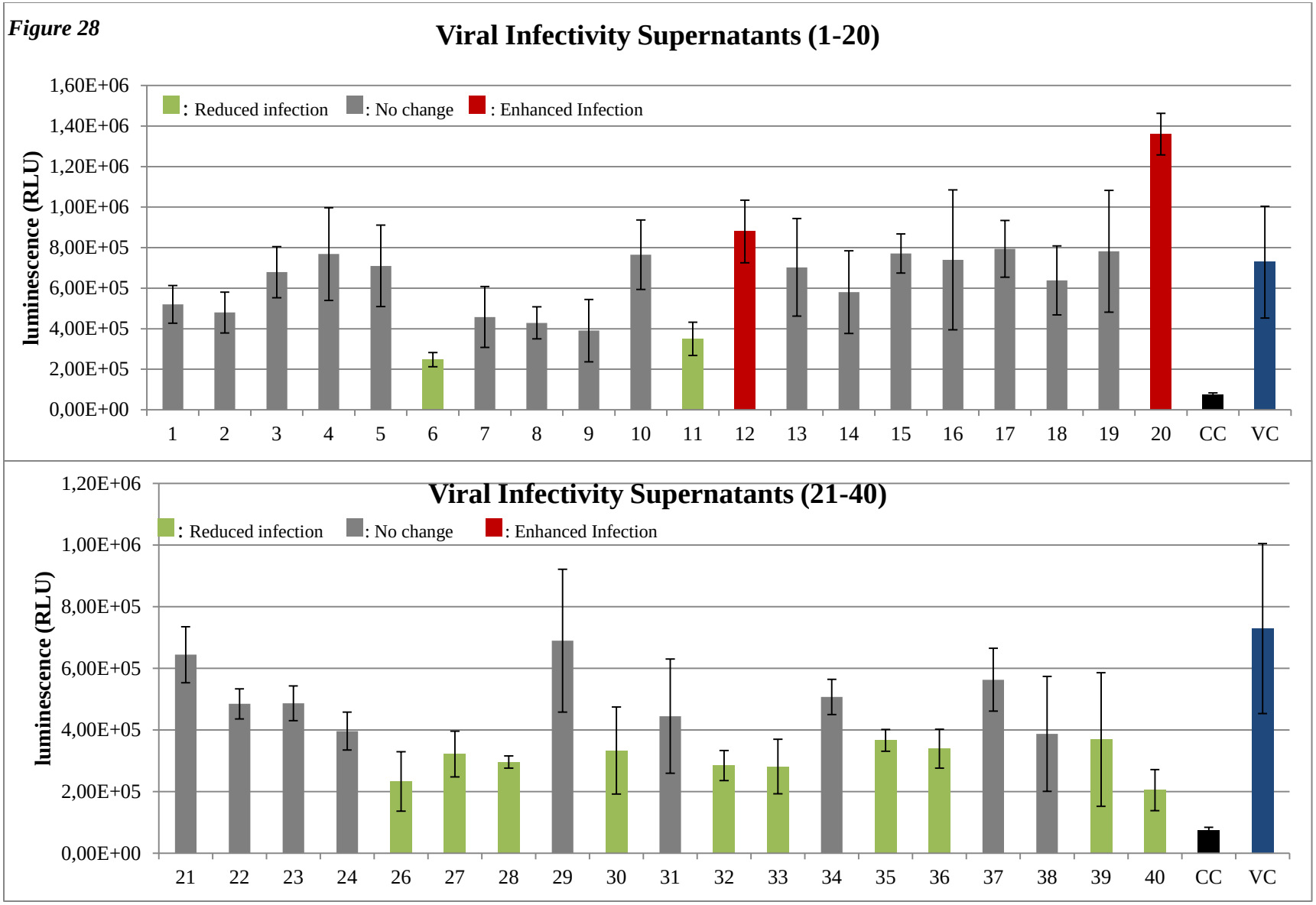
Viral Infectivity Supernatants (1-20)
: Reduced infection
: No change
: Enhanced Infection
luminescence (RLU)
1,60E+06
1,40E+06
1,20E+06
1,00E+06
8,00E+05
6,00E+05
4,00E+05
2,00E+05
0,00E+00
1 2 3 4 5 6 7 8 9 10 11 12 13 14 15 16 17 18 19 20 CC VC
Viral Infectivity Supernatants (21-40)
: Reduced infection
: No change
: Enhanced Infection
luminescence (RLU)
1,20E+06
1,00E+06
8,00E+05
6,00E+05
4,00E+05
2,00E+05
0,00E+00
21 22 23 24 26 27 28 29 30 31 32 33 34 35 36 37 38 39 40 CC VC

Figure 28: CD4MAb-mediated inhibition of HIV-1 replication

Viral Inhibition due to CD4-MAbs. By means of Luciferase assay, pseudoviral infection of TZMbls were assessed. The TZMBls cells were incubated with concentrated CD4-MAbs supernatant prior (2h) to addition of pseudovirus (ZM53). Viral infection was allowed for 48 h. Triplicates of experiments were used and average luminescence was determined. Error bars represent standard deviation (μ±1sd).

VC: Viral Control CC: Cell control

Two tail t-test relative to viral control (VC, in blue). Green: Reduced Infection ($P<0.05$); Grey: No significant difference ($P>0.05$); Red; Enhanced Infection ($P>0.05$).

3.3.2.4. PBMC Assay (See Appendix D)

Activated PBMCs express a wide-range of cytokines, one of which is Interferon-gamma (Fan et al., 1998, Vaquero et al., 1986, Sullivan et al., 2000). Interferon-gamma (INF-γ) is a critical secreted cytokine that is involved in further lymphocyte and macrophage activation during an immune response (Schroder et al., 2004). In our study, we wished to examine the activation of PBMC by PHA by assessing the levels of INF-γ secreted into the cell culture media. We reasoned that this might provide some rudimentary insights into whether any of the CD4-MAbs, had any negative effects on lymphocyte proliferation and activation during PHA stimulation As shown in Appendix D, ii, none of the antibodies appeared to exert significant inhibitory effects on PHA-mediated IFN-γ secretion. While the results of this rudimentary assay establish a basic platform for analysing potential immunosuppressive effects of the CD4 antibodies on T-cell activation, and suggest that many of those identified in this study may not exert significant inhibition in this regard, we acknowledge that far more detailed and rigorous cellular and biochemical analyses, beyond the scope of this work, will need to be performed in order to address this important question satisfactorily.

3.4. DISCUSSION

In this chapter we described the generation of a panel of anti-CD4 monoclonal antibodies that could potentially serve as novel candidate anti-HIV therapies. These were derived from mice immunized with purified recombinant 2dCD4-WT. Supernatants derived from 40 anti-CD4 monoclonal antibody hybridomas that had been selected and expanded were collected and characterised. Using purified CD4 D1 (m1.1) and D2 we were thus able to define the domain specificity of each of the CD4-Mabs, and this data provided further evidence for the structural integrity of recombinant CD4 D2. We also verified and confirmed the inhibitory potential of the Mab-containing supernatants against HIV-1 *in vitro* by a CD4-gp120 competition ELISA assay, and in cell culture by an HIV-1 pseudovirion inhibition assay.

Recombinant individual D1 (m1.1) (Chen et al., 2011), wild-type D2 and 4dCD4 variants were generated using bacterial host cells. A major disadvantage of expressing mammalian proteins in *E. coli* is the inability of these host cells to effect post-translational modifications, which may be important for the structure and function of the protein (Yin et al., 2007). Furthermore, the lack of chaperones and presence of a heavily reducing intracellular microenvironment prevent proper protein folding and disulphide bond formation. (Baneyx, 1999). Our laboratory, and part of this project, addresses the redox state of the expressed CD4 (Cerutti et al., 2010, Cerutti et al., 2014). Therefore, structural and functional integrity of the protein is critical. Protein expression in mammalian cells is ideal as it eliminates the mentioned inconveniences of the *E.coli* expression system, producing correctly folded and soluble protein. Typically, CD4 has been expressed from mammalian cell cultures (Kwong et al., 1998, Ryu et al., 1990). However, mammalian cell culture is tedious, time-consuming, costly and yields of protein tend to be relatively low (Yin et al., 2007). In this project, we have provided indications that a 2dCD4 expressed in *E.coli* is capable of being refolded into a native structure *in vitro*, and can be used as an immunogen for the generation of anti-CD4 antibody with anti-HIV properties. The generated CD4-MAbs ultimately were able to bind strongly to not only 2dCD4 variants, but to 4dCD4, and cognate epitopes within the individual CD4 domains 1 and 2 specifically. Moreover, together with the data described in Chapter 2, the finding that a set of antibodies elicited to a 2-domain CD4 immunogen bind robustly to CD4 D2 provides further evidence that this protein is structurally

similar to CD4-D2 as it occurs in the context of the native CD4 structure,. These experiments have therefore reinforced our confidence in the expression of CD4 in *E.coli* host cells, which is much more economical and less time-consuming than using mammalian cell expression systems.

Despite almost 30 years since the discovery of HIV/AIDS, an effective vaccine remains to be found. High mutation rates (Korber et al., 2001), glycosylation masking and inaccessible neutralising epitopes (Johnson et al., 2009, Poignard et al., 2001) on the envelope glycoprotein are some of the few reasons why the development of vaccine immunogens that can elicit neutralizing antibodies targeting HIV directly have not been successful. Targeting host cell CD4 with an antibody to inhibit HIV infection could be a potential approach to overcoming such challenges and provide an alternate therapy. While the generation of anti-CD4 MAbs as potent viral inhibitors has been considered for some time, it remains a difficult task due to risk of compromising the critical physiological role played by CD4 in adaptive immunity (Cobbold et al., 1984, Goronzy et al., 1986, Dalgleish et al., 1984). Currently proceeding into phase III clinical trials, Ibalizumab is the only anti-CD4 MAb that inhibits HIV infection without causing immune suppression (Jacobson et al., 2009, Norris D, 2006, Khanlou H, 2011, TaiMed_Biologics_Inc, 2011). With Ibalizumab as a novel class of drug against HIV, we propose that several other undiscovered epitopes exist on CD4 which can be targeted by MAbs without mediating immunosuppressive effects. Moreover, with the emergence of HIV strains that are resistant to all existing antiretroviral therapies (Gupta et al., 2009), including Ibalizumab (Toma et al., 2011, Pace et al., 2013), there is an urgent ongoing need for the development of alternative antiviral therapies targeting different sites on both the virus and host molecules.

Notwithstanding this, nearly half of the MAbs raised against the 2dCD4 immunogen were shown to target domain 2 of CD4. Furthermore, eight of these were able to inhibit viral infection as demonstrated from the pseudoviral assay (Figure 28). Non-immunosuppressive anti-HIV Ibalizumab was confirmed to bind to the domain 2 of CD4 (Song et al., 2010, Freeman et al., 2010, Burkly et al., 1992), although its mechanism of action does not involve blocking of CD4-gp120 binding (Burkly et al., 1992, Moore et al., 1992). Rather, the mode of action of Ibalizumab is suspected to involve inhibiting the conformational changes in either CD4 or gp120 that ultimately lead to viral entry. We therefore have at our disposal an entire new panel of potentially novel CD4 domain 2 targeting antibodies with anti-HIV properties which are able to

restrict gp120 binding. This therefore indicates that epitopes of the MAbs generated in this study are different to those of Ibalizumab: these may be more proximal to or overlap with residues in D1, or these MAbs may bind to D2 via approaches that sterically inhibit gp120 binding. It is plausible that the Fc portion of the antibody has a role to play in obstructing gp120 binding. It would therefore be interesting to verify whether the gp120 inhibitory effect is still possible with the use of Fab fragments.

It has been suggested that CD4 is susceptible to redox changes that affect its physiological role. For instance, CD4 has been observed to form disulphide-linked dimers during T-cell activation (Lynch et al., 1999, Moldovan et al., 2002). Whilst more research needs to be conducted, it has been reported that reduced, monomeric forms of CD4 represented the preferred state of the receptor for HIV entry (Matthias et al., 2010), since reduction of the disulphide bond in the second domain of CD4 supports higher levels of HIV infection. (Matthias et al., 2002, Cerutti et al., 2014). It is undoubtedly interesting to speculate whether HIV corrupts the CD4-redox physiology in order to enhance infection. With wild-type CD4 and a panel of Cys/Ala CD4 mutants at our disposal, we therefore sought to find out whether we could identify any CD4 Mabs that had specific binding preferences for distinct CD4 redox isomers. Based on the evidence of the importance of disulphide bonds in CD4, the discovery of a redox-dependent antibody would indicate that significant conformational changes occur in CD4 during redox alterations. Furthermore, such an antibody could potentially lock CD4 in a redox state that is not permissive to viral entry. Intriguingly, while the CD4-Mabs showed no difference in binding to either wild-type or D2 cysteine deficient two-domain CD4, the latter had reduced binding ability to a 2dCD4 in which all cysteines were ablated (2dCD4-CΔA). D1-specific MAbs did not show any binding to 2dCD4-CΔA.

CHAPTER 4:
CONCLUSION

In this study we described the generation of recombinant bacterial expressed individual domains 1(D1) and 2 (D2) of CD4. D1 and D2 were effectively expressed, purified and based on the several lines of biochemical evidence, were structurally and functionally intact. Reducing and non-reducing SDS-PAGE showed the occurrence of intact disulphide bonds in both of the recombinant proteins. Far-UV CD-spectrum showed preservation of the secondary structure. The biophysical assessment of stable mutant D1 (m1.1) showed consistency with the previous study on which this recombinant protein was based (Chen et al., 2011). The expression of recombinant wild-type D2, which has only been mentioned once in the literature (Matthias et al., 2010), indicated a correctly folded structure. For future studies, using these individual domains, it could be possible to further characterise the structural and functional roles of the domains of CD4 independently. With our laboratory focusing on redox changes in the CD4 molecule, the individual domains of CD4 would provide insight for assessing the states of the disulphide bonds in 2dCD4. Future analyses, including time-dependent assays and determination of the redox potential would allow quantitative description of the disulphide bonds. With previous research indicating that the redox state the disulphide bonds influences viral infection (Matthias et al., 2010, Matthias and Hogg, 2003, Matthias et al., 2002), these further experiments on individual domains D1 and D2, will provide insights into the role of CD4 structural dynamics during HIV viral entry and infection.

Ibalizumab, currently in phase III of clinical trials, is the only recognised anti-CD4 MAb that has demonstrated effectiveness in inhibiting HIV infection. As such, the development of anti-CD4 MAbs against HIV remains a mostly untapped field. With growing HIV resistance against Ibalizumab (Toma et al., 2011, Pace et al., 2013), the urgency of seeking novel anti-CD4 MAbs is further stressed. In the second part of the project, we have successfully generated a panel of 40 anti-CD4 MAbs; all of which could inhibit CD4-gp120 binding and limiting pseudoviral infection *in vitro*. Undoubtedly, our research represents preliminary work – further analyses and experiments need to be conducted. Purifying and further characterising the epitopes and potencies of the MAbs needs to be undertaken. An important piece of work remains verifying whether the MAbs have any immunosuppressive effects. A basic PBMC assay allowing the detection of secreted INF-γ was begun (Appendix D). This represents a future platform for assessment of secreted cytokines, of which the levels are indicative of immunosuppression.

Additionally, with the use of the recombinant individual D1 and D2 domains of CD4, it was possible to define the domain specificities of each CD4-MAb. Ibalizumab targeting the domain 2 of CD4, allows for gp120 binding to CD4, but limits viral entry by restricting the conformational changes that ensues. Here, whether targeting D1 or D2, the MAbs could actually inhibit gp120-CD4 binding. Thus, these MAbs potentially signify alternate binding epitopes and mechanism of action in preventing viral entry. Our work therefore lays down the basis for development of these novel anti-CD4 MAbs therapies against HIV.

REFERENCES

ABU-RADDAD, L. J., PATNAIK, P. & KUBLIN, J. G. 2006. Dual infection with HIV and malaria fuels the spread of both diseases in sub-Saharan Africa. *Science,* 314**,** 1603-6.

AIDSINFO, F. 2014. *HIV Treatment: FDA-Approved HIV Medicines* [Online]. Available: http://aidsinfo.nih.gov/education-materials/fact-sheets/21/58/fda-approved-hiv-medicines [Accessed 13.01 2015].

ALTERS, S. E., SAKAI, K., STEINMAN, L. & OI, V. T. 1990. Mechanisms of anti-CD4-mediated depletion and immunotherapy. A study using a set of chimeric anti-CD4 antibodies. *Journal of immunology,* 144**,** 4587-92.

ANDERSON, D., CHAMBERS, K., HANNA, N., LEONARD, J., REFF, M., NEWMAN, R., BALDONI, J., DUNLEAVY, D., REDDY, M., SWEET, R. & TRUNEH, A. 1997. A primatized MAb to human CD4 causes receptor modulation, without marked reduction in CD4+ T cells in chimpanzees: in vitro and in vivo characterization of a MAb (IDEC-CE9.1) to human CD4. *Clinical immunology and immunopathology,* 84**,** 73-84.

ASHISH, JUNCADELLA, I. J., GARG, R., BOONE, C. D., ANGUITA, J. & KRUEGER, J. K. 2008. Conformational rearrangement within the soluble domains of the CD4 receptor is ligand-specific. *The Journal of biological chemistry,* 283**,** 2761-72.

AUFFRAY, C., PIATIER-TONNEAU, D. & KROEMER, G. 1991. CD4-targeted immune intervention: a strategy for the therapy of AIDS and autoimmune disease. *Trends in biotechnology,* 9**,** 124-31.

AUVERT, B., TALJAARD, D., LAGARDE, E., SOBNGWI-TAMBEKOU, J., SITTA, R. & PUREN, A. 2005. Randomized, controlled intervention trial of male circumcision for reduction of HIV infection risk: the ANRS 1265 Trial. *PLoS medicine,* 2**,** e298.

BACK, N. K., SMIT, L., DE JONG, J. J., KEULEN, W., SCHUTTEN, M., GOUDSMIT, J. & TERSMETTE, M. 1994. An N-glycan within the human immunodeficiency virus type 1 gp120 V3 loop affects virus neutralization. *Virology,* 199**,** 431-8.

BAILEY, R. C., MOSES, S., PARKER, C. B., AGOT, K., MACLEAN, I., KRIEGER, J. N., WILLIAMS, C. F., CAMPBELL, R. T. & NDINYA-ACHOLA, J. O. 2007. Male circumcision for HIV prevention in young men in Kisumu, Kenya: a randomised controlled trial. *Lancet,* 369**,** 643-56.

BANEYX, F. 1999. Recombinant protein expression in Escherichia coli. *Current opinion in biotechnology,* 10**,** 411-21.

BAR, K. J., TSAO, C. Y., IYER, S. S., DECKER, J. M., YANG, Y., BONSIGNORI, M., CHEN, X., HWANG, K. K., MONTEFIORI, D. C., LIAO, H. X., HRABER, P., FISCHER, W., LI, H., WANG, S., STERRETT, S., KEELE, B. F., GANUSOV, V. V., PERELSON, A. S., KORBER, B. T., GEORGIEV, I., MCLELLAN, J. S., PAVLICEK, J. W., GAO, F., HAYNES, B. F., HAHN, B. H., KWONG, P. D. & SHAW, G. M. 2012. Early low-titer neutralizing antibodies impede HIV-1 replication and select for virus escape. *PLoS Pathog,* 8**,** e1002721.

BERNSTEIN, H. B., PLASTERER, M. C., SCHIFF, S. E., KITCHEN, C. M., KITCHEN, S. & ZACK, J. A. 2006. CD4 expression on activated NK cells: ligation of CD4 induces cytokine expression and cell migration. *J Immunol,* 177**,** 3669-76.

BOON, L., HOLLAND, B., GORDON, W., LIU, P., SHIAU, F., SHANAHAN, W., REIMANN, K. A. & FUNG, M. 2002. Development of anti-CD4 MAb hu5A8 for treatment of HIV-1 infection: preclinical assessment in non-human primates. *Toxicology,* 172**,** 191-203.

BOR, J., HERBST, A. J., NEWELL, M. L. & BARNIGHAUSEN, T. 2013. Increases in adult life expectancy in rural South Africa: valuing the scale-up of HIV treatment. *Science,* 339**,** 961-5.

BOUTWELL, C. L., ROLLAND, M. M., HERBECK, J. T., MULLINS, J. I. & ALLEN, T. M. 2010. Viral evolution and escape during acute HIV-1 infection. *The Journal of infectious diseases,* 202 Suppl 2**,** S309-14.

BRIGGS, J. A., WILK, T., WELKER, R., KRAUSSLICH, H. G. & FULLER, S. D. 2003. Structural organization of authentic, mature HIV-1 virions and cores. *The EMBO journal,* 22**,** 1707-15.

BROMLEY, S. K., BURACK, W. R., JOHNSON, K. G., SOMERSALO, K., SIMS, T. N., SUMEN, C., DAVIS, M. M., SHAW, A. S., ALLEN, P. M. & DUSTIN, M. L. 2001. The immunological synapse. *Annual review of immunology,* 19**,** 375-96.

BUCHACHER, A., PREDL, R., STRUTZENBERGER, K., STEINFELLNER, W., TRKOLA, A., PURTSCHER, M., GRUBER, G., TAUER, C., STEINDL, F., JUNGBAUER, A. & ET AL. 1994. Generation of human monoclonal antibodies against HIV-1 proteins; electrofusion and Epstein-Barr virus transformation for peripheral blood lymphocyte immortalization. *AIDS research and human retroviruses,* 10**,** 359-69.

BURKLY, L. C., OLSON, D., SHAPIRO, R., WINKLER, G., ROSA, J. J., THOMAS, D. W., WILLIAMS, C. & CHISHOLM, P. 1992. Inhibition of HIV infection by a novel CD4 domain 2-specific monoclonal antibody. Dissecting the basis for its inhibitory effect on HIV-induced cell fusion. *Journal of immunology,* 149**,** 1779-87.

BURTON, D. R., AHMED, R., BAROUCH, D. H., BUTERA, S. T., CROTTY, S., GODZIK, A., KAUFMANN, D. E., MCELRATH, M. J., NUSSENZWEIG, M. C., PULENDRAN, B., SCANLAN, C. N., SCHIEF, W. R., SILVESTRI, G., STREECK, H., WALKER, B. D., WALKER, L. M., WARD, A. B., WILSON, I. A. & WYATT, R. 2012a. A Blueprint for HIV Vaccine Discovery. *Cell host & microbe,* 12**,** 396-407.

BURTON, D. R., AHMED, R., BAROUCH, D. H., BUTERA, S. T., CROTTY, S., GODZIK, A., KAUFMANN, D. E., MCELRATH, M. J., NUSSENZWEIG, M. C., PULENDRAN, B., SCANLAN, C. N., SCHIEF, W. R., SILVESTRI, G., STREECK, H., WALKER, B. D., WALKER, L. M., WARD, A. B., WILSON, I. A. & WYATT, R. 2012b. A Blueprint for HIV Vaccine Discovery. *Cell Host Microbe,* 12**,** 396-407.

BURTON, D. R., BARBAS, C. F., 3RD, PERSSON, M. A., KOENIG, S., CHANOCK, R. M. & LERNER, R. A. 1991. A large array of human monoclonal antibodies to type 1 human immunodeficiency virus from combinatorial libraries of asymptomatic seropositive individuals. *Proceedings of the National Academy of Sciences of the United States of America,* 88**,** 10134-7.

BURTON, D. R., PYATI, J., KODURI, R., SHARP, S. J., THORNTON, G. B., PARREN, P. W., SAWYER, L. S., HENDRY, R. M., DUNLOP, N., NARA, P. L. & ET AL. 1994. Efficient neutralization of primary isolates of HIV-1 by a recombinant human monoclonal antibody. *Science,* 266**,** 1024-7.

CALARESE, D. A., LEE, H. K., HUANG, C. Y., BEST, M. D., ASTRONOMO, R. D., STANFIELD, R. L., KATINGER, H., BURTON, D. R., WONG, C. H. & WILSON, I. A. 2005. Dissection of the carbohydrate specificity of the broadly neutralizing anti-HIV-1 antibody 2G12. *Proceedings of the National Academy of Sciences of the United States of America,* 102**,** 13372-7.

CALARESE, D. A., SCANLAN, C. N., ZWICK, M. B., DEECHONGKIT, S., MIMURA, Y., KUNERT, R., ZHU, P., WORMALD, M. R., STANFIELD, R. L., ROUX, K. H., KELLY, J. W., RUDD, P. M., DWEK, R. A., KATINGER, H., BURTON, D. R. & WILSON, I. A. 2003. Antibody domain exchange is an immunological solution to carbohydrate cluster recognition. *Science,* 300**,** 2065-71.

CAPON, D. J. & WARD, R. H. 1989. Antiviral effects of CD4 derivatives. *Current opinion in immunology,* 2**,** 433-8.

CARR, C. M. & KIM, P. S. 1993. A spring-loaded mechanism for the conformational change of influenza hemagglutinin. *Cell,* 73**,** 823-32.

CARTERON, N. L., WOFSY, D. & SEAMAN, W. E. 1988. Induction of immune tolerance during administration of monoclonal antibody to L3T4 does not depend on depletion of L3T4+ cells. *Journal of immunology,* 140**,** 713-6.

CERUTTI, N., KILLICK, M., JUGNARAIN, V., PAPATHANASOPOULOS, M. & CAPOVILLA, A. 2014. Disulfide reduction in CD4 Domain 1 or 2 is essential for interaction with HIV gp120, which impairs Thioredoxin-driven CD4 dimerization. *The Journal of biological chemistry*.

CERUTTI, N., MENDELOW, B. V., NAPIER, G. B., PAPATHANASOPOULOS, M. A., KILLICK, M., KHATI, M., STEVENS, W. & CAPOVILLA, A. 2010. Stabilization of HIV-1 gp120-CD4 receptor complex through targeted interchain disulfide exchange. *The Journal of biological chemistry,* 285**,** 25743-52.

CHAILLON, A., BRAIBANT, M., HUE, S., BENCHARIF, S., ENARD, D., MOREAU, A., SAMRI, A., AGUT, H. & BARIN, F. 2012. Human immunodeficiency virus type-1 (HIV-1) continues to evolve in presence of broadly neutralizing antibodies more than ten years after infection. *PLoS One,* 7**,** e44163.

CHAO, B. H., COSTOPOULOS, D. S., CURIEL, T., BERTONIS, J. M., CHISHOLM, P., WILLIAMS, C., SCHOOLEY, R. T., ROSA, J. J., FISHER, R. A. & MARAGANORE, J. M. 1989. A 113-amino acid fragment of CD4 produced in Escherichia coli blocks human immunodeficiency virus-induced cell fusion. *The Journal of biological chemistry,* 264**,** 5812-7.

CHEN, V. M. & HOGG, P. J. 2006. Allosteric disulfide bonds in thrombosis and thrombolysis. *Journal of thrombosis and haemostasis : JTH,* 4**,** 2533-41.

CHEN, W., FENG, Y., GONG, R., ZHU, Z., WANG, Y., ZHAO, Q. & DIMITROV, D. S. 2011. Engineered single human CD4 domains as potent HIV-1 inhibitors and components of vaccine immunogens. *Journal of virology,* 85**,** 9395-405.

CHUN, T. W., CARRUTH, L., FINZI, D., SHEN, X., DIGIUSEPPE, J. A., TAYLOR, H., HERMANKOVA, M., CHADWICK, K., MARGOLICK, J., QUINN, T. C., KUO, Y. H., BROOKMEYER, R., ZEIGER, M. A., BARDITCH-CROVO, P. & SILICIANO, R. F. 1997. Quantification of latent tissue reservoirs and total body viral load in HIV-1 infection. *Nature,* 387**,** 183-8.

CHUN, T. W., FINZI, D., MARGOLICK, J., CHADWICK, K., SCHWARTZ, D. & SILICIANO, R. F. 1995. In vivo fate of HIV-1-infected T cells: quantitative analysis of the transition to stable latency. *Nat Med,* 1**,** 1284-90.

COBBOLD, S. P., JAYASURIYA, A., NASH, A., PROSPERO, T. D. & WALDMANN, H. 1984. Therapy with monoclonal antibodies by elimination of T-cell subsets in vivo. *Nature,* 312**,** 548-51.

CORBETT, E. L., WATT, C. J., WALKER, N., MAHER, D., WILLIAMS, B. G., RAVIGLIONE, M. C. & DYE, C. 2003. The growing burden of tuberculosis: global trends and interactions with the HIV epidemic. *Archives of internal medicine,* 163**,** 1009-21.

COSIMI, A. B., DELMONICO, F. L., WRIGHT, J. K., WEE, S. L., PREFFER, F. I., JOLLIFFE, L. K. & COLVIN, R. B. 1990. Prolonged survival of nonhuman primate renal allograft recipients treated only with anti-CD4 monoclonal antibody. *Surgery,* 108**,** 406-13; discussion 413-4.

CRAWFORD, J. M., EARL, P. L., MOSS, B., REIMANN, K. A., WYAND, M. S., MANSON, K. H., BILSKA, M., ZHOU, J. T., PAUZA, C. D., PARREN, P. W., BURTON, D. R., SODROSKI, J. G., LETVIN, N. L. & MONTEFIORI, D. C. 1999. Characterization of primary isolate-like variants of simian-human immunodeficiency virus. *Journal of virology,* 73**,** 10199-207.

DALEY, C. L., SMALL, P. M., SCHECTER, G. F., SCHOOLNIK, G. K., MCADAM, R. A., JACOBS, W. R., JR. & HOPEWELL, P. C. 1992. An outbreak of tuberculosis with accelerated progression among persons infected with the human immunodeficiency virus. An analysis using restriction-fragment-length polymorphisms. *The New England journal of medicine,* 326**,** 231-5.

DALGLEISH, A. G., BEVERLEY, P. C., CLAPHAM, P. R., CRAWFORD, D. H., GREAVES, M. F. & WEISS, R. A. 1984. The CD4 (T4) antigen is an essential component of the receptor for the AIDS retrovirus. *Nature,* 312**,** 763-7.

DARBY, N. J., FREEDMAN, R. B. & CREIGHTON, T. E. 1994. Dissecting the mechanism of protein disulfide isomerase: catalysis of disulfide bond formation in a model peptide. *Biochemistry,* 33**,** 7937-47.

DAWSON, L. & YU, X. F. 1998. The role of nucleocapsid of HIV-1 in virus assembly. *Virology,* 251**,** 141-57.

DE CLERCQ, E. 2009. Anti-HIV drugs: 25 compounds approved within 25 years after the discovery of HIV. *International journal of antimicrobial agents,* 33**,** 307-20.

DEBAISIEUX, S., RAYNE, F., YEZID, H. & BEAUMELLE, B. 2012. The ins and outs of HIV-1 Tat. *Traffic,* 13**,** 355-63.

DELMONICO, F. L., KNOWLES, R. W., COLVIN, R. B., CAVENDER, D. E., KAWAI, T., BEDLE, M., STROKA, D., PREFFER, F. I., HAUG, C. & COSIMI, A. B. 1993. Immunosuppression of cynomolgus renal allograft

recipients with humanized OKT4A monoclonal antibodies. *Transplantation proceedings,* 25**,** 784-5.

DENISOVA, G., RAVIV, D., MONDOR, I., SATTENTAU, Q. J. & GERSHONI, J. M. 1997. Conformational transitions in CD4 due to complexation with HIV envelope glycoprotein gp120. *Journal of immunology,* 158**,** 1157-64.

DOI, E. & JIRGENSONS, B. 1970. Circular dichroism studies on the acid denaturation of gamma-immunoglobulin G and its fragments. *Biochemistry,* 9**,** 1066-73.

DONOGHUE, N., YAM, P. T., JIANG, X. M. & HOGG, P. J. 2000. Presence of closely spaced protein thiols on the surface of mammalian cells. *Protein science : a publication of the Protein Society,* 9**,** 2436-45.

DOORES, K. J. & BURTON, D. R. 2010. Variable loop glycan dependency of the broad and potent HIV-1-neutralizing antibodies PG9 and PG16. *Journal of virology,* 84**,** 10510-21.

DORIA-ROSE, N. A., KLEIN, R. M., DANIELS, M. G., O'DELL, S., NASON, M., LAPEDES, A., BHATTACHARYA, T., MIGUELES, S. A., WYATT, R. T., KORBER, B. T., MASCOLA, J. R. & CONNORS, M. 2010. Breadth of human immunodeficiency virus-specific neutralizing activity in sera: clustering analysis and association with clinical variables. *Journal of virology,* 84**,** 1631-6.

DORIA-ROSE, N. A., KLEIN, R. M., MANION, M. M., O'DELL, S., PHOGAT, A., CHAKRABARTI, B., HALLAHAN, C. W., MIGUELES, S. A., WRAMMERT, J., AHMED, R., NASON, M., WYATT, R. T., MASCOLA, J. R. & CONNORS, M. 2009. Frequency and phenotype of human immunodeficiency virus envelope-specific B cells from patients with broadly cross-neutralizing antibodies. *Journal of virology,* 83**,** 188-99.

DORR, P., WESTBY, M., DOBBS, S., GRIFFIN, P., IRVINE, B., MACARTNEY, M., MORI, J., RICKETT, G., SMITH-BURCHNELL, C., NAPIER, C., WEBSTER, R., ARMOUR, D., PRICE, D., STAMMEN, B., WOOD, A. & PERROS, M. 2005. Maraviroc (UK-427,857), a potent, orally bioavailable, and selective small-molecule inhibitor of chemokine receptor CCR5 with broad-spectrum anti-human immunodeficiency virus type 1 activity. *Antimicrobial agents and chemotherapy,* 49**,** 4721-32.

DOUEK, D. C., PICKER, L. J. & KOUP, R. A. 2003. T cell dynamics in HIV-1 infection. *Annual review of immunology,* 21**,** 265-304.

EROSHKIN, A. M., LEBLANC, A., WEEKES, D., POST, K., LI, Z., RAJPUT, A., BUTERA, S. T., BURTON, D. R. & GODZIK, A. 2014. bNAber: database of broadly neutralizing HIV antibodies. *Nucleic acids research,* 42**,** D1133-9.

ETEMAD-MOGHADAM, B., SUN, Y., NICHOLSON, E. K., KARLSSON, G. B., SCHENTEN, D. & SODROSKI, J. 1999. Determinants of neutralization resistance in the envelope glycoproteins of a simian-human immunodeficiency virus passaged in vivo. *Journal of virology,* 73**,** 8873-9.

FAN, J., NISHANIAN, P., BREEN, E. C., MCDONALD, M. & FAHEY, J. L. 1998. Cytokine gene expression in normal human lymphocytes in response to stimulation. *Clinical and diagnostic laboratory immunology,* 5**,** 335-40.

FISCHER, W., GANUSOV, V. V., GIORGI, E. E., HRABER, P. T., KEELE, B. F., LEITNER, T., HAN, C. S., GLEASNER, C. D., GREEN, L., LO, C. C., NAG, A., WALLSTROM, T. C., WANG, S., MCMICHAEL, A. J., HAYNES, B. F., HAHN, B. H., PERELSON, A. S., BORROW, P., SHAW, G. M., BHATTACHARYA, T. & KORBER, B. T. 2010. Transmission of single HIV-1 genomes and dynamics of early immune escape revealed by ultra-deep sequencing. *PloS one,* 5**,** e12303.

FREEMAN, M. M., SEAMAN, M. S., RITS-VOLLOCH, S., HONG, X., KAO, C. Y., HO, D. D. & CHEN, B. 2010. Crystal structure of HIV-1 primary receptor CD4 in complex with a potent antiviral antibody. *Structure,* 18**,** 1632-41.

FRISCH, M., BIGGAR, R. J., ENGELS, E. A. & GOEDERT, J. J. 2001. Association of cancer with AIDS-related immunosuppression in adults. *JAMA : the journal of the American Medical Association,* 285**,** 1736-45.

GARCIA-PEREZ, J., RUEDA, P., ALCAMI, J., ROGNAN, D., ARENZANA-SEISDEDOS, F., LAGANE, B. & KELLENBERGER, E. 2011. Allosteric model of maraviroc binding to CC chemokine receptor 5 (CCR5). *The Journal of biological chemistry,* 286**,** 33409-21.

GARNER, A. P., BIALUCHA, C. U., SPRAGUE, E. R., GARRETT, J. T., SHENG, Q., LI, S., SINESHCHEKOVA, O., SAXENA, P., SUTTON, C. R., CHEN, D., CHEN, Y., WANG, H., LIANG, J., DAS, R., MOSHER, R., GU, J., HUANG, A., HAUBST, N., ZEHETMEIER, C., HABERL, M., ELIS, W., KUNZ, C., HEIDT, A. B., HERLIHY, K., MURTIE, J., SCHULLER, A., ARTEAGA, C. L., SELLERS, W. R. & ETTENBERG, S. A. 2013. An antibody that locks HER3 in the inactive conformation inhibits tumor growth driven by HER2 or neuregulin. *Cancer Res,* 73**,** 6024-35.

GAUDUIN, M. C., PARREN, P. W., WEIR, R., BARBAS, C. F., BURTON, D. R. & KOUP, R. A. 1997. Passive immunization with a human monoclonal antibody protects hu-PBL-SCID mice against challenge by primary isolates of HIV-1. *Nature medicine,* 3**,** 1389-93.

GELDERBLOM, H. R., HAUSMANN, E. H., OZEL, M., PAULI, G. & KOCH, M. A. 1987. Fine structure of human immunodeficiency virus (HIV) and immunolocalization of structural proteins. *Virology,* 156**,** 171-6.

GORONZY, J., WEYAND, C. M. & FATHMAN, C. G. 1986. Long-term humoral unresponsiveness in vivo, induced by treatment with monoclonal antibody against L3T4. *The Journal of experimental medicine,* 164**,** 911-25.

GOTTLIEB, M. S. 2006. Pneumocystis pneumonia--Los Angeles. 1981. *American journal of public health,* 96**,** 980-1; discussion 982-3.

GRAM, G. J., BOLMSTEDT, A., SCHONNING, K., BILLER, M., HANSEN, J. E. & OLOFSSON, S. 2002. Detection of orientation-specific anti-gp120 antibodies by a new N-glycanase protection assay. *APMIS : acta pathologica, microbiologica, et immunologica Scandinavica,* 110**,** 123-31.

GRAY, E. S., TAYLOR, N., WYCUFF, D., MOORE, P. L., TOMARAS, G. D., WIBMER, C. K., PUREN, A., DECAMP, A., GILBERT, P. B., WOOD, B., MONTEFIORI, D. C., BINLEY, J. M., SHAW, G. M., HAYNES, B. F., MASCOLA, J. R. & MORRIS, L. 2009. Antibody specificities associated with neutralization breadth in plasma from human immunodeficiency virus type 1 subtype C-infected blood donors. *Journal of virology,* 83**,** 8925-37.

GREGSON, S., GARNETT, G. P., NYAMUKAPA, C. A., HALLETT, T. B., LEWIS, J. J., MASON, P. R., CHANDIWANA, S. K. & ANDERSON, R. M. 2006. HIV decline associated with behavior change in eastern Zimbabwe. *Science,* 311**,** 664-6.

GRIMWADE, K., FRENCH, N., MBATHA, D. D., ZUNGU, D. D., DEDICOAT, M. & GILKS, C. F. 2004. HIV infection as a cofactor for severe falciparum malaria in adults living in a region of unstable malaria transmission in South Africa. *AIDS,* 18**,** 547-54.

GUPTA, R. K., HILL, A., SAWYER, A. W., COZZI-LEPRI, A., VON WYL, V., YERLY, S., LIMA, V. D., GUNTHARD, H. F., GILKS, C. & PILLAY, D. 2009. Virological monitoring and resistance to first-line highly active antiretroviral therapy in adults infected with HIV-1 treated under WHO guidelines: a systematic review and meta-analysis. *The Lancet. Infectious diseases,* 9**,** 409-17.

HAYNES, B. F., KELSOE, G., HARRISON, S. C. & KEPLER, T. B. 2012. B-cell-lineage immunogen design in vaccine development with HIV-1 as a case study. *Nature biotechnology,* 30**,** 423-33.

HEALEY, D., DIANDA, L., MOORE, J. P., MCDOUGAL, J. S., MOORE, M. J., ESTESS, P., BUCK, D., KWONG, P. D., BEVERLEY, P. C. & SATTENTAU, Q. J. 1990a. Novel anti-CD4 monoclonal antibodies separate human immunodeficiency virus infection and fusion of CD4+ cells from virus binding. *J Exp Med,* 172**,** 1233-42.

HEALEY, D., DIANDA, L., MOORE, J. P., MCDOUGAL, J. S., MOORE, M. J., ESTESS, P., BUCK, D., KWONG, P. D., BEVERLEY, P. C. & SATTENTAU, Q. J. 1990b. Novel anti-CD4 monoclonal antibodies separate human immunodeficiency virus infection and fusion of CD4+ cells from virus binding. *The Journal of experimental medicine,* 172**,** 1233-42.

HELLING, B., KONIG, M., DALKEN, B., ENGLING, A., KROMER, W., HEIM, K., WALLMEIER, H., HAAS, J., WILDEMANN, B., FRITZ, B., JONULEIT, H., KUBACH, J., DINGERMANN, T., RADEKE, H. H., OSTERROTH, F., UHEREK, C., CZELOTH, N. & SCHUTTRUMPF, J. 2015. A specific CD4 epitope bound by tregalizumab mediates activation of regulatory T cells by a unique signaling pathway. *Immunol Cell Biol,* 93**,** 396-405.

HEMELAAR, J., GOUWS, E., GHYS, P. D. & OSMANOV, S. 2006. Global and regional distribution of HIV-1 genetic subtypes and recombinants in 2004. *AIDS,* 20**,** W13-23.

HEMELAAR, J., GOUWS, E., GHYS, P. D. & OSMANOV, S. 2011. Global trends in molecular epidemiology of HIV-1 during 2000-2007. *AIDS,* 25**,** 679-89.

HERZOG, C., WALKER, C., MULLER, W., RIEBER, P., REITER, C., RIETHMULLER, G., WASSMER, P., STOCKINGER, H., MADIC, O. & PICHLER, W. J. 1989. Anti-CD4 antibody treatment of patients with rheumatoid arthritis: I. Effect on clinical course and circulating T cells. *Journal of autoimmunity,* 2**,** 627-42.

HOLMES, C. B., LOSINA, E., WALENSKY, R. P., YAZDANPANAH, Y. & FREEDBERG, K. A. 2003. Review of human immunodeficiency virus type 1-related opportunistic infections in sub-Saharan Africa. *Clinical infectious diseases : an official publication of the Infectious Diseases Society of America,* 36**,** 652-62.

JACOBSON, J. M., KURITZKES, D. R., GODOFSKY, E., DEJESUS, E., LARSON, J. A., WEINHEIMER, S. P. & LEWIS, S. T. 2009. Safety, pharmacokinetics, and antiretroviral activity of multiple doses of ibalizumab (formerly TNX-355), an anti-CD4 monoclonal antibody, in human immunodeficiency virus type 1-infected adults. *Antimicrobial agents and chemotherapy,* 53**,** 450-7.

JOHNSON, V. A., BRUN-VEZINET, F., CLOTET, B., GUNTHARD, H. F., KURITZKES, D. R., PILLAY, D., SCHAPIRO, J. M. & RICHMAN, D. D. 2009. Update of the drug resistance mutations in HIV-1: December 2009. *Topics in HIV medicine : a publication of the International AIDS Society, USA,* 17**,** 138-45.

JOHNSON, W. E. & DESROSIERS, R. C. 2002. Viral persistence: HIV's strategies of immune system evasion. *Annual review of medicine,* 53**,** 499-518.

KATZ, B. A. & KOSSIAKOFF, A. 1986. The crystallographically determined structures of atypical strained disulfides engineered into subtilisin. *The Journal of biological chemistry,* 261**,** 15480-5.

KEELE, B. F., GIORGI, E. E., SALAZAR-GONZALEZ, J. F., DECKER, J. M., PHAM, K. T., SALAZAR, M. G., SUN, C., GRAYSON, T., WANG, S., LI, H., WEI, X., JIANG, C., KIRCHHERR, J. L., GAO, F., ANDERSON, J. A., PING, L. H., SWANSTROM, R., TOMARAS, G. D., BLATTNER, W. A., GOEPFERT, P. A., KILBY, J. M., SAAG, M. S., DELWART, E. L., BUSCH, M. P., COHEN, M. S., MONTEFIORI, D. C., HAYNES, B. F., GASCHEN, B., ATHREYA, G. S., LEE, H. Y., WOOD, N., SEOIGHE, C., PERELSON, A. S., BHATTACHARYA, T., KORBER, B. T., HAHN, B. H. & SHAW, G. M. 2008. Identification and characterization of transmitted and early founder virus envelopes in primary HIV-1 infection. *Proceedings of the National Academy of Sciences of the United States of America,* 105**,** 7552-7.

KHANLOU H, G. J. J., SCHRADER S, TOWNER W, WEINHEIMER S, LEWIS S. 2011. Safety, Efficacy, and Pharmacokinetics of Ibalizumab in Treatment-Experienced HIV-1 Infected Patients: a Phase 2b Study. *51st Interscience Conference on Antimicrobial Agents and Chemotherapy (ICAAC).* Chicago, IL.

KOCH, M., PANCERA, M., KWONG, P. D., KOLCHINSKY, P., GRUNDNER, C., WANG, L., HENDRICKSON, W. A., SODROSKI, J. & WYATT, R. 2003. Structure-based, targeted deglycosylation of HIV-1 gp120 and effects on neutralization sensitivity and antibody recognition. *Virology,* 313**,** 387-400.

KORBER, B., GASCHEN, B., YUSIM, K., THAKALLAPALLY, R., KESMIR, C. & DETOURS, V. 2001. Evolutionary and immunological implications of contemporary HIV-1 variation. *British medical bulletin,* 58**,** 19-42.

KURITZKES, D. R., JACOBSON, J., POWDERLY, W. G., GODOFSKY, E., DEJESUS, E., HAAS, F., REIMANN, K. A., LARSON, J. L., YARBOUGH, P. O., CURT, V. & SHANAHAN, W. R. 2004. Antiretroviral activity of the anti-CD4 monoclonal antibody TNX-355 in patients infected with HIV type 1. *Journal of Infectious Diseases,* 189**,** 286-291.

KWONG, P. D. & MASCOLA, J. R. 2012. Human antibodies that neutralize HIV-1: identification, structures, and B cell ontogenies. *Immunity,* 37**,** 412-25.

KWONG, P. D., WYATT, R., ROBINSON, J., SWEET, R. W., SODROSKI, J. & HENDRICKSON, W. A. 1998. Structure of an HIV gp120 envelope glycoprotein in complex with the CD4 receptor and a neutralizing human antibody. *Nature,* 393**,** 648-59.

LAWRENCE, D. A., SONG, R. & WEBER, P. 1996. Surface thiols of human lymphocytes and their changes after in vitro and in vivo activation. *Journal of leukocyte biology,* 60**,** 611-8.

LEE, B., SHARRON, M., BLANPAIN, C., DORANZ, B. J., VAKILI, J., SETOH, P., BERG, E., LIU, G., GUY, H. R., DURELL, S. R., PARMENTIER, M., CHANG, C. N., PRICE, K., TSANG, M. & DOMS, R. W. 1999a. Epitope mapping of CCR5 reveals multiple conformational states and distinct but overlapping structures involved in chemokine and coreceptor function. *The Journal of biological chemistry,* 274**,** 9617-26.

LEE, B., SHARRON, M., MONTANER, L. J., WEISSMAN, D. & DOMS, R. W. 1999b. Quantification of CD4, CCR5, and CXCR4 levels on lymphocyte subsets, dendritic cells, and differentially conditioned monocyte-derived macrophages. *Proc Natl Acad Sci U S A,* 96**,** 5215-20.

LIAO, H. X., LYNCH, R., ZHOU, T., GAO, F., ALAM, S. M., BOYD, S. D., FIRE, A. Z., ROSKIN, K. M., SCHRAMM, C. A., ZHANG, Z., ZHU, J., SHAPIRO, L., MULLIKIN, J. C., GNANAKARAN, S., HRABER, P., WIEHE, K., KELSOE, G., YANG, G., XIA, S. M., MONTEFIORI, D. C., PARKS, R., LLOYD, K. E., SCEARCE, R. M., SODERBERG, K. A., COHEN, M., KAMANGA, G., LOUDER, M. K., TRAN, L. M., CHEN, Y., CAI, F., CHEN, S., MOQUIN, S., DU, X., JOYCE, M. G., SRIVATSAN, S., ZHANG, B., ZHENG, A., SHAW, G. M., HAHN, B. H., KEPLER, T. B., KORBER, B. T., KWONG, P. D., MASCOLA, J. R. & HAYNES, B. F. 2013. Co-evolution of a broadly neutralizing HIV-1 antibody and founder virus. *Nature,* 496**,** 469-76.

LIU, J., BARTESAGHI, A., BORGNIA, M. J., SAPIRO, G. & SUBRAMANIAM, S. 2008. Molecular architecture of native HIV-1 gp120 trimers. *Nature,* 455**,** 109-13.

LYNCH, G. W., SLAYTOR, E. K., ELLIOTT, F. D., SAURAJEN, A., TURVILLE, S. G., SLOANE, A. J., CAMERON, P. U., CUNNINGHAM, A. L. & HALLIDAY, G. M. 2003. CD4 is expressed by epidermal Langerhans' cells predominantly as covalent dimers. *Experimental dermatology,* 12**,** 700-11.

LYNCH, G. W., SLOANE, A. J., RASO, V., LAI, A. & CUNNINGHAM, A. L. 1999. Direct evidence for native CD4 oligomers in lymphoid and monocytoid cells. *European journal of immunology,* 29**,** 2590-602.

MACARTHUR, M. W. & THORNTON, J. M. 1991. Influence of proline residues on protein conformation. *J Mol Biol,* 218**,** 397-412.

MADDON, P. J., LITTMAN, D. R., GODFREY, M., MADDON, D. E., CHESS, L. & AXEL, R. 1985. The isolation and nucleotide sequence of a cDNA encoding the T cell surface protein T4: a new member of the immunoglobulin gene family. *Cell,* 42**,** 93-104.

MAEKAWA, A., SCHMIDT, B., FAZEKAS DE ST GROTH, B., SANEJOUAND, Y. H. & HOGG, P. J. 2006. Evidence for a domain-swapped CD4 dimer as the coreceptor for binding to class II MHC. *Journal of immunology,* 176**,** 6873-8.

MALIM, M. H. & EMERMAN, M. 2008. HIV-1 accessory proteins--ensuring viral survival in a hostile environment. *Cell host & microbe,* 3**,** 388-98.

MASCOLA, J. R., LEWIS, M. G., STIEGLER, G., HARRIS, D., VANCOTT, T. C., HAYES, D., LOUDER, M. K., BROWN, C. R., SAPAN, C. V., FRANKEL, S. S., LU, Y., ROBB, M. L., KATINGER, H. & BIRX, D. L. 1999.

Protection of Macaques against pathogenic simian/human immunodeficiency virus 89.6PD by passive transfer of neutralizing antibodies. *Journal of virology,* 73**,** 4009-18.

MASCOLA, J. R., STIEGLER, G., VANCOTT, T. C., KATINGER, H., CARPENTER, C. B., HANSON, C. E., BEARY, H., HAYES, D., FRANKEL, S. S., BIRX, D. L. & LEWIS, M. G. 2000. Protection of macaques against vaginal transmission of a pathogenic HIV-1/SIV chimeric virus by passive infusion of neutralizing antibodies. *Nature medicine,* 6**,** 207-10.

MATTHEWS, T., SALGO, M., GREENBERG, M., CHUNG, J., DEMASI, R. & BOLOGNESI, D. 2004. Enfuvirtide: the first therapy to inhibit the entry of HIV-1 into host CD4 lymphocytes. *Nature reviews. Drug discovery,* 3**,** 215-25.

MATTHIAS, L. J., AZIMI, I., TABRETT, C. A. & HOGG, P. J. 2010. Reduced monomeric CD4 is the preferred receptor for HIV. *The Journal of biological chemistry,* 285**,** 40793-9.

MATTHIAS, L. J. & HOGG, P. J. 2003. Redox control on the cell surface: implications for HIV-1 entry. *Antioxidants & redox signaling,* 5**,** 133-8.

MATTHIAS, L. J., YAM, P. T., JIANG, X. M., VANDEGRAAFF, N., LI, P., POUMBOURIOS, P., DONOGHUE, N. & HOGG, P. J. 2002. Disulfide exchange in domain 2 of CD4 is required for entry of HIV-1. *Nature immunology,* 3**,** 727-32.

MCCUTCHAN, F. E. 2006. Global epidemiology of HIV. *Journal of medical virology,* 78 Suppl 1**,** S7-S12.

MCSHANE, H. 2005. Co-infection with HIV and TB: double trouble. *International journal of STD & AIDS,* 16**,** 95-100; quiz 101.

MIDDELBERG, A. P. 2002. Preparative protein refolding. *Trends Biotechnol,* 20**,** 437-43.

MOIR, S., PERREAULT, J. & POULIN, L. 1996. Postbinding events mediated by human immunodeficiency virus type 1 are sensitive to modifications in the D4-transmembrane linker region of CD4. *Journal of virology,* 70**,** 8019-28.

MOLDOVAN, M. C., YACHOU, A., LEVESQUE, K., WU, H., HENDRICKSON, W. A., COHEN, E. A. & SEKALY, R. P. 2002. CD4 dimers constitute the functional component required for T cell activation. *Journal of immunology,* 169**,** 6261-8.

MOORE, J. P., SATTENTAU, Q. J., KLASSE, P. J. & BURKLY, L. C. 1992. A monoclonal antibody to CD4 domain 2 blocks soluble CD4-induced conformational changes in the envelope glycoproteins of human immunodeficiency virus type 1 (HIV-1) and HIV-1 infection of CD4+ cells. *Journal of virology,* 66**,** 4784-93.

MOORE, J. P., SATTENTAU, Q. J., YOSHIYAMA, H., THALI, M., CHARLES, M., SULLIVAN, N., POON, S. W., FUNG, M. S., TRAINCARD, F., PINKUS, M. & ET AL. 1993. Probing the structure of the V2 domain of human immunodeficiency virus type 1 surface glycoprotein gp120 with a panel of eight monoclonal antibodies: human immune response to the V1 and V2 domains. *Journal of virology,* 67**,** 6136-51.

MOORE, J. P. & SODROSKI, J. 1996. Antibody cross-competition analysis of the human immunodeficiency virus type 1 gp120 exterior envelope glycoprotein. *Journal of virology,* 70**,** 1863-72.

MOORE, P. L., GRAY, E. S., WIBMER, C. K., BHIMAN, J. N., NONYANE, M., SHEWARD, D. J., HERMANUS, T., BAJIMAYA, S., TUMBA, N. L., ABRAHAMS, M. R., LAMBSON, B. E., RANCHOBE, N., PING, L., NGANDU, N., ABDOOL KARIM, Q., ABDOOL KARIM, S. S., SWANSTROM, R. I., SEAMAN, M. S., WILLIAMSON, C. & MORRIS, L. 2012. Evolution of an HIV glycan-dependent broadly neutralizing antibody epitope through immune escape. *Nature medicine,* 18**,** 1688-92.

MUSTER, T., STEINDL, F., PURTSCHER, M., TRKOLA, A., KLIMA, A., HIMMLER, G., RUKER, F. & KATINGER, H. 1993. A conserved neutralizing epitope on gp41 of human immunodeficiency virus type 1. *Journal of virology,* 67**,** 6642-7.

MYSZKA, D. G., SWEET, R. W., HENSLEY, P., BRIGHAM-BURKE, M., KWONG, P. D., HENDRICKSON, W. A., WYATT, R., SODROSKI, J. & DOYLE, M. L. 2000. Energetics of the HIV gp120-CD4 binding reaction. *Proceedings of the National Academy of Sciences of the United States of America,* 97**,** 9026-31.

NICHOLSON, L. K., YAMAZAKI, T., TORCHIA, D. A., GRZESIEK, S., BAX, A., STAHL, S. J., KAUFMAN, J. D., WINGFIELD, P. T., LAM, P. Y., JADHAV, P. K. & ET AL. 1995. Flexibility and function in HIV-1 protease. *Nature structural biology,* 2**,** 274-80.

NOIVA, R. 1994. Enzymatic catalysis of disulfide formation. *Protein expression and purification,* 5**,** 1-13.

NORRIS D, M. J., GATHE J, ET AL. 2006. Phase 2 efficacy and safety of the novel entry inhibitor, TNX-355, in combination with optimized background regimen (OBR). *16th International AIDS Conference.* Toronto, Canada.

OVERBAUGH, J. & RUDENSEY, L. M. 1992. Alterations in potential sites for glycosylation predominate during evolution of the simian immunodeficiency virus envelope gene in macaques. *Journal of virology,* 66**,** 5937-48.

OZEL, M., PAULI, G. & GELDERBLOM, H. R. 1988. The organization of the envelope projections on the surface of HIV. *Archives of virology,* 100**,** 255-66.

PACE, C. S., FORDYCE, M. W., FRANCO, D., KAO, C. Y., SEAMAN, M. S. & HO, D. D. 2013. Anti-CD4 monoclonal antibody ibalizumab exhibits breadth and potency against HIV-1, with natural resistance mediated by the loss of a V5 glycan in envelope. *Journal of acquired immune deficiency syndromes,* 62**,** 1-9.

PARREN, P. W., BURTON, D. R. & SATTENTAU, Q. J. 1997. HIV-1 antibody--debris or virion? *Nature medicine,* 3**,** 366-7.

PATTERSON, S., GROSS, J., ENGLISH, N., STACKPOOLE, A., BEDFORD, P. & KNIGHT, S. C. 1995. CD4 expression on dendritic cells and their infection by human immunodeficiency virus. *J Gen Virol,* 76 (Pt 5)**,** 1155-63.

PEJCHAL, R., DOORES, K. J., WALKER, L. M., KHAYAT, R., HUANG, P. S., WANG, S. K., STANFIELD, R. L., JULIEN, J. P., RAMOS, A., CRISPIN, M., DEPETRIS, R., KATPALLY, U., MAROZSAN, A., CUPO, A., MALOVESTE, S., LIU, Y., MCBRIDE, R., ITO, Y., SANDERS, R. W., OGOHARA, C., PAULSON, J. C., FEIZI, T., SCANLAN, C. N., WONG, C. H., MOORE, J. P., OLSON, W. C., WARD, A. B., POIGNARD, P., SCHIEF, W. R., BURTON, D. R. & WILSON, I. A. 2011. A potent and broad neutralizing antibody recognizes and penetrates the HIV glycan shield. *Science,* 334**,** 1097-103.

PETERSON, A. & SEED, B. 1988. Genetic analysis of monoclonal antibody and HIV binding sites on the human lymphocyte antigen CD4. *Cell,* 54**,** 65-72.

PIANTADOSI, A., PANTELEEFF, D., BLISH, C. A., BAETEN, J. M., JAOKO, W., MCCLELLAND, R. S. & OVERBAUGH, J. 2009. Breadth of neutralizing antibody response to human immunodeficiency virus type 1 is affected by factors early in infection but does not influence disease progression. *Journal of virology,* 83**,** 10269-74.

POIGNARD, P., SAPHIRE, E. O., PARREN, P. W. & BURTON, D. R. 2001. gp120: Biologic aspects of structural features. *Annual review of immunology,* 19**,** 253-74.

QIN L., Z. M., G. REITHMULLER, P. REIBER, CHEN Y. 2001. Monoclonal Anti-CD4 Antibody MT310 Binds HIV-1 gp120 Binding Site on CD4. *TSINGHUA SCIENCE AND TECHNOLOGY,* Vol. 6**,** 257 - 259.

RATNER, L., HASELTINE, W., PATARCA, R., LIVAK, K. J., STARCICH, B., JOSEPHS, S. F., DORAN, E. R., RAFALSKI, J. A., WHITEHORN, E. A., BAUMEISTER, K. & ET AL. 1985. Complete nucleotide sequence of the AIDS virus, HTLV-III. *Nature,* 313**,** 277-84.

REIMANN, K. A., BURKLY, L. C., BURRUS, B., WAITE, B. C., LORD, C. I. & LETVIN, N. L. 1993. In vivo administration to rhesus monkeys of a CD4-specific monoclonal antibody capable of blocking AIDS virus replication. *AIDS research and human retroviruses,* 9**,** 199-207.

REIMANN, K. A., CATE, R. L., WU, Y., PALMER, L., OLSON, D., WAITE, B. C., LETVIN, N. L. & BURKLY, L. C. 1995. In vivo administration of CD4-specific monoclonal antibody: effect on provirus load in rhesus monkeys chronically infected with the simian immunodeficiency virus of macaques. *AIDS research and human retroviruses,* 11**,** 517-25.

REIMANN, K. A., KHUNKHUN, R., LIN, W., GORDON, W. & FUNG, M. 2002. A humanized, nondepleting anti-CD4 antibody that blocks virus entry inhibits virus replication in rhesus monkeys chronically infected with simian immunodeficiency virus. *AIDS research and human retroviruses,* 18**,** 747-55.

REIMANN, K. A., LIN, W., BIXLER, S., BROWNING, B., EHRENFELS, B. N., LUCCI, J., MIATKOWSKI, K., OLSON, D., PARISH, T. H., ROSA, M. D., OLESON, F. B., HSU, Y. M., PADLAN, E. A., LETVIN, N. L. & BURKLY, L. C. 1997. A humanized form of a CD4-specific monoclonal antibody exhibits decreased antigenicity and prolonged plasma half-life in rhesus monkeys while retaining its unique biological and antiviral properties. *AIDS research and human retroviruses,* 13**,** 933-43.

RICHMAN, D. D., WRIN, T., LITTLE, S. J. & PETROPOULOS, C. J. 2003. Rapid evolution of the neutralizing antibody response to HIV type 1 infection. *Proceedings of the National Academy of Sciences of the United States of America,* 100**,** 4144-9.

RIZZUTO, C. D., WYATT, R., HERNANDEZ-RAMOS, N., SUN, Y., KWONG, P. D., HENDRICKSON, W. A. & SODROSKI, J. 1998. A conserved HIV gp120 glycoprotein structure involved in chemokine receptor binding. *Science,* 280**,** 1949-53.

ROBEN, P., MOORE, J. P., THALI, M., SODROSKI, J., BARBAS, C. F., 3RD & BURTON, D. R. 1994. Recognition properties of a panel of human recombinant Fab fragments to the CD4 binding site of gp120 that show differing abilities to neutralize human immunodeficiency virus type 1. *Journal of virology,* 68**,** 4821-8.

RUBARTELLI, A., BAJETTO, A., ALLAVENA, G., WOLLMAN, E. & SITIA, R. 1992. Secretion of thioredoxin by normal and neoplastic cells through a leaderless secretory pathway. *The Journal of biological chemistry,* 267**,** 24161-4.

RYU, S. E., KWONG, P. D., TRUNEH, A., PORTER, T. G., ARTHOS, J., ROSENBERG, M., DAI, X. P., XUONG, N. H., AXEL, R., SWEET, R. W. & ET AL. 1990. Crystal structure of an HIV-binding recombinant fragment of human CD4. *Nature,* 348**,** 419-26.

SAHA, P., BARUA, B., BHATTACHARYYA, S., BALAMURALI, M. M., SCHIEF, W. R., BAKER, D. & VARADARAJAN, R. 2011. Design and characterization of stabilized derivatives of human CD4D12 and CD4D1. *Biochemistry,* 50**,** 7891-900.

SALAZAR-GONZALEZ, J. F., BAILES, E., PHAM, K. T., SALAZAR, M. G., GUFFEY, M. B., KEELE, B. F., DERDEYN, C. A., FARMER, P., HUNTER, E., ALLEN, S., MANIGART, O., MULENGA, J., ANDERSON, J. A., SWANSTROM, R., HAYNES, B. F., ATHREYA, G. S., KORBER, B. T., SHARP, P. M., SHAW, G. M. & HAHN, B. H. 2008. Deciphering human immunodeficiency virus type 1 transmission and early envelope diversification by single-genome amplification and sequencing. *Journal of virology,* 82**,** 3952-70.

SAPHIRE, E. O., PARREN, P. W., PANTOPHLET, R., ZWICK, M. B., MORRIS, G. M., RUDD, P. M., DWEK, R. A., STANFIELD, R. L., BURTON, D. R. & WILSON, I. A. 2001. Crystal structure of a neutralizing human IGG against HIV-1: a template for vaccine design. *Science,* 293**,** 1155-9.

SARAFIANOS, S. G., MARCHAND, B., DAS, K., HIMMEL, D. M., PARNIAK, M. A., HUGHES, S. H. & ARNOLD, E. 2009. Structure and function of HIV-1 reverse transcriptase: molecular mechanisms of polymerization and inhibition. *Journal of molecular biology,* 385**,** 693-713.

SATHER, D. N., ARMANN, J., CHING, L. K., MAVRANTONI, A., SELLHORN, G., CALDWELL, Z., YU, X., WOOD, B., SELF, S., KALAMS, S. & STAMATATOS, L. 2009. Factors associated with the development of cross-reactive neutralizing antibodies during human immunodeficiency virus type 1 infection. *Journal of virology,* 83**,** 757-69.

SCHMIDT, B., HO, L. & HOGG, P. J. 2006. Allosteric disulfide bonds. *Biochemistry,* 45**,** 7429-33.

SCHRODER, A. R., SHINN, P., CHEN, H., BERRY, C., ECKER, J. R. & BUSHMAN, F. 2002. HIV-1 integration in the human genome favors active genes and local hotspots. *Cell,* 110**,** 521-9.

SCHRODER, K., HERTZOG, P. J., RAVASI, T. & HUME, D. A. 2004. Interferon-gamma: an overview of signals, mechanisms and functions. *Journal of leukocyte biology,* 75**,** 163-89.

SCHUBERT, U., FERRER-MONTIEL, A. V., OBLATT-MONTAL, M., HENKLEIN, P., STREBEL, K. & MONTAL, M. 1996. Identification of an ion channel activity of the Vpu transmembrane domain and its involvement in the regulation of virus release from HIV-1-infected cells. *FEBS letters,* 398**,** 12-8.

SEVIER, C. S. & KAISER, C. A. 2002. Formation and transfer of disulphide bonds in living cells. *Nature reviews. Molecular cell biology,* 3**,** 836-47.

SHANKARAPPA, R., MARGOLICK, J. B., GANGE, S. J., RODRIGO, A. G., UPCHURCH, D., FARZADEGAN, H., GUPTA, P., RINALDO, C. R., LEARN, G. H., HE, X., HUANG, X. L. & MULLINS, J. I. 1999. Consistent viral evolutionary changes associated with the progression of human immunodeficiency virus type 1 infection. *Journal of virology,* 73**,** 10489-502.

SHARMA, D., BALAMURALI, M. M., CHAKRABORTY, K., KUMARAN, S., JEGANATHAN, S., RASHID, U., INGALLINELLA, P. & VARADARAJAN, R. 2005. Protein minimization of the gp120 binding region of human CD4. *Biochemistry,* 44**,** 16192-202.

SHIBATA, R., IGARASHI, T., HAIGWOOD, N., BUCKLER-WHITE, A., OGERT, R., ROSS, W., WILLEY, R., CHO, M. W. & MARTIN, M. A. 1999. Neutralizing antibody directed against the HIV-1 envelope glycoprotein can completely block HIV-1/SIV chimeric virus infections of macaque monkeys. *Nature medicine,* 5**,** 204-10.

SILICIANO, R. F. & GREENE, W. C. 2011. HIV latency. *Cold Spring Harb Perspect Med,* 1**,** a007096.

SIMEK, M. D., RIDA, W., PRIDDY, F. H., PUNG, P., CARROW, E., LAUFER, D. S., LEHRMAN, J. K., BOAZ, M., TARRAGONA-FIOL, T., MIIRO, G., BIRUNGI, J., POZNIAK, A., MCPHEE, D. A., MANIGART, O., KARITA, E., INWOLEY, A., JAOKO, W., DEHOVITZ, J., BEKKER, L. G., PITISUTTITHUM, P., PARIS, R., WALKER, L. M., POIGNARD, P., WRIN, T., FAST, P. E., BURTON, D. R. & KOFF, W. C. 2009. Human immunodeficiency virus type 1 elite neutralizers: individuals with broad and potent neutralizing activity identified by using a high-throughput neutralization assay together with an analytical selection algorithm. *Journal of virology,* 83**,** 7337-48.

SINGH, S. M. & PANDA, A. K. 2005. Solubilization and refolding of bacterial inclusion body proteins. *J Biosci Bioeng,* 99**,** 303-10.

SONG, R., FRANCO, D., KAO, C. Y., YU, F., HUANG, Y. & HO, D. D. 2010. Epitope mapping of ibalizumab, a humanized anti-CD4 monoclonal antibody with anti-HIV-1 activity in infected patients. *Journal of virology,* 84**,** 6935-42.

SORENSEN, H. P., SPERLING-PETERSEN, H. U. & MORTENSEN, K. K. 2003. Dialysis strategies for protein refolding: preparative streptavidin production. *Protein Expr Purif,* 31**,** 149-54.

SPELLMAN, M. W., LEONARD, C. K., BASA, L. J., GELINEO, I. & VAN HALBEEK, H. 1991. Carbohydrate structures of recombinant soluble human CD4 expressed in Chinese hamster ovary cells. *Biochemistry,* 30**,** 2395-406.

SPINA, C. A., PRINCE, H. E. & RICHMAN, D. D. 1997. Preferential replication of HIV-1 in the CD45RO memory cell subset of primary CD4 lymphocytes in vitro. *J Clin Invest,* 99**,** 1774-85.

SREERAMA, N., VENYAMINOV, S. Y. & WOODY, R. W. 2000. Estimation of protein secondary structure from circular dichroism spectra: inclusion of denatured proteins with native proteins in the analysis. *Analytical biochemistry,* 287**,** 243-51.

STAMATATOS, L., MORRIS, L., BURTON, D. R. & MASCOLA, J. R. 2009. Neutralizing antibodies generated during natural HIV-1 infection: good news for an HIV-1 vaccine? *Nature medicine,* 15**,** 866-70.

STANFIELD, R. L., GORNY, M. K., WILLIAMS, C., ZOLLA-PAZNER, S. & WILSON, I. A. 2004. Structural rationale for the broad neutralization of HIV-1 by human monoclonal antibody 447-52D. *Structure,* 12**,** 193-204.

SULLIVAN, K. E., CUTILLI, J., PILIERO, L. M., GHAVIMI-ALAGHA, D., STARR, S. E., CAMPBELL, D. E. & DOUGLAS, S. D. 2000. Measurement of cytokine secretion, intracellular protein expression, and mRNA in resting and stimulated peripheral blood mononuclear cells. *Clinical and diagnostic laboratory immunology,* 7**,** 920-4.

SULLIVAN, N., SUN, Y., SATTENTAU, Q., THALI, M., WU, D., DENISOVA, G., GERSHONI, J., ROBINSON, J., MOORE, J. & SODROSKI, J. 1998. CD4-Induced conformational changes in the human immunodeficiency virus type 1 gp120 glycoprotein: consequences for virus entry and neutralization. *Journal of virology,* 72**,** 4694-703.

SWEET, R. W., TRUNEH, A. & HENDRICKSON, W. A. 1991. CD4: its structure, role in immune function and AIDS pathogenesis, and potential as a pharmacological target. *Current opinion in biotechnology,* 2**,** 622-33.

TAGER, M., KRONING, H., THIEL, U. & ANSORGE, S. 1997. Membrane-bound proteindisulfide isomerase (PDI) is involved in regulation of surface expression of thiols and drug sensitivity of B-CLL cells. *Experimental hematology,* 25**,** 601-7.

TAIMED_BIOLOGICS_INC 2011. A Phase 1, Randomized, Double-Blinded, Placebo-Controlled, Sequential Dose-Escalation Study of the Safety, Tolerability, Pharmacokinetics and Pharmacodynamics of Subcutaneously Administered Ibalizumab in HIV-Negative, At-Risk Volunteers. *In:* INC, T. B. (ed.). Bethesda ClinicalTrials.gov. Bethesda (MD): National Library of Medicine (US).

TAN, Q., ZHU, Y., LI, J., CHEN, Z., HAN, G. W., KUFAREVA, I., LI, T., MA, L., FENALTI, G., ZHANG, W., XIE, X., YANG, H., JIANG, H., CHEREZOV, V., LIU, H., STEVENS, R. C., ZHAO, Q. & WU, B. 2013. Structure of the CCR5 chemokine receptor-HIV entry inhibitor maraviroc complex. *Science,* 341**,** 1387-90.

THORNTON, J. M. 1981. Disulphide bridges in globular proteins. *Journal of molecular biology,* 151**,** 261-87.

TITE, J. P., SLOAN, A. & JANEWAY, C. A., JR. 1986. The role of L3T4 in T cell activation: L3T4 may be both an Ia-binding protein and a receptor that transduces a negative signal. *The Journal of molecular and cellular immunology : JMCI,* 2**,** 179-90.

TOMA, J., WEINHEIMER, S. P., STAWISKI, E., WHITCOMB, J. M., LEWIS, S. T., PETROPOULOS, C. J. & HUANG, W. 2011. Loss of asparagine-linked glycosylation sites in variable region 5 of human immunodeficiency virus type 1 envelope is associated with resistance to CD4 antibody ibalizumab. *Journal of virology,* 85**,** 3872-80.

TRKOLA, A., POMALES, A. B., YUAN, H., KORBER, B., MADDON, P. J., ALLAWAY, G. P., KATINGER, H., BARBAS, C. F., 3RD, BURTON, D. R., HO, D. D. & ET AL. 1995. Cross-clade neutralization of primary isolates of human immunodeficiency virus type 1 by human monoclonal antibodies and tetrameric CD4-IgG. *Journal of virology,* 69**,** 6609-17.

TRKOLA, A., PURTSCHER, M., MUSTER, T., BALLAUN, C., BUCHACHER, A., SULLIVAN, N., SRINIVASAN, K., SODROSKI, J., MOORE, J. P. & KATINGER, H. 1996. Human monoclonal antibody 2G12 defines a distinctive neutralization epitope on the gp120 glycoprotein of human immunodeficiency virus type 1. *Journal of virology,* 70**,** 1100-8.

TSUMOTO, K., EJIMA, D., KUMAGAI, I. & ARAKAWA, T. 2003. Practical considerations in refolding proteins from inclusion bodies. *Protein Expr Purif,* 28**,** 1-8.

VAN DER MERWE, P. A. & DAVIS, S. J. 2003. Molecular interactions mediating T cell antigen recognition. *Annu Rev Immunol,* 21**,** 659-84.

VAQUERO, C., SANCEAU, J., WEISSENBACH, J., BERANGER, F. & FALCOFF, R. 1986. Regulation of human gamma-interferon and beta-interferon gene expression in PHA-activated lymphocytes. *Journal of interferon research,* 6**,** 161-70.

VERKOCZY, L., KELSOE, G., MOODY, M. A. & HAYNES, B. F. 2011. Role of immune mechanisms in induction of HIV-1 broadly neutralizing antibodies. *Current opinion in immunology,* 23**,** 383-90.

WALKER, L. M., PHOGAT, S. K., CHAN-HUI, P. Y., WAGNER, D., PHUNG, P., GOSS, J. L., WRIN, T., SIMEK, M. D., FLING, S., MITCHAM, J. L., LEHRMAN, J. K., PRIDDY, F. H., OLSEN, O. A., FREY, S. M., HAMMOND, P. W., KAMINSKY, S., ZAMB, T., MOYLE, M., KOFF, W. C., POIGNARD, P. & BURTON, D. R. 2009. Broad and potent neutralizing antibodies from an African donor reveal a new HIV-1 vaccine target. *Science,* 326**,** 285-9.

WANG, J. H., MEIJERS, R., XIONG, Y., LIU, J. H., SAKIHAMA, T., ZHANG, R., JOACHIMIAK, A. & REINHERZ, E. L. 2001. Crystal structure of the human CD4 N-terminal two-domain fragment complexed to a class II MHC molecule. *Proceedings of the National Academy of Sciences of the United States of America,* 98**,** 10799-804.

WANG, J. H., YAN, Y. W., GARRETT, T. P., LIU, J. H., RODGERS, D. W., GARLICK, R. L., TARR, G. E., HUSAIN, Y., REINHERZ, E. L. & HARRISON, S. C. 1990. Atomic structure of a fragment of human CD4 containing two immunoglobulin-like domains. *Nature,* 348**,** 411-8.

WEI, X., DECKER, J. M., WANG, S., HUI, H., KAPPES, J. C., WU, X., SALAZAR-GONZALEZ, J. F., SALAZAR, M. G., KILBY, J. M., SAAG, M. S., KOMAROVA, N. L., NOWAK, M. A., HAHN, B. H., KWONG, P. D. & SHAW, G. M. 2003. Antibody neutralization and escape by HIV-1. *Nature,* 422**,** 307-12.

WEISSENHORN, W., DESSEN, A., HARRISON, S. C., SKEHEL, J. J. & WILEY, D. C. 1997. Atomic structure of the ectodomain from HIV-1 gp41. *Nature,* 387**,** 426-30.

WHITE, T. A., BARTESAGHI, A., BORGNIA, M. J., MEYERSON, J. R., DE LA CRUZ, M. J., BESS, J. W., NANDWANI, R., HOXIE, J. A., LIFSON, J. D., MILNE, J. L. & SUBRAMANIAM, S. 2010. Molecular architectures of trimeric SIV and HIV-1 envelope glycoproteins on intact viruses: strain-dependent variation in quaternary structure. *PLoS pathogens,* 6**,** e1001249.

WHO_MEDIA_CENTRE. 2014. *HIV/AIDS Fact Sheet* [Online]. Geneva, Switzerland: WHO. Available: http://www.who.int/mediacentre/factsheets/fs360/en/ [Accessed 24 March 2014].

WOLINSKY, S. M., KORBER, B. T., NEUMANN, A. U., DANIELS, M., KUNSTMAN, K. J., WHETSELL, A. J., FURTADO, M. R., CAO, Y., HO, D. D. & SAFRIT, J. T. 1996. Adaptive evolution of human immunodeficiency virus-type 1 during the natural course of infection. *Science,* 272**,** 537-42.

WOLLMAN, E. E., KAHAN, A. & FRADELIZI, D. 1997. Detection of membrane associated thioredoxin on human cell lines. *Biochemical and biophysical research communications,* 230**,** 602-6.

WORLD_HEALTH_ORGANISATION 2007. WHO case definitions of HIV for surveillance and revised clinical staging and immunological classification of HIV-related disease in adults and children. *In:* WORLD_HEALTH_ORGANISATION (ed.). Geneva, Switzerland.

WORLD_HEALTH_ORGANISATION 2011. Global Tuberculosis Control. *In:* WHO_REPORT (ed.). Geneva, Switzerland: WHO.

WORLD_HEALTH_ORGANISATION 2013. World Health Statistics *In:* WHO (ed.) *World Health Statistics.* Geneva: WHO.

WORLD_HEALTH_ORGANIZATION. 2014. *The top 10 causes of death* [Online]. World Health Organization. Available: http://www.who.int/mediacentre/factsheets/fs310/en/ [Accessed 21.05.2015 2015].

WU, H., KWONG, P. D. & HENDRICKSON, W. A. 1997. Dimeric association and segmental variability in the structure of human CD4. *Nature,* 387**,** 527-30.

WU, H., MYSZKA, D. G., TENDIAN, S. W., BROUILLETTE, C. G., SWEET, R. W., CHAIKEN, I. M. & HENDRICKSON, W. A. 1996. Kinetic and structural analysis of mutant CD4 receptors that are defective in HIV gp120 binding. *Proc Natl Acad Sci U S A,* 93**,** 15030-5.

WU, J., YANG, J. T. & WU, C. S. 1992. Beta-II conformation of all-beta proteins can be distinguished from unordered form by circular dichroism. *Analytical biochemistry,* 200**,** 359-64.

WU, X., YANG, Z. Y., LI, Y., HOGERKORP, C. M., SCHIEF, W. R., SEAMAN, M. S., ZHOU, T., SCHMIDT, S. D., WU, L., XU, L., LONGO, N. S., MCKEE, K., O'DELL, S., LOUDER, M. K., WYCUFF, D. L., FENG, Y., NASON, M., DORIA-ROSE, N., CONNORS, M., KWONG, P. D., ROEDERER, M., WYATT, R. T., NABEL, G. J. & MASCOLA, J. R. 2010. Rational design of envelope identifies broadly neutralizing human monoclonal antibodies to HIV-1. *Science,* 329**,** 856-61.

WU, X., ZHOU, T., ZHU, J., ZHANG, B., GEORGIEV, I., WANG, C., CHEN, X., LONGO, N. S., LOUDER, M., MCKEE, K., O'DELL, S., PERFETTO, S., SCHMIDT, S. D., SHI, W., WU, L., YANG, Y., YANG, Z. Y., YANG, Z., ZHANG, Z., BONSIGNORI, M., CRUMP, J. A., KAPIGA, S. H., SAM, N. E., HAYNES, B. F.,

SIMEK, M., BURTON, D. R., KOFF, W. C., DORIA-ROSE, N. A., CONNORS, M., MULLIKIN, J. C., NABEL, G. J., ROEDERER, M., SHAPIRO, L., KWONG, P. D. & MASCOLA, J. R. 2011. Focused evolution of HIV-1 neutralizing antibodies revealed by structures and deep sequencing. *Science,* 333**,** 1593-602.

WYATT, R., KWONG, P. D., DESJARDINS, E., SWEET, R. W., ROBINSON, J., HENDRICKSON, W. A. & SODROSKI, J. G. 1998. The antigenic structure of the HIV gp120 envelope glycoprotein. *Nature,* 393**,** 705-11.

WYATT, R., MOORE, J., ACCOLA, M., DESJARDIN, E., ROBINSON, J. & SODROSKI, J. 1995. Involvement of the V1/V2 variable loop structure in the exposure of human immunodeficiency virus type 1 gp120 epitopes induced by receptor binding. *Journal of virology,* 69**,** 5723-33.

XIAO, X., CHEN, W., FENG, Y., ZHU, Z., PRABAKARAN, P., WANG, Y., ZHANG, M. Y., LONGO, N. S. & DIMITROV, D. S. 2009. Germline-like predecessors of broadly neutralizing antibodies lack measurable binding to HIV-1 envelope glycoproteins: implications for evasion of immune responses and design of vaccine immunogens. *Biochemical and biophysical research communications,* 390**,** 404-9.

YACHOU, A. & SEKALY, R. P. 1999. Binding of soluble recombinant HIV envelope glycoprotein, rgp120, induces conformational changes in the cellular membrane-anchored CD4 molecule. *Biochemical and biophysical research communications,* 265**,** 428-33.

YIN, J., LI, G., REN, X. & HERRLER, G. 2007. Select what you need: a comparative evaluation of the advantages and limitations of frequently used expression systems for foreign genes. *Journal of biotechnology,* 127**,** 335-47.

YIN, Y., WANG, X. X. & MARIUZZA, R. A. 2012. Crystal structure of a complete ternary complex of T-cell receptor, peptide-MHC, and CD4. *Proceedings of the National Academy of Sciences of the United States of America,* 109**,** 5405-10.

ZEIRA, M., BYRN, R. A. & GROOPMAN, J. E. 1990. Inhibition of serum-enhanced HIV-1 infection of U937 monocytoid cells by recombinant soluble CD4 and anti-CD4 monoclonal antibody. *AIDS research and human retroviruses,* 6**,** 629-39.

ZHOU, T., GEORGIEV, I., WU, X., YANG, Z. Y., DAI, K., FINZI, A., KWON, Y. D., SCHEID, J. F., SHI, W., XU, L., YANG, Y., ZHU, J., NUSSENZWEIG, M. C., SODROSKI, J., SHAPIRO, L., NABEL, G. J., MASCOLA, J. R. & KWONG, P. D. 2010. Structural basis for broad and potent neutralization of HIV-1 by antibody VRC01. *Science,* 329**,** 811-7.

ZHU, J., WU, X., ZHANG, B., MCKEE, K., O'DELL, S., SOTO, C., ZHOU, T., CASAZZA, J. P., MULLIKIN, J. C., KWONG, P. D., MASCOLA, J. R. & SHAPIRO, L. 2013. De novo identification of VRC01 class HIV-1-neutralizing antibodies by next-generation sequencing of B-cell transcripts. *Proceedings of the National Academy of Sciences of the United States of America,* 110**,** E4088-97.

ZWICK, M. B., LABRIJN, A. F., WANG, M., SPENLEHAUER, C., SAPHIRE, E. O., BINLEY, J. M., MOORE, J. P., STIEGLER, G., KATINGER, H., BURTON, D. R. & PARREN, P. W. 2001. Broadly neutralizing antibodies targeted to the membrane-proximal external region of human immunodeficiency virus type 1 glycoprotein gp41. *Journal of virology,* 75**,** 10892-905.

APPENDICES

APPENDIX A

a. For Bacterial Transformation/Culture/Plating:

i. Ampicillin 1000x Stock Solution* (*per 10 mL): Weigh out 1 g Ampicillin (Sigma-Aldrich, MO, U.S.A). Dissolve by vigourous agitation in 5 mL high-quality Millipore® distilled water and 5 mL 100 % ethanol. Store at -20^{o}C.

ii. Transformation Buffer (per 100 mL): Weigh out 1.4702 g $CaCl_2.2H_2O$ (100 mM) (Sigma-Aldrich, MO, U.S.A) and 0.3024 g PIPES-HCl (10 mM). Dissolve in 80 mL of high-quality Millipore® distilled water. Add 15 mL of glycerol (15 %). PH to 7.0 with NaOH (Sigma-Aldrich, MO, U.S.A). Make up to 100 mL with high-quality Millipore® distilled water. Sterilize by autoclaving on liquid cycle (121^{o}C, 1kg/cm^2, 20 minutes). Allow to cool and store at 4^{o}C.

iii. Luria Bertani (LB) broth (per 1L): Weigh out 10 g tryptone (Sigma-Aldrich, MO, U.S.A), 10 g yeast extract (Sigma-Aldrich, MO, U.S.A) and 5.0 g NaCl (Sigma-Aldrich, MO, U.S.A). Dissolve into 1L distilled water Sterilize by autoclaving on liquid cycle (121^{o}C, 1kg/cm^2, 20 minutes) and allow to cool. Store at room temperature.

iv. Agar LB (per 200ml): Weigh out 2 g tryptone (Sigma-Aldrich, MO, U.S.A), 2 g yeast extract (Sigma-Aldrich, MO, U.S.A), 3 g agar and 1g NaCl ((Sigma-Aldrich, MO, U.S.A). Dissolve into 1L distilled water. Sterilize by autoclaving on liquid cycle (121^{o}C, 1kg/cm^2, 20 minutes) and allow to cool. Store at room temperature. Melt before use.

b. For Agarose Gel Electrophoresis:

i. EDTA 0.5 M Stock Solution (per 200ml): Weigh out 37.22 g EDTA ((Sigma-Aldrich, MO, U.S.A). Dissolve in 150 mL high-quality Millipore® distilled water. PH to 8.0 with NaOH. Store at room temperature.

ii. Tris-acetate EDTA (TAE) Buffer, 50X stock (per 1L): Weigh out 242 g tris base. Add 57.1 mL glacial acetic acid (Merck, Darmstadt, Germany) and 100 mL 0.5 EDTA (Sigma-Aldrich, MO, U.S.A). Add 800 mL of distilled water. Adjust pH to 8.0 with HCl. Make up to 1 L with distilled water. Store at room temperature.

iii. 1% Agarose gel: Weigh out 1g agarose powder (Sigma-Aldrich, MO, U.S.A). Add 100 ml of 1X Tris acetate EDTA (TAE) buffer and heat in a microwave until the agarose completely dissolved. Allow to cool at room temperature before the addition of 7.5 µl Ethidium Bromide (0.5µg/ml) (Promega, U.S.A). Pour in a Bio-Rad Gel Chamber System (Bio-Rad) and allow to set.

c. For SDS-PAGE:

i. Monomer Solution (30.8 % T, 2.7 % C_{bis}), (per 200 mL): Weigh out 60 g acrylamide (Sigma-Aldrich, MO, U.S.A) and 1.6 g bisacrylamide (Merck). Dissolve in 200 mL of distilled water. Store in the dark at 4^{o}C.

ii. Stacking gel buffer, 4X (0.5 M tris.cl, pH 6.8) (per 50 mL): Weigh out 3.0 g tris-cl (0.5 M) (Sigma-Aldrich, MO, U.S.A). Dissolve in 40ml distilled water. Adjust pH to 6.8 with HCl. Make up to 50.0 ml with distilled water. Store at 4^{o}C in the dark.

iii. Running gel buffer, 4X (1.5 M tris.cl pH 8.8) (per 200 mL): Weigh out 36.3 g tris-cl (Sigma-Aldrich, MO, U.S.A). Dissolve into 150ml distilled water. Adjust pH to 8.8 with HCl. Make up to 200 ml with distilled water. Store in the dark at 4^{o}C

iv. Loading Buffer, 2X (0.125M tris-cl, 4% SDS, 20% v/v glycerol, 0,2M DTT, 0,02% bromophenol blue, pH6.8) (per 10ml): Weigh out 0.31 DTT (Sigma-Aldrich, MO, U.S.A). Add 2.5 ml 4x stacking gel buffer, 4.0 ml 10% SDS (Sigma-Aldrich, MO, U.S.A), 2.0 ml glycerol and 2 mg bromophenol blue. Adjust pH to 6.8 with HCl. Dissolve and make up to 10 ml with distilled water. Store 0.5 ml aliquots at -20^{o}C.

v. 10% SDS (per 100 ml): Weigh out 10g SDS (Sigma-Aldrich, MO, U.S.A). Dissolve in 100 ml distilled water. Store at room temperature.

vi. 10% Ammonium Persulphate (per 1 mL): Weigh out 1 g Ammonium Persulphate (Sigma-Aldrich, MO, U.S.A). Dissolve in 1 mL of syringe-quality distilled water. Use immediately. Do not store.

vii. Tank buffer, 10X (per 1L): Weigh out 30.28 g tris.cl (Sigma-Aldrich, MO, U.S.A), 144.13g glycine (Sigma-Aldrich, MO, U.S.A) and 10g SDS (Sigma-Aldrich, MO, U.S.A). Disolve into 1L of distilled water. Store at room temperature.

d. For Coomassie Blue Staining and Western Blots

i. Transfer buffer (per 1L): Add 200ml methanol into 800 mL of 1X Tank Buffer.

ii. Coomassie Blue stain (per 1L): Add 500 ml methanol and 100 ml acetic acid into 400 ml distilled water. Dissolve in 0.25g Coomassie R250. Store at room temperature.

iii. Destain Solution (per 1L): Add 50 ml ethanol and 70ml acetic acid into 850ml distilled water. Distilled water is then added to make up to 1L. Store at room temperature.

iv. ***10X TBS (per 1L):*** Weigh out 10 g NaCl (Sigma-Aldrich, MO, U.S.A), 30 g Tris (Sigma-Aldrich, MO, U.S.A) and 2.0 g of KCl (Sigma-Aldrich, MO, U.S.A). Dissolve into 950 mL of distilled water. Adjust pH to 7.4 with HCl. Make up to 1 L with distilled water. Store at 4^{o}C.

v. ***T-TBS (0.05% Tween, per 1L):*** Add 500 µL of Tween® 20 (Sigma-Aldrich, MO, U.S.A) into 1L of 1X TBS. Dissolve. Store at 4^{o}C.

vi. ***BSA Blocking Solution (10 mg/mL):*** Weigh out 50 mg of BSA (Sigma-Aldrich, MO, U.S.A). Dissolve into 50 mL of 1X TBS. Use immediately.

e. For Protein Isolation

i. ***Solubilisation buffer (per 50ml)***: Weigh out 24.03g urea (8M) (VWR), 0.18766 gylcine (50mM) (Sigma-Aldrich, MO, U.S.A), 0.068g imidazole (20mM) (Sigma-Aldrich, MO, U.S.A), and 1.46 g NaCl (Sigma-Aldrich, MO, U.S.A). Dissolve in 20 mL distilled water. Add 7.00µL β-mercaptoethanol (2 mM) (Sigma-Aldrich, MO, U.S.A). Adjust pH to 7.4 with HCl. Make up to 50 mL with distilled water. Store at room temperature.

ii. ***Folding Buffer A (per 1 L):*** Weigh out 3.75 g glycine (50 mM) (Sigma-Aldrich, MO, U.S.A), 100 g sucrose (10 %) (Sigma-Aldrich, MO, U.S.A), 0.31 g GSH (Glutathione, reduced, 1 mM) (Sigma-Aldrich, MO, U.S.A), 0.061 g GSSG (Glutathione disulphide, oxidised, 0.1 mM) (Sigma-Aldrich, MO, U.S.A) and 240 g Urea (4 M) (VWR International). Dissolve in 500 mL of distilled water. Add 2.0 mL 0.5 M stock EDTA (Sigma-Aldrich, MO, U.S.A) and 7.8 mL of 2 M of stock NaOH (Sigma-Aldrich, MO, U.S.A). PH to 9.6 with HCl or NaOH. Make to 1 L with distilled water. Chill before use (4^{o}C).

iii. ***Folding Buffer B (per 1 L):*** Weigh out 1.59 g Na_2CO_3 (15 mM) ((Sigma-Aldrich, MO, U.S.A), 2.93 g $NaHCO_3$ (35 mM) (Sigma-Aldrich, MO, U.S.A), 100 g sucrose (10 %) (Sigma-Aldrich, MO, U.S.A), 0.031 g GSH (Glutathione, reduced, 0.1 mM) (Sigma-Aldrich, MO, U.S.A) and 0.006 g (Glutathione disulphide, oxidised, 0.01 mM) (Sigma-Aldrich, MO, U.S.A). Dissolve in 950 mL of distilled water. Add 2.0 mL 0.5 M stock EDTA (Sigma-Aldrich, MO, U.S.A). PH to 9.6 with HCl or NaOH. Make up to 1 L wih distilled water. Chill before use (4^oC).

iv. ***Nickel Sulphate 0.1 M Stock Solution (per 10 mL):*** Weigh out 0.15476 g of $NiSO_4$ (Sigma-Aldrich, MO, U.S.A). Dissolve in 10 mL of high-quality Millipore® distilled water.

f. Wash buffers:

i. ***Base solution (per 100 mL):*** Weigh out 48.05 g urea (8M) (VWR International), 0.37532 g glycine (50mM) (Sigma-Aldrich, MO, U.S.A), 0.068g imidazole (20mM) (Sigma-Aldrich, MO, U.S.A) and 1.46 g NaCl (Sigma-Aldrich, MO, U.S.A). Dissolve in 40 mL distilled water. Add 14.00µL β-mercaptoethanol (Sigma-Aldrich, MO, U.S.A) (2 mM) and 10 mL of 10X PBS ((Sigma-Aldrich, MO, U.S.A). Make up to 100 mL with distilled water. Store at room temperature. Syringe/vacuum filter through 1 µL filter. Store at room temperature.

ii. ***For 20 mM imidazole (per100ml):*** Dissolve 0.13616 g Imidazole (Sigma-Aldrich, MO, U.S.A) into base solution. Adjust pH to 7.4 with HCl.

iii. ***For 50 mM imidazole (per100ml):*** Dissolve 0.3404g Imidazole (Sigma-Aldrich, MO, U.S.A) into base solution. Adjust pH to 7.4 with HCl. Store at room temperature.

iv. ***For 75 mM imidazole (per100ml):*** Dissolve 0.5106 g Imidazole (Sigma-Aldrich, MO, U.S.A) into base solution. Adjust pH to 7.4 with HCl. Store at room temperature.

v. ***For 100 mM imidazole (per100ml):*** Dissolve 0.6809 g Imidazole (Sigma-Aldrich, MO, U.S.A) into base solution. Adjust pH to 7.4 with HCl. Store at room temperature.

vi. ***Protein Elution Buffer (500 mM imidazole, per 50 ml):*** Dissolve 1.702 g Imidazole (Sigma-Aldrich, MO, U.S.A) into base solution. Adjust pH to 7.4 with HCl. Store at room temperature.

g. For Tricine SDS-PAGE

i. ***Anode buffer (per 1L):*** Weigh out 24.3 g tris base (Sigma-Aldrich, MO, U.S.A). Dissolve in 500 ml distilled water. Adjust pH to 8.9 with HCl. Make up to 1 L with distilled water. Store at 4^{o}C.

ii. ***Cathode buffer (per 1L):*** Weigh out 12.11g tris base (0.1M) ((Sigma-Aldrich, MO, U.S.A) and 17.19 g tricine (0.1M) (Sigma-Aldrich, MO, U.S.A), 1g SDS (0.1% w/v) (Sigma-Aldrich, MO, U.S.A). Dissolve in 1L distilled water. Do no adjust pH. Store at 4^{o}C.

iii. ***Tris.cl/SDS, pH 6.8 (0.5M tris.cl, 0.4% SDS) (per 100ml):*** Weigh out 6.05g tris base (Sigma-Aldrich, MO, U.S.A) dissolve in 40ml of distilled water adjust pH to 6.8 with HCl, make up to 100ml with distilled water , syringe water through a 0.45µm filter, dissolve in 0.4g SDS. Store at 4^{o}C.

iv. ***Tricine gel DTT-containing loading buffer, 6X (0.1 M Tris, 24 % w/v glycerol, 8 % w/v SDS, 0.2 M DTT) (per 10ml)***: Weigh out 1 g SDS (Sigma-Aldrich, MO, U.S.A), 0.93 g DDT (Sigma-Aldrich, MO, U.S.A) and 1.2 mg Bromophenol blue.

Add 7 ml 4x tris.cl/SDS (pH 6.8) and 3.0 ml glycerol. Make up to 10 ml with distilled water. Store 0.5ml aliquots at -20^{o}C.

v. ***Tricine gel DTT-free loading buffer, 6X:*** Same as above, exclude DTT.

h. For Mammalian Cell Cultures

i. PBMC Culture Media

RPMI-1640 Medium (with sodium bicarbonate, without L-glutamine) (Sigma-Aldrich, MO, U.S.A); supplemented with 1x Glutamax (2 mM), 1x P/S (100 units of Penicillin and 0.1 mg/ml of Streptomycin; Sigma-Aldrich, MO, U.S.A), 1x IL – 2 (3%) (Sigma-Aldrich, MO, U.S.A), 10%/20% FCS (Biochrom Heat Inactivated, UK)

ii. Freeze Media for PBMC (90% FCS, 10% DMSO)

In 9 mL of FCS (Biochrom Heat Inactivated, UK), add 1 mL of sterile syringe-filtered cell culture grade DMSO (Sigma-Aldrich, MO, U.S.A). Mix before use.

APPENDIX B: Protocols

a. Poly-Acrylamide Gels

Mini-PROTEAN® Bio-Rad gel casting glass plates (12.5cm x 6.5 cm x 1.5 mm) were firstly washed with soapy water, rinsed with distilled water, and cleaned with 70% ethanol. The plates were assembled on the casting standing and it was ensured that there were no leaks. Running gels were prepared (described below), with Ammonium Persulphate (APS) (Sigma-Aldrich, MO, U.S.A) and Tetra-methyl-ethylene-diamine (TEMED) (Sigma-Aldrich, MO, U.S.A) being added last. Running gel was poured into casting plates and topped with isopropanol in order to level the gels. Running gels was allowed to set. Once set, isopropanol was discarded and remaining isopropanol was allowed to air-dry. Stacking gels were prepared (described below), with APS and TEMED being added last. Stacking gels was poured onto set running gel. Combs were carefully placed to prevent air bubbles. Stacking gels were allowed to set. Gels could be used immediately or were wrapped in moistened paper-towels and stored at 4^{o}C until use.

Appropriate loading buffer was added to protein samples accordingly. If required, samples were incubated onto a water-bath at 100^{o}C for 10 minutes. Casted gel plates were assembled into the electrophoresis cell. Appropriate buffer is added to corresponding chambers. Markers and gel samples are loaded into wells using a syringe. Gel electrophoresis is conducted (200 V, 15mA per gel) until proteins were resolved.

i. **SDS-PAGE Gels (10% Running gels, 2 gels, 1.5 mm)**

Running Gel (10%)	
Monomer Solution	10.0 mL
4X Running Buffer	7.5 mL
10% SDS	300 µL
Distilled Water	12 mL
10% APS	150 µL
TEMED	10 µL

Stacking Gel	
Monomer Solution	0.88 mL
4X Stacking Buffer	1.66 mL
10% SDS	66 µL
Distilled Water	4.0 mL
10% APS	33.4 µL
TEMED	10 µL

ii. **Tricine Gels (15% Running gels, 2 gels, 1.5 mm)**

Running Gel (15%)	
Monomer Solution	4.9 mL
Tris.Cl/SDS	5.0 mL
Glycerol	1.59 µL
Distilled Water	3.5 mL
10% APS	50 µL
TEMED	10 µL

Stacking Gel	
Monomer Solution	1.62 mL
Tris.Cl/SDS	3.10 mL
Glycerol	-
Distilled Water	7.78 mL
10% APS	50 µL
TEMED	10 µL

b. Plasmid extraction/Mini-Prep. (GenElute™ Plasmid Miniprep Kit, Sigma-Aldrich)

i. Pellet cells from 1 – 5 mL overnight culture (10 minutes, 2000 rpm). Discard the supernatant.

ii. Resuspend in 200 µL of resuspension solution (RNAse-containing). Pipette gently to mix.

iii. Add 200 µL of lysis solution. Invert gently to mix (4 – 6 times) and allow to clear (< 5 minutes).

iv. Add 350 µL of neutralising solution. Invert gently to mix (4 – 6 times). Pellet debris by centrifugation at maximum speed.

v. Attach binding column to collection tube. Prepare binding column by adding 500 mL of column preparation solution to the binding column. Centrifuge (>12000 xg, 1 minute) and discard flow-through.

vi. Transfer clear lysate to the binding column. Centrifuge (>12000 xg, 1 minute) and discard flow.through.

vii. Add 750 µL of wash solution to column. Centrifuge (>12000 xg, 1 minute) and discard flow-through.

viii. Dry-spin column. Centrifuge (>12000 xg, 1 minute) and discard collection tube.

ix. Attach column to a new collection tube. Add 100 µL of elution buffer to column. Centrifuge (>12000 xg, 1 minute). Collect flow-through containing purified plasmid DNA.

c. Isolation and purification of DNA (High Pure PCR product purification kit, Roche®)

i. Visualise under UV and isolate resolved bands of interest from agarose gel by cutting the desired band out.

ii. Place cut agarose gel slice into sterile capped 1.5 mL microtube.

iii. Add 300 µL of binding buffer per 100 mg of agarose to the microtube. Dissolve the agarose by incubating the microtube at 56^{o}C for 10 minutes. Vortex every 2 – 3 minutes.

iv. Add 150 µL of isopropanol to every 100 mg agarose gel. Vortex.

v. Attach a High Pure ® filtration tube a to a collection tube. Pipette contents of microtube into the filtration tube (no more than 700 µL). Centrifuge 30 – 60s at maximum speed between 15 – 25 ^{o}C. Discard flow-through and reconnect the filter tube to the collection tube.

vi. Add 150 µL of wash buffer to filter tube. Centrifuge at maximum speed for 1 minute. Discard flow-through. Reconnect the filter tube to the collection tube.

vii. Add 200 µL of wash buffer to filter tube. Centrifuge at maximum speed for 1 minute. Discard the collection tube. Reconnect the filter tube to a new 1.5 mL collection tube.

viii. Add 50 - 100 µL of elution buffer to filter tube. Centrifuge at maximum speed for 1 minute. Collect flow-through containing purified DNA.

APPENDIX C: Diagrams, Tables and Graphs

a) Amino acid sequence alignment of D1 (m1.1) and D2 (WT) relative to 2dCD4.

In green: Mutations; In yellow: Histidine tags

1 **50**

Two-domain_CD4 KKVVLGKKGD TVELTCTASQ KKSIQFHWKN SNQIKILGNQ GSFLTKGPSK

Cd4_D1(m1.1) MKKVVIGKKGD TVELTCTASQ KKSIQFHWKN SNQIKILGNQ GSFLTKGPSK

Cd4_D2_(WT) ----------

51 **100**

Two-domain_CD4 LNDRADSRRS LWDQGNFPLI IKNLKIEDSD TYICEVEDQK EEVQLLVFG

Cd4_D1(m1.1) LNDRVDSRRS LWDQGNFPLI IKNLKPEDSD TYICEVEDQK EEVQLIVLG

Cd4_D2_(WT) ----------MG

101 **150**

Two-domain_CD4 LTANSDTHLL QGQSLTLTLE SPPGSSPSVQ CRSPRGKNIQ GGKTLSVSQL

Cd4_D1(m1.1) HHHHHH----------

Cd4_D2_(WT) LTANSDTHLL QGQSLTLTLE SPPGSSPSVQ CRSPRGKNIQ GGKTLSVSQL

151 **190**

Two-domain_CD4 ELQDSGTWTC TVLQNQKKVE FKIDIVVLAF QKAS----------

Cd4_D1(m1.1) ----------

Cd4_D2_(WT) ELQDSGTWTC TVLQNQKKVE FKIDIVVLAF QKLEHHHHHH

b) In silico derived-data of D1(m1.1)and D2 (WT) relative to 2dCD4.

D1 (m1.1)

Analysis	Entire Protein
Length	108 amino acids
Molecular Weight	12392.35
1 microgram =	80.695 pMoles
Molar Extinction Coefficient	12900
A_{280} corr. to	0.96 mg/mL
A_{280} corr. ff 1 mg/mL	1.04 AU
Isoelectric Point	8.94
Charge at pH 7	3.36

Table 2: In silico derived-data of D1(m1.1)

Amino Acids	Number count	% by weight	% by frequency
Charged (RKHYCDE)	39	40.13	36.11
Acidic (DE)	13	12.67	12.04
Basic (KR)	16	16.92	14.81
Polar (NCQSTY)	29	25.67	26.85
Hydrophobic (AILFWV)	30	28.23	27.78

D2 (WT)

Analysis	Entire Protein
Length	94 amino acids
Molecular Weight	10358.12
1 microgram =	96.543 pMoles
Molar Extinction Coefficient	5930
A_{280} corr. to	1.75 mg/mL
A_{280} corr. of 1 mg/mL	0.57 AU
Isoelectric Point	8.06
Charge at pH 7	1.36

Table 3: In silico derived-data of D2 (Wt)

Amino Acids	Number count	% by weight	% by frequency
Charged (RKHYCDE)	24	29.43	25.53
Acidic (DE)	7	8.21	7.45
Basic (KR)	8	10.18	8.51
Polar (NCQSTY)	32	32.89	34.04
Hydrophobic (AILFWV)	26	28.12	27.66

c) Ramachandran Plots

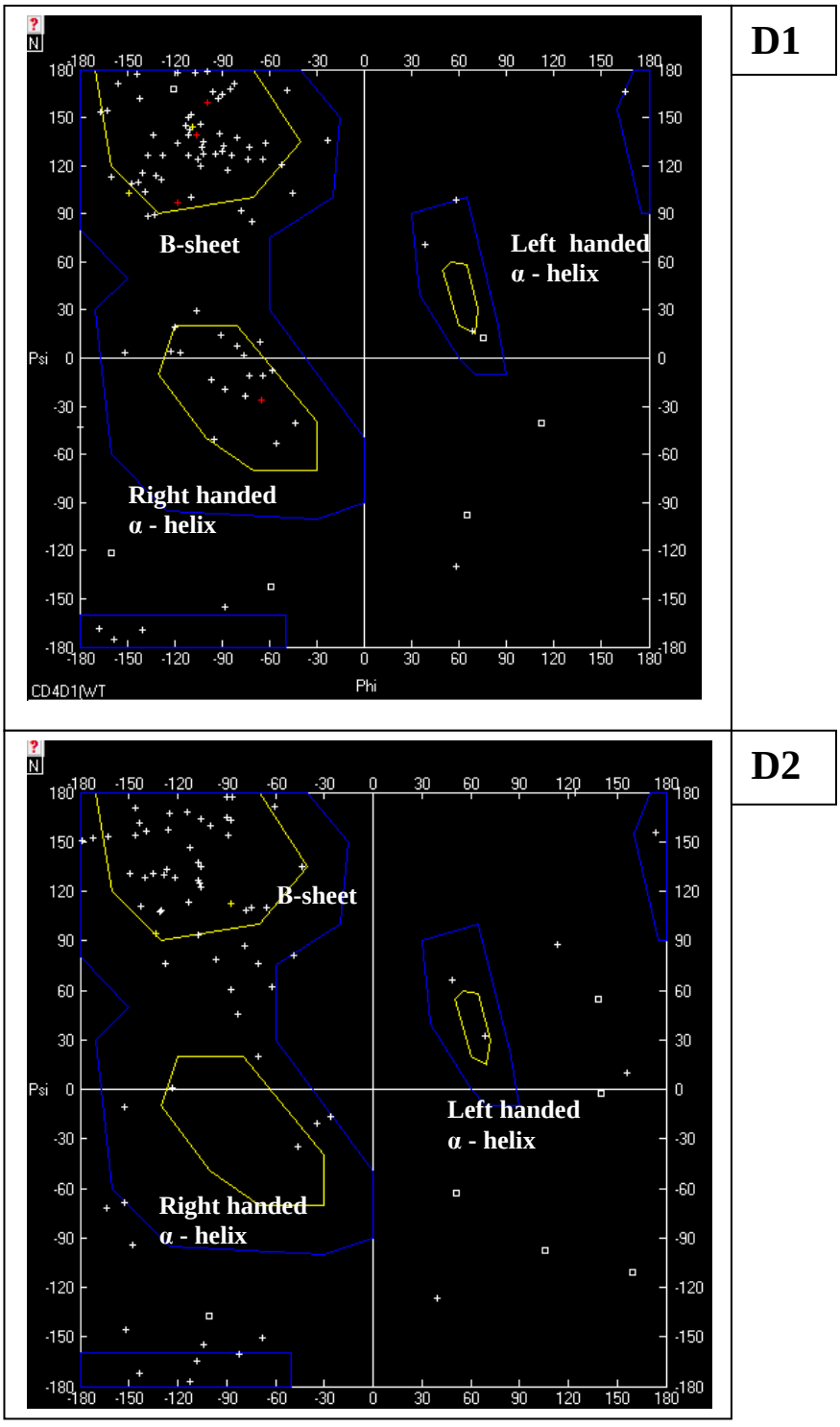

Figure 29: Ramachandran Plots of D1 (m1.1) and D2.

d) Far-UV CD Voltage/Wavelength

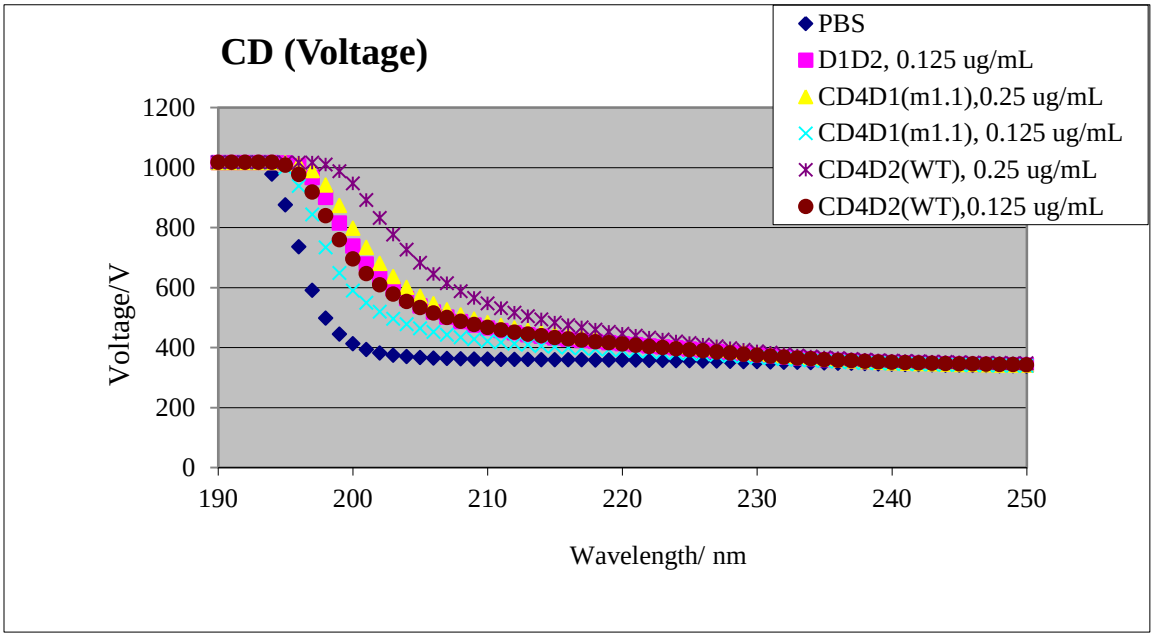

Figure 30: CD-Analysis (V/nm)

During CD-analyses, the voltage experienced against wavelength was plotted in order to validate the region of the Far-CD UV plot (Figure 15) where stable measurements were made. Stable, constant voltage of ~400 V from ~210nm represents valid measurements. Increasing voltage to 1000 V below 210nm represent non-valid measurements.

e) Viral Inhibition with serum m79

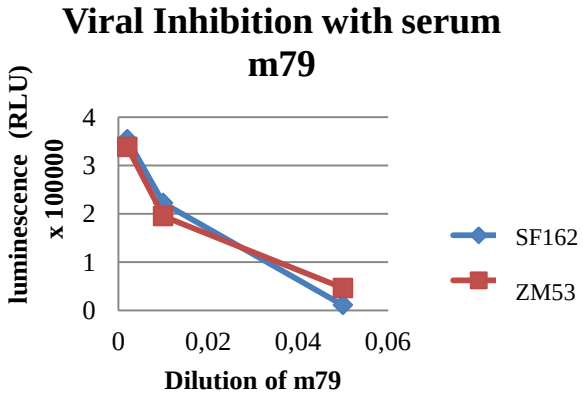

Figure 31: Preliminary Analysis of CD4MAb-mediated inhibition of HIV-1 pseudovirus replication

Serum m79, which was derived from rabbit immunized with gp120-CD4 complex, had shown significant viral inhibition against both SF162 and ZM53.

f) Previous Expression of individual domains 1 and 2 of CD4

Domain	Reference	Name of Domain in Original Publication	Description and Mutations	Expression	Purification
D1	Chen et al.(2011)	mD1.1	L5I, A55V, I76P, L96I, F98L; C-terminal His-tag	HB2151 *E. coli*; Soluble fraction of periplasm	Metal Ion Affinity (IMAC) using Ni-nitrotriacetic acid (NTA); followed by size exclusion chromatography
D1	Chen et al.(2011)	mD1.1	L5I, A55V, I76P, L96I, F98L; C-terminal His-tag	*HEK293;* Soluble from supernatant	Metal Ion Affinity (IMAC) using Ni-nitrotriacetic acid (NTA); followed by size exclusion chromatography
D1	Chen et al.(2011)	mD1.1 – CH2	L5I, A55V, I76P, L96I, F98L; Fusion protein with IgG1 CH2 domain	*HEK293;* Soluble from supernatant	Protein A Sepharose 4 Fast Flow; followed by size exclusion chromatography
D1	Chen et al.(2011)	mD1.2	L5I, A55V, I76P, L96I, F98L; C-terminal His-tag	*E. coli*; Soluble fraction of periplasm	Metal Ion Affinity (IMAC) using Ni-nitrotriacetic acid (NTA); followed by size exclusion chromatography
D1	Chen et al.(2011)	mD1.2	L5Y, S23N, I76P, L96V, F98V; C-terminal His-tag	*HEK293;* Soluble from supernatant	Metal Ion Affinity (IMAC) using Ni-nitrotriacetic acid (NTA); followed by size exclusion chromatography

D1	Saha et al. (2011)	CD4D1a	L5K, G6A, L51I, V86L, F98T; N-terminal His-tag	*E. coli*; Insoluble fraction as inclusion bodies	Solubilisation with 8 M guanidine hydrochloride in PBS, Ni-NTA affinity and imidazole elution, refolding by dialysis against PBS
D1	Sharma et al. (2005)	CD4D1	V3T, L5A, I76T, L96A, F98A N-terminal His-tag	*E. coli*; Insoluble fraction as inclusion bodies	Solubilisation with 6 M guanidine hydrochloride in PBS, Ni-NTA affinity and imidazole elution, refolding by dialysis against PBS
D2	Commercially available from: ProSpec-Tany TechnoGene Ltd., Rehovot, Israel (Cat. No.: CYT-315) Matthias et al. (2010)	CD-4	Residues 125 – 202; Histidine tagged	*E. coli*	Has not been publicly described

Table 4: Previous Expression of individual domains 1 and 2 of CD4

a) Restriction Analysis

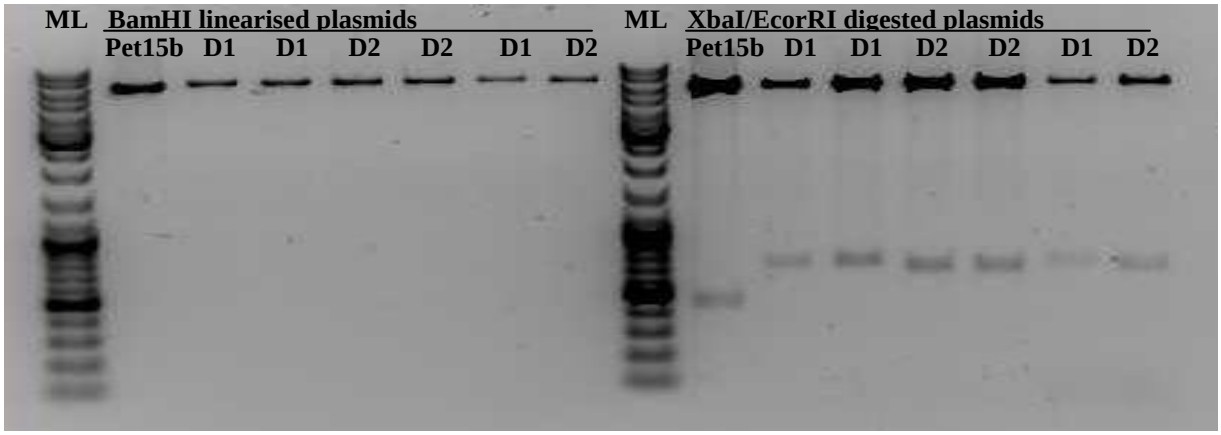

Figure 33: Restriction Analysis of D1 and D2 in pET15b vector

Molecular screening for successful ligation was confirmed by 1.5 % gel electrophoresis of *BamHI* and *XbaI/EcorRI* digested plasmids. Linearised plasmid (i.e. *BamHI* digestion) produced the expected single bands at about 6000 bp. The absence of any other DNA contaminants or un-ligated inserts is stressed. Inserts derived from *XbaI/EcorRI* restriction analysis were visualised (D1 (m1.1): 691 bp, D2: 649 bp). This confirmed success of ligation and isolation of pet15b – D1 and –D2 plasmids.

ML: Molecular ladder (Thermo Scientific O'GeneRuler *DNA Ladder* Mix, SM1173)

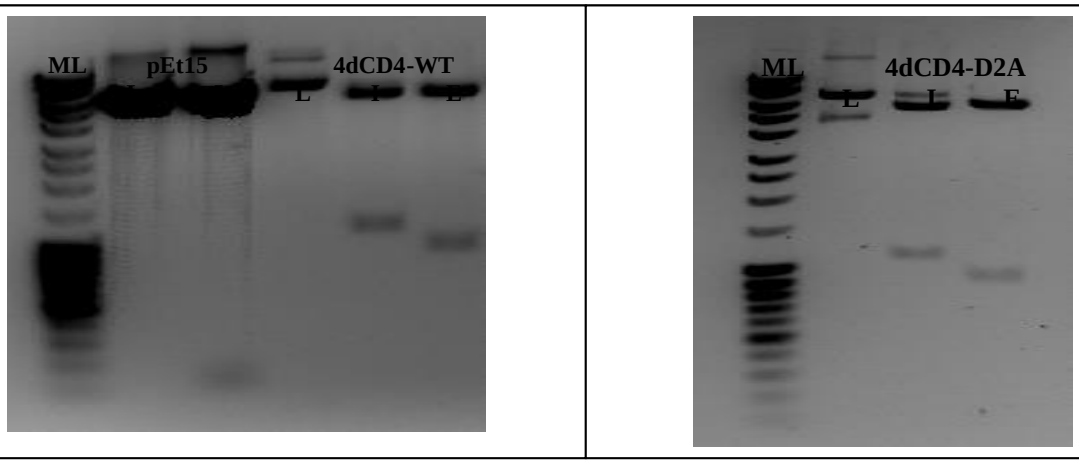

Figure 32: Restriction Analysis of 4dCD4-Wt and 4dCD4-D2A in pET15b vector

Molecular screening for successful ligation was confirmed by 1.0 % gel electrophoresis. Control pET15b and ligated vector were linearised with *XbaI* (**L**). Single significant band was observed, with ligated DNA occurring at higher molecular weight compared to pET15b control. Digestion with *XbaI/XhoI* allowed for identification of insert (1226 bp) in the ligated products (**I**). Control pET15b, subjected to *XbaI/XhoI* produced expected fragment of 109 bp. EcoRI digestion essentially caused linearization of control pET15b (**E**). In the case of ligated products, EcoRI digestion produced two fragments, due to presence of extra EcoRI restriction site present in 4dCD4 insert.

ML: Molecular ladder (Thermo Scientific O'GeneRuler *DNA Ladder* Mix, SM1173)

APPENDIX D: PBMC-based IFN-G Stimulation Assay

a. Material and Methods

i. PBMC cell isolation

Human buffy coats (purchased from the South African National Blood Services), which had been separated from whole blood by initial hard-spin, were used for extraction of peripheral blood mononuclear cells (PBMC). Approximately 200 ml of human buffy coat was diluted with an equal volume of 1x PBS (Sigma-Aldrich, MO, U.S.A) (Total of 400 mL). Twenty-five millitres (25 mL) of the diluted buffy coat was then layered onto 20 mL Ficoll-Paque^{TM} (GE HealthCare, LifeSicences, UK) in a 50 ml centrifuge tube at room temperature. The tubes were centrifuged at 800 g for 30 minutes at room temp (maximum acceleration, no brakes). The buffy layer was then carefully removed from on top of the Ficoll layer and diluted into PBS (25 mL PBS per tube). The PBMC were gently mixed and centrifuged at 3200 g for 20 minutes at 16^{o}C (max. acceleration, brakes on). The supernatant was discarded and the pellet resuspended in 5 mL of PBS. A total of 50 mL of PBS was then added to the tubes, which were then centrifuged at 450 g for 10 min at 10^{o}C (max. acceleration, brakes on). The supernatant was discarded, the cells washed again, and the PBMC pellet from each tube resuspended in 2 mL of PBS. The cells were counted by trypan blue (Gibco©, LifeTechnology, U.S.A) exclusion using a haemocytometer before being stored in cryogenic 2 mL microtubes in freeze media (10% DMSO and 90% FCS) at -80^{o}C (10 million cells in 1.5 mL per vial).

ii. PBMC culture and stimulation

Twenty million PBMCs were quickly thawed and washed thrice with room temperature PBS by centrifuging (3200 g, 3 minutes, max. acceleration, brakes on) before resuspension in 5 mL of RPMI cell culture media (See Appendix A.g.i.) containing 20% Fetal Calf Serum (FCS) (Biochrom Heat Inactivated FCS, UK). In order to allow for the cells to settle following thawing, these were firstly seeded in a 75 cm^2 culture flask (Easy Nunc, Nunclon D, Denmark) in a total

of 30 mL of cell culture medium and allowed to incubate at 37^{o}C in a humidified atmosphere containing 5% CO_2 (standard conditions) overnight.

The PBMCs were then transferred to a 50 mL centrifuge tube and centrifuged at 3200 g for 15 minutes at room temperature (max. acceleration, brakes on). The supernatant was discarded and the PBMC pellet resuspended in 5 mL of culture media containing 10% FCS (Biochrom Heat Inactivated FCS, UK). Cells were counted and plated into 24-well culture plates (10^6 cells in 1 ml of medium per well) (ThermoScientific^{TM} Nunc^{TM} MicroWell^{TM} 24-Well Microplate/ Nunclon^{TM}-D, Denmark). The cells were incubated for 48 hours under standard conditions prior to stimulation with Phytohaemagglutinin (Sigma-Adrich, MO, U.S.A) (PHA, 5 ug/mL). The cells then incubated for a further 48 hours. Supernatants were collected and clarified by centrifugation at 10000 g for 5 min and stored at -20^{o}C.

iii. Assessment of supernatant inhibition of INF-γ

Into 96-well plates (ThermoScientific^{TM} Nunc^{TM} MicroWell^{TM} 96-Well Microplate/ Nunclon^{TM}-D, Denmark), 10^5 cells per well in a total of 200 µL of culture media, were plated. In order to assess data statistically, triplicates of experimental wells were used. The cells were incubated at 37^{o}C/5% CO_2 for 48 hours prior to stimulation with PHA (Sigma-Adrich, MO, U.S.A) at 5 µg/mL. Anti-CD4 antibody-containing mouse hybridoma supernatants were then added to the PBMC cultures at a dilution of 1:100. As a positive control for CD4+ T-cell activation inhibition, the mouse monoclonal anti-CD4 antibody mt310 (Santa Cruz Biotechnology, TX, U.S.A) was added to a final concentration of 1 µg/mL. An irrelevant antibody, the anti-HIV monoclonal antibody (IgG1b12), which binds the viral envelope glycoprotein (gp120), was added at the same concentration as a negative control. Reactions were performed in triplicate, and the plates incubated for a further 48 hours. The levels of INF-γ in supernatant samples from each well were analysed by the INF-γ detection assay described below.

iv. INF-γ detection

Secretion of human INF-γ from PHA-stimulated PBMCs was used as a crude marker of T-cell activation, and this was detected by sandwich ELISA using the DuoSet® ELISA Development System from R&D Systems (cat. No.: DY285, MN, U.S.A). Reagents and a standard ELISA protocol provided by the manufacturer were used. In order to assess data statistically, triplicates of experimental wells were used. One hundred microlitres of anti-IFN capture antibody diluted in PBS at 4.0 µg/mL was added to wells of 96-well plate (Nunc©, MaxiSorp, Denmark). PBS blank controls were included. The plate was sealed and incubated overnight at room temperature. The coating solution was aspirated from wells and washed with wash buffer (1x PBS, 0.05% Tween) (Sigma-Aldrich, MO, U.S.A) thrice. The plates were then blocked with 300 µL of blocking buffer (10mg/mL BSA in PBS-T) (Sigma-Adrich, MO, U.S.A) for 1 hour. The blocking solution was removed and the wells washed 3 times before the addition of either 100 µL of thawed PBMC supernatant samples, or recombinant human INF-γ control (0 - 1000 pg/ml). Following a 2 hour incubation at room temperature, the wells were aspirated and washed, and 100 µL of detection antibody diluted in reagent diluent at 50 ng/mL was added to the plate wells, which were incubated for a further 2 hours at room temperature. The plates were washed after removal of the detector antibody solution, and 100 µL of Streptavidin-HRP (1:200 in reagent diluents) was added. Following aspiration and washes, 100 µL of TMB-Ultra substrate (Thermo-Pierce, U.S.A) was added. Plate was incubated for 20 min at 37^{o}C onto a rotary plate. Sulphuric acid, 100 µL at 1 M, was added to wells to quench reaction. The solution optical densities were determined using a plate reader (Fast read, 570/450 nm measure filter, 37^{o}C; Bio-Rad Model 650 Microplate reader; CA, U.S.A).

a. Results

There was enhanced expression and secretion of INF-γ, indicative of robust PHA-mediated PBMC/T-cell activation (Figure 33). Based on standards, above 1 mg/mL of INF-γ was detected.

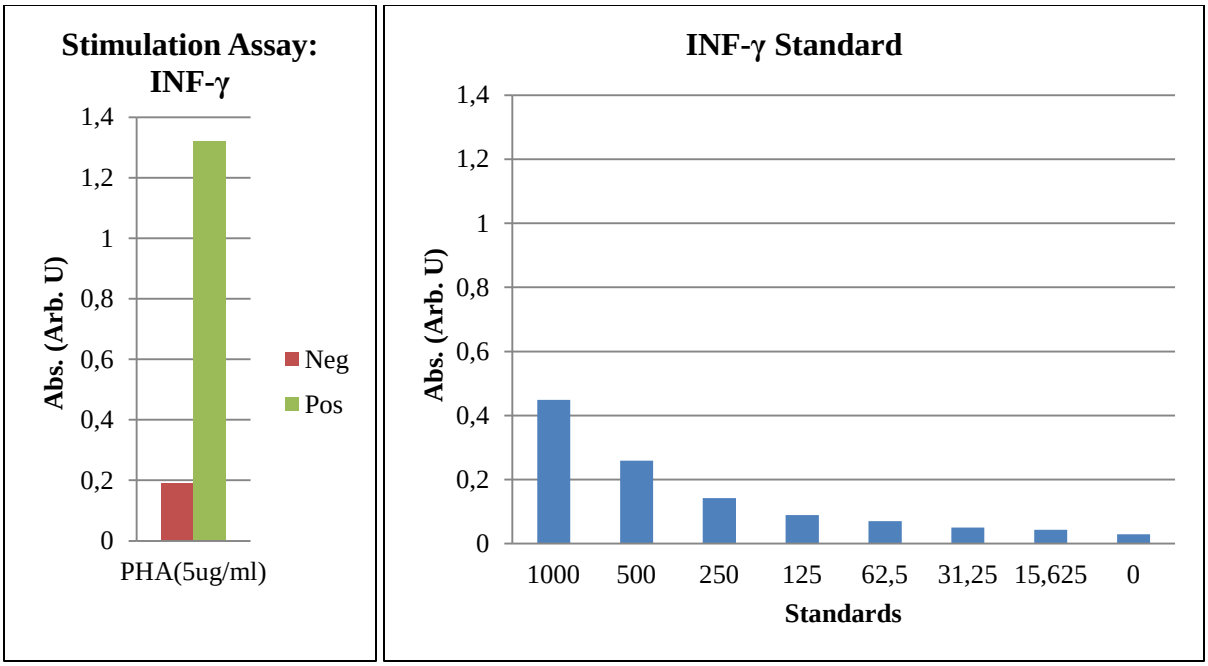

Figure 34: Preliminary detection of INF- γ produced by PBMCs

INF-γ detection in PHA stimulated and unstimulated PBMCs. Almost 6.5-fold more INF-γ was detected in the cell culture media of PHA stimulated PBMC (green) when compared to unstimulated cells (red), representing concentrations above 1 mg/mL INF-γ.

i. Preliminary analysis of inhibitory effects of CD4MAb1-40 on T-Cell activation

After confirming the secretion of INF-γ, we set out to verify whether the CD4MAb1-40 had any effect in the PHA-stimulated assay. The experiment, as described above, was set up in 96-well plates instead (10^5 cells per well). Supernatants (1:100) were added to corresponding wells and the plate was incubated for 48h prior to INF-γ detection. Additionally, mt310 (1ug/ml) and IgG1b12 (1µg/ml) were also included in the setup as controls. Mt310 is a known anti-CD4 antibody (positive control), whereas IgG1b12 is an anti-gp120 antibody (Negative control). It was observed that none of the CD4-MAbs, mt310 and IgG1b12 caused any reduction in INF-γ secretion following PHA stimulation, indicative of maintenance of PBMC/T-cell activation (Figure 34).

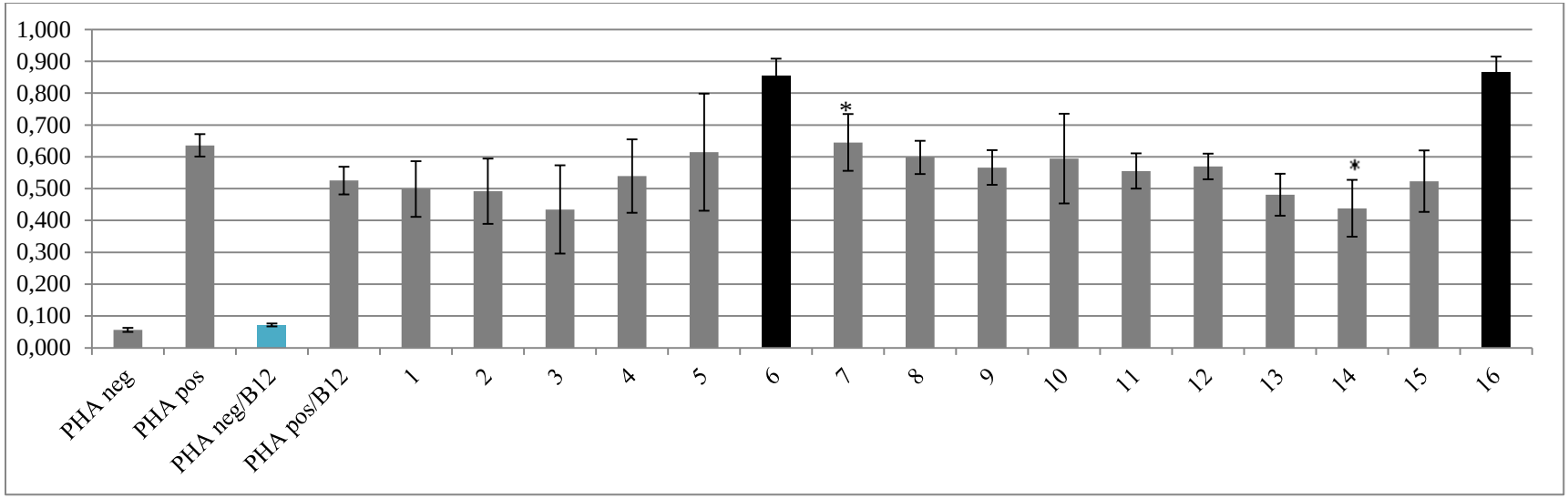
1,000
0,900
0,800
0,700
0,600
0,500
0,400
0,300
0,200
0,100
0,000
PHA neg
PHA pos
PHA neg/B12
PHA pos/B12
1
2
3
4
5
6
7
8
9
10
11
12
13
14
15
16
*
*

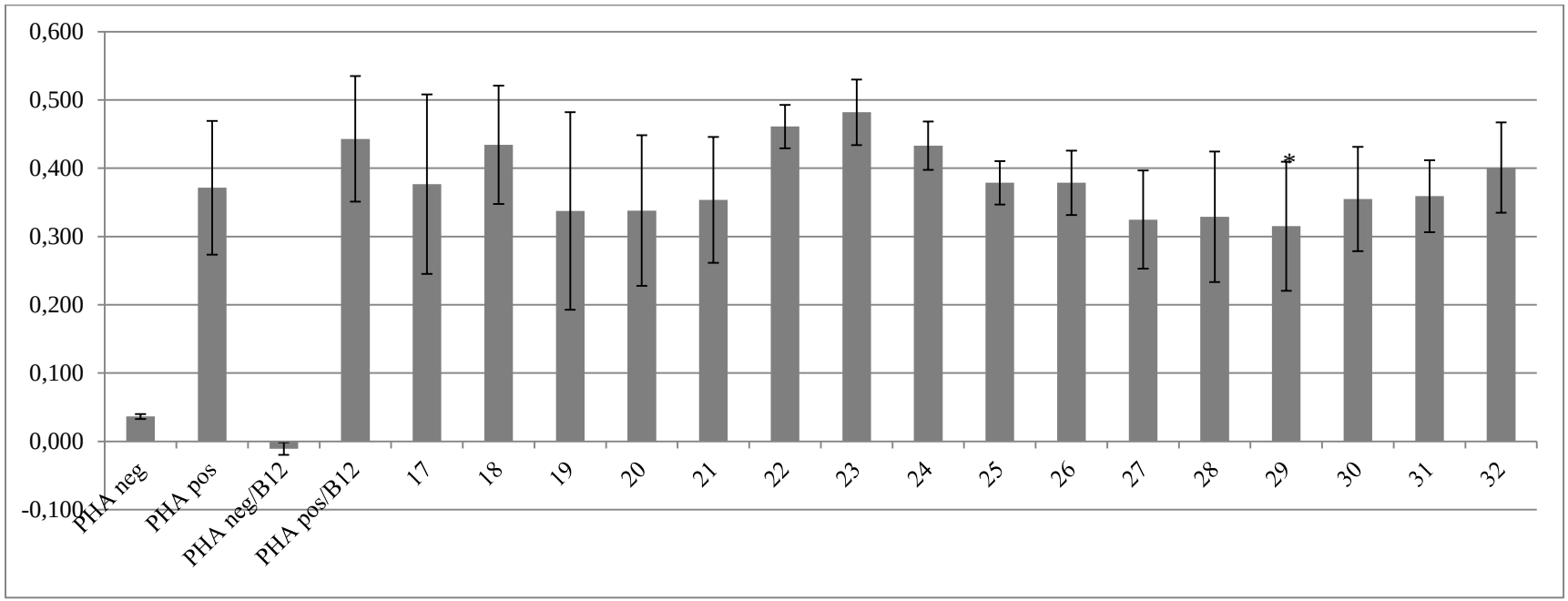
0,600
0,500
0,400
0,300
0,200
0,100
0,000
-0,100
PHA neg
PHA pos
PHA neg/B12
PHA pos/B12
17
18
19
20
21
22
23
24
25
26
27
28
29
30
31
32
*

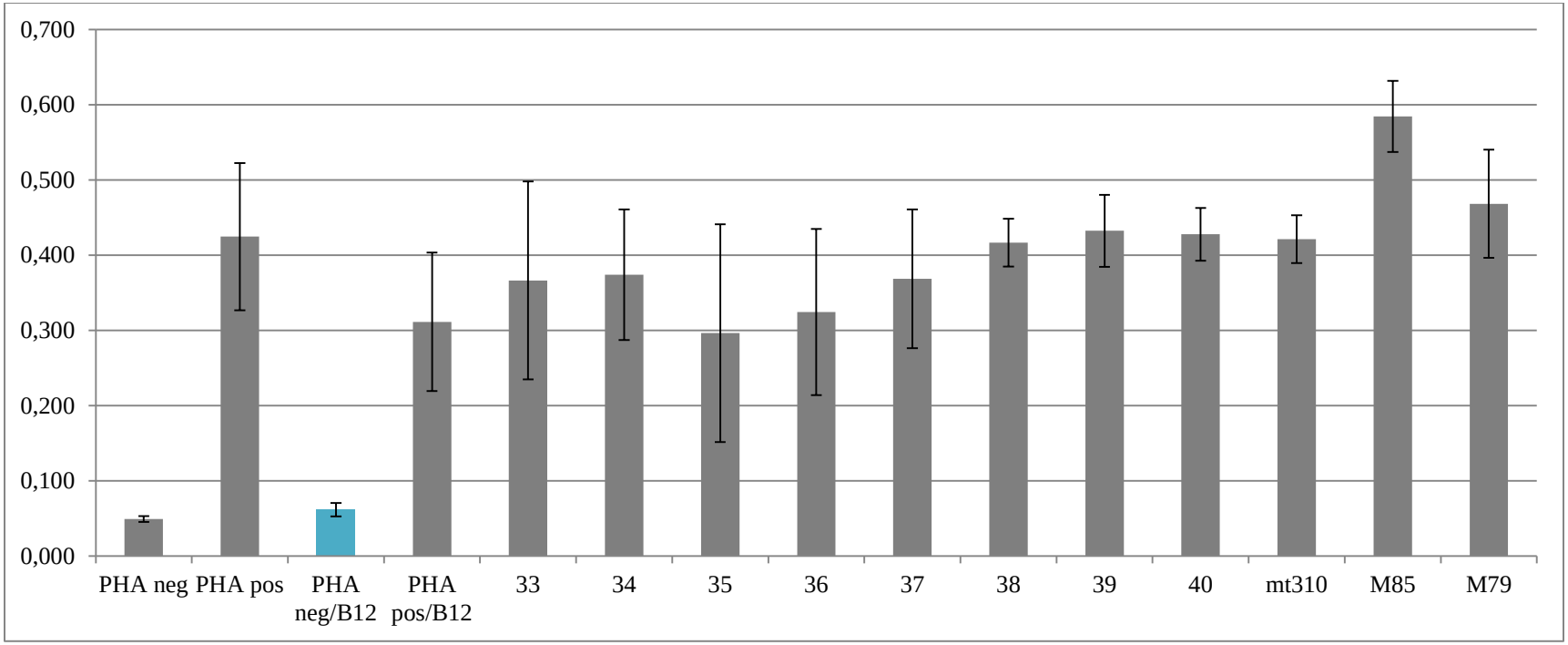

Figure 35: Preliminary Analysis of Inhibitory effects of CD4MAb1-40 on T-Cell activation

PBMC Stimulation Assay with supernatant (1:100), background corrected. As opposed to PHA stimulated experiments, the absence of PHA did not result in PBMC stimulation and INF-γ was not overexpressed. Supernatants and antibodies did not have any observable effect on INF-γ expression. It is likely the effect of PHA as a mitogenic stimulant results in net PBMC activation that overshadows the influence of the supernatants and antibodies. NB: Samples 6 and 16 were ignored due to excessive evaporation of media on the wells during incubation.

Triplicates of experimental data were used for calculating means; error bars represent standard deviation (μ±1sd). Two-tail T-test of experimental versus PHA pos./IgG1b12 as control was conducted (in blue); * indicates significant differences ($p<0.05$) relative to PHA pos/IgG1b12. Whilst these might indicate statistically significant differences, these may not be biologically significant - theoretically, PHA acting as a mitogen promotes cellular activation irrespective of CD4MAb presence. M85 and M79, used as further controls, are sera from rabbits that were immunised with a gp120-CD4 complex that had shown potent pseudoviral inhibition in our laboratory.

APPENDIX E: Analysis of CD4MAb-mediated inhibition of CD4-gp120 binding *in vitro*

CD4MAb Supernatant dilution	1	2	3	4	5	6	7
0.1	0.065	0.084	0.033	0.047	0.059	0.076	0.058
0.01	0.218	0.197	0.131	0.153	0.161	0.151	0.205
0.001	0.316	0.330	0.275	0.277	0.308	0.225	0.364
0	0.403	0.436	0.466	0.420	0.415	0.429	0.522

CD4MAb Supernatant dilution	8	9	10	11	12	13	14
0.1	0.077	0.091	0.064	0.082	0.077	0.031	0.056
0.01	0.231	0.243	0.255	0.218	0.116	0.129	0.147
0.001	0.354	0.383	0.399	0.324	0.258	0.223	0.239
0	0.536	0.568	0.522	0.533	0.538	0.364	0.413

CD4MAb Supernatant dilution	15	16	17	18	19	20	21
0.1	0.041	0.067	0.022	0.032	0.028	0.013	0.024
0.01	0.115	0.154	0.103	0.101	0.106	0.104	0.084
0.001	0.202	0.237	0.162	0.191	0.152	0.156	0.225
0	0.392	0.420	0.222	0.275	0.269	0.222	0.239

CD4MAb Supernatant dilution	22	23	24	25	26	27	28
0.1	0.034	0.021	0.031	0.018	0.008	0.018	0.019
0.01	0.077	0.094	0.108	0.088	0.105	0.076	0.099
0.001	0.205	0.163	0.157	0.166	0.169	0.159	0.174
0	0.237	0.219	0.226	0.229	0.218	0.213	0.234

CD4MAb Supernatant dilution	29	30	31	32	33	34	35
0.1	0.012	0.025	0.029	0.015	0.026	0.029	0.020
0.01	0.099	0.232	0.219	0.108	0.121	0.115	0.090
0.001	0.166	0.221	0.223	0.146	0.152	0.155	0.125
0	0.245	0.243	0.242	0.198	0.207	0.195	0.147

CD4MAb Supernatant dilution	36	37	38	39	40
0.1	0.030	0.021	0.014	0.017	0.025
0.01	0.090	0.060	0.065	0.081	0.070
0.001	0.136	0.121	0.122	0.127	0.118
0	0.187	0.184	0.156	0.159	0.175

Table 5: ***In vitro gp120 binding inhibition assay***

Inhibition of gp120 (200 ng/ml) binding to 4dCD4-Wt following pre-incubation with CD4-Mab-containing supernatants at dilutions of 0.1, 0.01, 0.001 and negative control (PBS). Absorbance readings (570 nm) reflect the level of gp120 binding. Triplicates of experimental data were used for calculating means.

APPENDIX F: TCID50 Calculation

The TCID50 of the frozen pseudoviruses stocks (produced and pre-determined by Dr. M. Killick) were as follows:

ZM53: 3,906,250 TCID50

SF162: 1,746,928 TCID50

An initial two-fold dilution (in DMEM) of viral stocks was made:

ZM53: 3,906,250/2 = ~1,950,000 TCID50

SF162: 1,746,928/2 = ~873,000 TCID50

Following determination of viral working concentration (see 3.3.2.1), the 1:500 dilution of pseudovirus was selected. Thus, working TCID50 of virus was follows:

ZM53: 1,950,000/500 = 3900 TCID50

SF162: 873,000/500 = ~1750TCID50

APPENDIX G: ETHIC WAIVER

Ref: W-AJW-130731-1 31/07/2013

TO WHOM IT MAY CONCERN:

Waiver: This certifies that the following research does not require clearance from the Human Research Ethics Committee (Medical).

Investigator: **Vinesh Jugnarain (363706)**

Project title: **The Generation and Characterisation of Monoclonal Domain-Specific CD4 Antibodies as Novel Anti-HIV Ligands**

Reason: This is an *in vitro* study using commercially available cells lines (HEK293 cells) and various CD4 variants expressed and synthesized by a company in Germany (Geneart, Regensburg, Germany). The study does not involve any human tissue samples or their derivatives.
[Although there is mention of a mouse immunisation protocol this will all be conducted externally in a commercial laboratory (ProMab, Biotechnology, CA, USA)].

Professor Angela Woodiwiss
Co-Chair: Human Research Ethics Committee (Medical)

copy: Anisa Keshav, Research Office, Senate House, Wits